Design Methodology for Subgrades and Bases Under Concrete Roads and Parking Lots

Test Methods & Results of Erosion Potential of Commonly Used Subgrade and Base Materials

Keivan Neshvadian Bakhsh
Graduate Research Assistant
Texas Transportation Institute

Dan Zollinger
Program Manager
Texas Transportation Institute

Texas A&M Transportation Institute

Please Note:

Accompanying the documents is a design spreadsheet for the purpose of incorporating the test procedures described and creates results regarding the best subbase option for a given concrete pavement scenario. As this design tool is being altered into a software program, the tool will be housed with the Pavement Structures Division of the National Ready Mixed Concrete Association. This division is able to run design scenarios and encourages outreach for further discussion (please contact Amanda Hult at ahult@nrmca.org or Brian Killingsworth at bkillingsworth@nrmca.org). The output of this design tool will be similar to the examples represented within the "Design Methodology for Subgrades and Bases Under Concrete Roads and Parking Lots" document.

ENGINEERING REPORT

SUBMITTED TO THE
READY MIXED CONCRETE (RMC) RESEARCH AND EDUCATION FOUNDATION

Design Methodology for Subgrades and Bases Under Concrete Roads and Parking Lots

Keivan Neshvadian Bakhsh
Graduate Research Assistant, Texas Transportation Institute

Dr. Dan Zollinger
Program Manager, Texas Transportation Institute

August 2014

TEXAS TRANSPORTATION INSTITUTE
The Texas A&M University System

Table of Contents

List of Figures

List of Tables

1. Background

When optimizing the design of concrete pavements for parking lots and roads, many factors need to be considered. Applications that are light duty, like a retail store parking lot or a residential road may only experience light passenger cars, school buses and periodic garbage trucks. Owners of low-volume roads are concerned with building low-cost pavements while reducing future maintenance costs. Using, and in some cases improving, the on-site soils can be useful in achieving the owner's goals. However, previous pavement design procedures may not have accounted for the viability of the on-site soils. The lack of fast moving, frequent heavy duty vehicular loading allows for use of chemically stabilized subgrade or the natural subgrade, when appropriately moisture conditioned and compacted.

When designing concrete pavements, designers consider the primary mechanisms for failure which are: faulting and fatigue cracking. Faulting can occur by fast moving, heavy loads, erodible subgrade, saturated soils and reduced load transfer efficiency. Greater detail is providing herein on the faulting mechanism. Fatigue cracking occurs due to repeated loading and flexing of the concrete pavement and is typically mitigated through appropriate concrete thickness, flexural strength and modulus of subgrade reaction.

Analysis of the Federal Highway Administration's (FHWA's) Long Term Pavement Performance (LTPP) data reveals that a pavement's foundation (subgrade and/or subbase) is one of the most critical design factors in achieving excellent performance for any type of pavement [1]. For pavement designers, one of the most important elements in optimizing the design of concrete pavements is determining whether a subbase or improved subgrade is required below the concrete slab and, if needed, the type and nature of the materials required. For highly trafficked highways, aggregate or stabilized subbases are commonly used to provide improved pavement performance; however; for light duty pavements these materials may not be necessary. When designing local streets, roadways and parking lots, designers need to be able to determine whether or not the natural subgrade can provide adequate performance or if alternate materials are needed. The design process detailed in this report assists the designer in making a decision regarding the need for a subbase or stabilized subgrade while specifically considering the soil type, local climate, and traffic loading.

Because of its rigidity, concrete pavement has a high degree of load-spreading capacity which typically results in low sublayer stresses and the potential for concrete pavement slabs to be placed directly on the compacted, natural subgrade. However, it has long been known that adequate subgrades are essential to good concrete pavement performance. As mentioned above, when adequate subgrade support is not achievable, the subgrade may need to be improved through stabilization or an additional sublayer may be required. These supporting layers should provide a stable construction platform, uniformly increased slab support, erosion resistance, and a gradual vertical transition in layer stiffness. From a construction perspective, providing sufficient strength for anticipated construction traffic loads should also be considered during the design phase, particularly if poor drainage conditions are expected during the service life.

Although subbase and subgrade strength are important factors in pavement design, other foundation properties besides strength need to be considered in the design of a foundation for concrete pavement. Sublayer erosion potential, which leads to faulting and potential slab cracking, is one of the key factors in designing the subgrade. The three main elements of erosion are the rate of erosion of the subbase or subgrade material, existence of moisture under the slab, and traffic loads [2]. Therefore, erosion is also linked to drainage and strength properties of the subbase and/or the subgrade.

Erosion potential and drainage considerations are important in the proper design and construction of a roadbed or foundation for concrete pavement. Accumulation of water along the slab/subbase interface combined with heavy loads can often initiate pumping, the transporting of eroded material, and finally the faulting of the joint. Pumping involves the transportation of abraded material from beneath the slab typically voiding the slab support in the vicinity of a joint. Erosion of slab support can often lead to high deflections and possibly other types of distress such as spalling of the joint, acceleration of the loss of load transfer, and reduction in bond between the slab and the sublayer which shortens the life of the pavement [1] [3] [4]. One method that has been utilized successfully to mitigate pumping in wet environmental regions is proper joint sealing that prevents moisture infiltration to the slab/subbase interface.

It is equally important not to overestimate the value of the permeability of a subbase layer. Where stability has been sacrificed for drainage, concrete pavements have performed poorly and have experienced unacceptable numbers of faulted joints and cracked slabs within a relatively short period. Alternatively, stabilization of the existing subgrade with cement, lime or fly ash has been a proven method to improve erosion resistance at the slab/subbase interface.

According to the American Concrete Institute (ACI) report ACI325.12R-02, foundation-related factors that can contribute to pavement distress are [5]:

- Non-uniformity of support caused by differences in subgrade soil strength or moisture;
- Non-uniform compaction;
- Poor drainage properties of the subbase or subgrade, which can enhance the potential for erosion under the action of slab pumping and lead to loss of support, and ultimately, faulting at the joints;
- Non-uniform frost heave; and
- Excessive swelling of expansive subgrade materials.

Other factors designers must consider when evaluating concrete pavement supporting layers are the axle loads, the distribution of the loads, and their frequency over the life of the pavement. When designing a light duty pavement such as a local road or parking lot, the axle loads and frequency are commonly significantly lower than highway type applications. Lighter loads will deflect the pavement less, resulting in less erosion of the sublayer, even when wet. This will allow, under certain conditions, concrete pavements to be built on compacted natural subgrade, stabilized subgrade, or thin aggregate bases and perform adequately. The following pavement design manuals and documents provide the following guidance on this topic:

- AASHTO 1993 Guide for the Design of Pavement Structures: “In cases where design traffic is less than 1 million ESALS, an additional subbase layer may not be needed.”

- ACI 330 R-08 Guide for the Design and Construction of Concrete Parking Lots: “It is not economical to use subbase material for the sole purpose of increasing k-values. Granular subbases are not normally used for concrete parking lots and should not be used as a construction expedient instead of proper subgrade preparation.” Also “Normally, pavements that carry less than 200 heavily loaded trucks/day will not be damaged by pumping, especially if speeds are low; therefore, they do not require subbases.”

- ACI 325.12 R-02 Guide for the Design of Jointed Concrete Pavements for Streets and Local Roads: “Experience suggests that for pavements that fall into residential classification (22 kip SAL, 34 kip TAL) the use of a subbase to increase structural capacity may or may not be cost effective in terms of long term performance of the pavement.” Also, “With adequate subgrade preparation and appropriate considerations for surface and subgrade drainage, concrete pavements designed for city streets may be built directly on subgrades because moisture conditions are such that strong slab support may not be needed.”

Historically, material properties directly related to erosion potential of the subbase or subgrade have not been explicitly included in the analysis and design of concrete pavement even though it has long been known to be an important design consideration. The contents of this report include a model that formulates the erosion related distresses in concrete pavement under specific traffic loads and local environmental conditions. The goal of this work is to help designers assess whether the natural, compacted subgrade at a project site is adequate for long term pavement performance or if subgrade stabilization or a subbase is required to meet the design criteria. It also provides the designer with a tool to evaluate the benefit of sealing joints. The erosion potential model presented herein addresses traffic loading and frequency, drainage conditions, and the exposure condition of the sublayers to water.

2. Sublayer Design

As previously discussed, low volume concrete pavements are typically designed against faulting and cracking for the duration of the service life. While subgrade/subbase characteristics impact the fatigue life of a concrete pavement, they have a much larger impact on the potential faulting of a pavement. Sublayer erosion is also a key to understanding the process of joint faulting. Based on field performance observations, faulting is identified as a major performance issue for many higher volume jointed concrete pavements [6]. For lower volume pavements, this has not typically been the case. However, engineers need to determine whether or not the natural compacted subgrade or chemically stabilized subgrade or aggregate base is the appropriate design material underneath the concrete pavement, as well as the benefit of joint sealing. Therefore, predicting the potential for in-service faulting through modeling at the design phase is important in order to mitigate this distress in jointed concrete pavement structures. Modeling erosion potential includes most of the factors already considered for other design distresses (i.e. cracking). These factors include traffic loading and frequency of loads; the existence of water and a pathway for the water to enter the sublayers; and the material properties of the subbase (Figure 1) [2] . Therefore, this report focuses on a methodology for assessing erosion potential and the resulting joint faulting through a design process that addresses all of the key parameters shown in Figure 1.

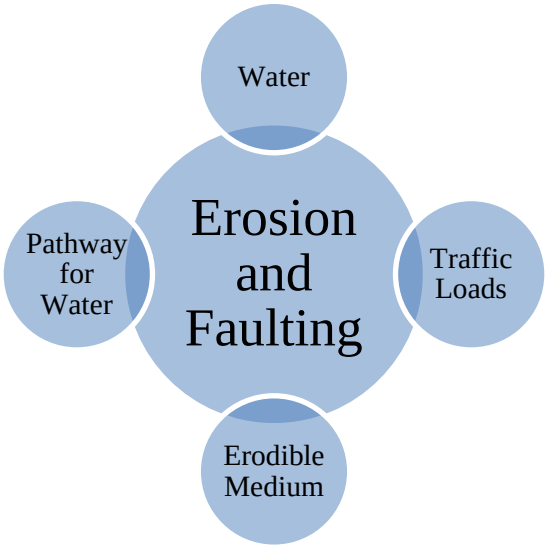

Figure 1 Main Elements Contributing in Subbase Erosion and PCC Faulting.

2.1 Traffic

Heavy axle loadings and their total number of repetitions are key components in pavement design. Applied loads are transmitted through the pavement structure to the subgrade as stresses, strains, and deflections and have a significant influence on the overall performance of the pavement. However, in the absence of heavy, repetitive loads, as is the case in light duty applications, the pavement will deflect less resulting in decreased erosion potential.

Under the same load, when the concrete slab thickness is reduced, the stress imposed by the traffic load through the pavement is distributed over a smaller area, transferring a higher stress level to the subbase/subgrade slab interface. Lower strength subgrades (i.e. lower compaction, higher moisture content, etc.) or consisting of highly plastic clays, may only sustain a limited amount of load applications. Reducing stress can be accomplished by simply building a thicker pavement section, stiffening of the joints, using stabilization, or placing a subbase.

2.2 Number of Wet Days

To give consideration to all factors that can affect the performance of the pavement, a careful climatic study in the locality of the proposed site should be made. Conditions that may cause the subgrade or subbase to become saturated over time, such as rising groundwater, surface water infiltration, and most importantly the potential for rainfall should be determined.

Soil properties may vary on a seasonal basis due to variations in the sublayer moisture levels. Trapped water directly beneath the slab greatly increases the potential for erosion. Drainage conditions and moisture flow through joints affect the potential for moisture to accumulate underneath the slab in the vicinity of the joints. One method of accounting for potential moisture accumulation below a pavement, thus providing a means to estimate erosion and faulting, is to determine the number of days when the slab subbase interface is wet. This is a function of the amount of rainfall (greater than 0.10 in), moisture infiltration through the joint and sublayers drainage. Section 3.2, provides greater detail regarding the calculation of the probability of the number of wet days used in the model for determining faulting.

One of the common methods for reducing moisture infiltration through a joint is the use of joint sealants. Sealants are used to fill the joint reservoir to prevent the intrusion of water and foreign incompressible materials and not to bond the two substrates together. The sealant strength characteristics are also important as is the ability to sustain the joint movement and maintain complete adhesion with the concrete substrate under different environmental conditions. Most concrete pavement joint sealants come in two categories, a low-modulus silicone or an asphaltic (hot pour) sealant. In general, the silicone sealants will withstand greater elongations at colder temperatures than asphaltic sealants. However, a successful installation of silicone sealant depends on having an extremely clean joint while asphaltic sealants may be more forgiving. In all cases, the manufacturer's recommendations must be closely followed. A properly installed joint sealant is considered to keep water completely out of the joint.

The design engineer will need to determine the necessity of joint sealants on a project-by-project basis. In certain climates or soil conditions, joint sealants may not be necessary. Many projects have performed adequately without sealants. The model contained in this report will provide the necessary information to help make that decision.

One of the key design details when using an open-graded aggregate for the subbase is to ensure the lowest elevation of the pavement section should be well drained in order for the water to exit the pavement system [7]. Proper drainage should be provided to minimize the presence of water in the pavement structure.

2.3 Erosion Resistance

Erosion resistance (i.e. the shear strength of the supporting layer) is a major factor to consider in the design of the supporting medium. Various subbase/subgrade materials have different resistance against erosion which is primarily a function of its shear strength. Erosion potential of soils can vary based on soil characterization, cohesion, moisture content and percent of material passing the #200 sieve. As is noted later in this report in Table 1, the natural soil Erosion Resistance is substantially reduced when saturated with water. A common construction practice is to chemically treat these soils with cement, lime or fly ash to modify those material properties resulting in improved erosion resistance, even when wet. The chemically treated soils are commonly used directly beneath concrete pavements under heavier traffic.

Erosion test results for subgrade soil, subbase materials and stabilized soils, varying from non-plastic pure sands to high plasticity clays, from a variety of locations across the United States are provided herein for reference. The Hamburg Wheel-Tracking Device (HWTD) was used in order to test the samples. The results presented in this report can be used for similar soils or subbase materials for a given project and may be found in section four of this report. HWTD testing may also be run on the project-specific materials to determine the precise erosion potential for a given soil. A proposed HWTD test method may be found in references from the reference list (Jung et al. 2010 or Jung and Zollinger, 2011).

Having proper tools for the design engineer is important in order to optimize the design of the pavement structure. This is one of the advantages of using models that include the effect of traffic as well as moisture and erosion potential. If the available tools are utilized to design and select the materials, the pavement will perform adequately while optimizing the cost of the project.

3. Erosion Model

The prediction of erosion explained herein is shown to be a function of the number of load repetitions to failure, number of wet days, and the erosion resistance of the subgrade/subbase. In the following sections, the model is explained in a step-by-step method for background information.

3.1 General Form of the Model

The erosion model follows a Gumbel cumulative probability function that is suitable for survival-failure analysis as it pertains to erosion damage due to traffic loading and moisture condition.

$$\%\boldsymbol{E} = \frac{\boldsymbol{f_i}}{\boldsymbol{f_0}} = \boldsymbol{e}^{-(\frac{\boldsymbol{\rho}}{\boldsymbol{D_i}-\Delta})^{\boldsymbol{\alpha}}} \qquad (\mathbf{1})$$

$$D_i = \boldsymbol{\Sigma}\frac{\boldsymbol{N_i}}{\boldsymbol{N_f}} \qquad (\mathbf{2})$$

where

%E	= Percent of erosion
f_i	= Level of faulting per load cycle i
f_0	= Ultimate faulting
D_i	= Damage ratio per load cycle i ($D_i = N_i/N_f$)
Δ	= Erosion initiation shift factor
α	= Erosion rate factor
ρ	= Erosion shape factor
N_i	= Effective Equivalent Single Axle Load per load cycle i, ($ESAL_i$)
N_f	= Ultimate loads to failure

The model calculates the percent erosion (%E) based on the ratio between the predicted faulting per load cycle to the ultimate amount of faulting which is determined from the erosion factors determined from the HWTD and explained in the paragraph below. Key factors in the model are determined from calibration analysis of testing on both low and high strength materials using the Hamburg device or from selected erosion inputs made by the design engineer. A common threshold for faulting is ¼" as most agencies try to repair the pavement at that point.

There are three factors associated with the erosion model illustrated in Figure 2 that are calibrated from test data inputted by the designer; Δ, α, and ρ. The erosion shift factor (Δ) is the delay period of time that the slab interface is protected from erosion damage due to non-separation between the slab and the supporting medium even though it has been exposed to traffic and climatic loading. This period may vary for different pavement structures, loading conditions, and climates. The erosion rate factor (α) and the erosion shape factor (ρ) are also calibrated that affect the rate of the damage. Figure 2 demonstrates how changing the value of α or ρ affects the distribution.

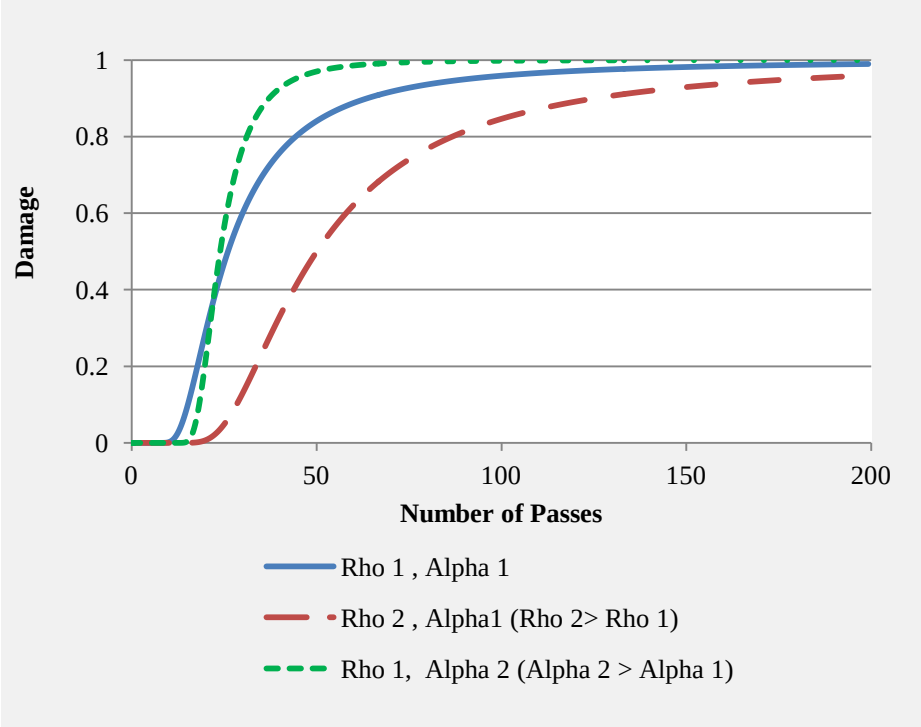

Figure 2 Sample Gumbel S-Shaped Distribution.

These factors are determined as part of the calibration process for different subgrade or subbase materials using data from the Hamburg testing. Another useful parameter derived from Hamburg testing is the erosion resistance (ER) of the material. The pavement designer can use this factor to differentiate one material from another with respect to its erodibility or even use it as an abbreviated input for calibration purposes. The factor applies to either the subgrade or the subbase and is a rate term defined as the amount of deflection at 1,000,000 load applications from the HWTD erosion test [3].

As was previously mentioned, erodibility, traffic loading, and existence of water underneath the slab are three main factors leading to erosion. As part of determining the damage ratio, D_i, is the determination of an equivalent traffic level (i.e. an erosion-based ESAL) and the allowable loads to failure N_f (i.e. $D_{i\,=}\ N_i/N_f$).

3.2 Calculation for Effective ESALs, N_i

The design ESAL is adjusted for the expected pavement drainage conditions. This is accomplished through consideration of the joint sealant condition, drainage characteristics, and the probability of rainfall:

$$\boldsymbol{N_i = ESAL_i * P}\ (\%) \qquad (3)$$

$$\boldsymbol{P}(\%) = \boldsymbol{f}(\boldsymbol{P_r}, \boldsymbol{P_{ss}}, \boldsymbol{P_{js}}) \qquad (4)$$

P (%) = Probability of wet days
P_r = Probability of rain (Number of storm days/365)

P_{js} = Probability of infiltration through the joint seal
P_{ss} = Probability of subsurface infiltration

As noted above, the design traffic is moderated by three different factors. The use of these factors basically delineates the portion of traffic distribution to that which is applied to the pavement when moisture exists underneath the pavement. Probability of rain, P_r, is simply a climatic factor defined as the number of days with rainfall greater than 2.5mm (0.1 in) [3].

Another important aspect of this model is the consideration of sealant quality, P_{js}. The sealant quality affects the infiltration of moisture into the slab/subbase interface and it is assumed that sealants installed correctly keep water out of the joint. Sealants should decrease the number of wet days in order to be an effective component of the design process. P_{ss} is the drainage factor and considers the effectiveness of the drainage system in terms of conducting the surface water out of the pavement through the interconnected voids (i.e. permeability) of the sublayers.

3.3 Ultimate Load and Shear Strength

As was mentioned, the damage ratio is the ratio between the design traffic (effective ESALs) and the allowable traffic level ($D_i = N_i/N_f$).

$$N_f = \mathbf{10}^{k_1 + k_2 r_i} \qquad (\mathbf{5})$$

$$r_i = \frac{\tau_i}{f_\tau} \qquad (\mathbf{6})$$

Where:
N_f = Ultimate loads to failure
k_i = Erosion fatigue damage calibration coefficients
τ_i = Interfacial Shear Stress between the concrete and supporting layer (FL^{-2})
f_τ = Shear Strength of the supporting layer (FL^{-2})

The erosive resistance of the slab/sublayer interface can be broken down into two segments; one relating to interfacial adhesive bond (as may be represented by the cohesive strength of the sublayer material) and the other related to interfacial sliding resistance. In this regard, two basic premises are stated:

1. The adhesive bond strength across the slab/sublayer interface can be defined by the cohesive shear strength of the sublayer (f_c) which can be determined from laboratory tri-axial testing (Figure 3); and
2. The coefficient of sliding friction (f_F) can be defined by the tangent of the φ angle also determined from tri-axial laboratory testing data (Figure 3).

Characterization of the interfacial adhesive bond between the slab and the sublayer in this manner is considered to be a manifestation of the shear capacity of the sublayer. Under field conditions, once the adhesive shear strength of the interface has been exceeded (due to lift-off), the sliding frictional resistance is in force and represented by the angle of friction (tan φ). It has

often been observed that the failure plane in a friction sliding test rarely occurs at the interface of the two materials used in the test but occurs in the layer having the lowest shear strength which has cast doubt on the validity of such test results.

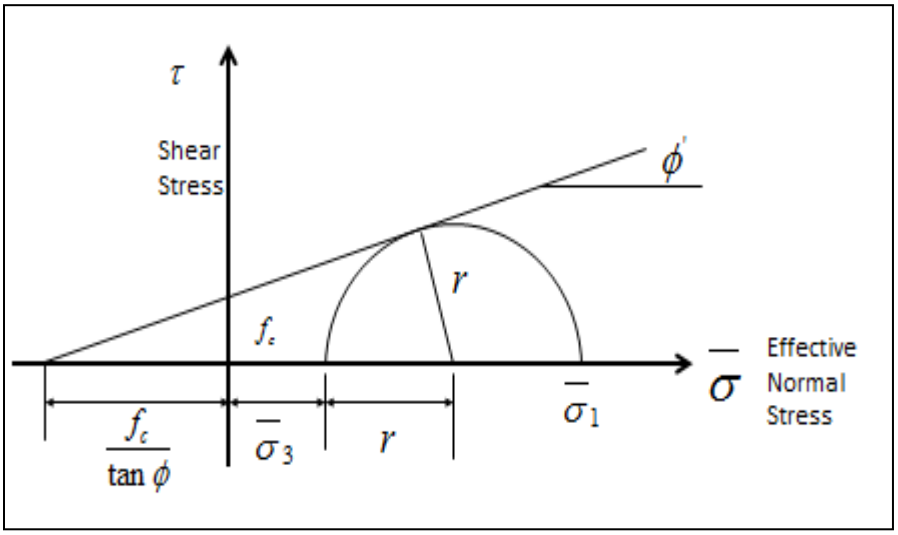

Figure 3 Shear Strength and Angle of Friction Determinations.

4. Required Test Data

This section defines the test data needed in order to represent key material characteristics required for the design process. The required parameters are listed below and discussed in further detail in subsequent sections:

- Sublayer gradation, Atterberg limits, and classification;
- Sublayer K value;
- Sublayer erosion potential; and
- Sublayers shear strength parameters (cohesion and angle of friction).

4.1 Basic Sublayer Tests

Samples of the sublayer should be obtained and basic properties such as liquid and plastic limits, moisture-density relationships, and grading should be determined. Sieve analyses on samples to provide grading curves can be performed according to ASTM D6913. Atterberg limits (liquid limit, plastic limit, and the plasticity index) for fine-grained materials can be determined using ASTM D4318. Materials should also be classified according to the unified soil classification system (ASTM D2487) [8] [9] [10].

4.2 Sublayer Support Tests

Sublayer materials are also characterized by their resistance to deformation under load, which can be either a measure of their strength (the stress needed to break or rupture a material) or stiffness (the relationship between stress and strain in the elastic range). The more resistant to deformation a sublayer is the more load stress it can support before reaching a critical deformation value. Therefore, the strength property of a soil can also be useful to determine and may be accomplished by performing tri-axial shear test (Figure 4).

There are also some other parameters such as the modulus of subgrade reaction k, California Bearing Ratio (CBR), resistance value R, or soil support value (SSV) that can be used to define sublayer strength. Modulus of subgrade reaction and CBR are briefly explained in Appendices A and B.

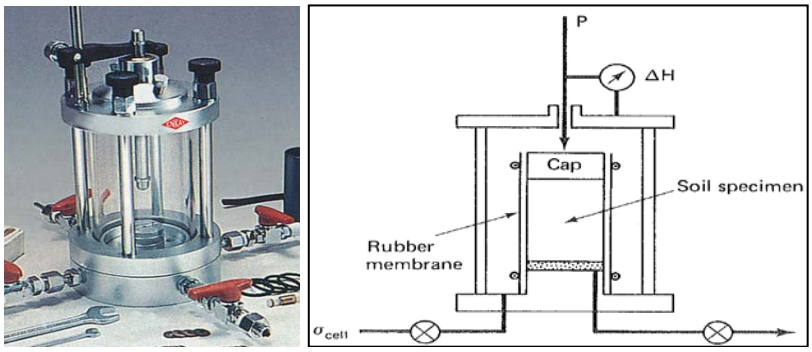

Figure 4 Tri-axial Test Apparatus.

4.3 Erosion Test

Even though erosion resistance is one of the key elements in achieving long-term pavement performance, material properties directly related to erosion resistance of a soil or subbase have not been explicitly included in the analysis and design of concrete pavements. Many erosion-related tests have been developed since the late 1970s using various testing devices, but few of those tests have provided a basis for a mechanistic design. Most of these laboratory tests involve the application of loads on the material and then defining erosion in terms of weight loss [11]. Jung and Zollinger presented a new lab test method to simulate erosion in the field that considers the mechanism of slab movements under traffic loads [3, 12]. This new laboratory test protocol involves measuring the erodibility of sublayer materials using the Hamburg Wheel-Tracking Device (HWTD) [3] [13]. The test consists of two component layers, one being a concrete cap with a joint and the other a soil or subbase material placed immediately under a concrete cap. The HWTD test device and erosion assessment procedure is further summarized in Appendix C.

An extended test program was recently performed on various soil types including sands, silts, and clays with different plasticity indices. Table 1 shows the summary of the erosion test results that can be used as an input for the erosion design procedure. Lab test data consists of the deflection of the passing wheel load and the number of load passes. Erodibility (ER) is the deflection as measured in millimeters (mm) at a million load applications. A higher ER indicates a higher rate of erosion and a lower resistance against erosion. For more detailed information on the results of this study refer to Test Methods & Results of Erosion Potential of Commonly Used Subgrade and Base Materials [14].

Table 1 Erodibility Values For Different Soil Categories.

No	Category	Group Symbol	PI	ER Wet (mm/10^6 loads)	ER Dry (mm/10^6 loads)
1	Poorly Graded Sand	SP	NP	4,500	90
2	Poorly Graded Sand with Silt	SP-SM	NP	2,400	20
3	Silty Sand	SM	2.09%	1,600	95
4	Sandy Silt	SM	9.91%	1,600	130
5	Sandy Lean Clay	s(CL)	13.36%	3,000	110
6	Sandy Lean Clay with Gravel	s(CL)g	17.34%	3,100	130
7	Lean Clay with Sand	CL	19.17%	900	60
8	Fat Clay with Sand	CH	39.96%	840	60

4.4 Shear Test on Subgrade

As previously discussed, shear parameters play a key role in the modeling of erosion behavior. Mohr-Coulomb shear failure criterion is used (Figure 3) to characterize the shear strength of the subbase/subgrade material. Shear parameters can be determined from the analysis of tri-axial testing data to determine the cohesion and friction angle of the material. Another way to determine these values is to estimate them using the gradation and plastic characteristics of the material. Table 2 shows the estimated values for cohesion and friction angle for the samples tested within this project. Appendix D includes estimation of shear strength parameters for all soil types.

Table 2 Estimated Values for Cohesion and Friction Angle for The Tested Samples [15, 16].

No	Group Symbol	Category	% of Fines	% of Sand	% of Gravel	PI	Friction Angle	Cohesion (psi)
1	SP	Poorly Graded Sand	1.8%	97.6%	0.6%	NP	37	0.00
2	SP-SM	Poorly Graded Sand with Silt	7.7%	91.8%	0.5%	NP	35	0.00
3	SM	Silty Sand	26.9%	69.3%	3.8%	2.09%	34	7.29
4	SM	Sandy Silt	32.7%	63.7%	3.6%	9.91%	34	7.29
5	s(CL)	Sandy Lean Clay	66.3%	30.7%	3.0%	13.36%	31	10.76
6	s(CL)g	Sandy Lean Clay with Gravel	62.3%	22.6%	15.1%	17.34%	31	10.76
7	CL	Lean Clay with Sand	79.3%	20.7%	0.0%	19.17%	28	12.50
8	CH	Fat Clay with Sand	81.7%	18.3%	0.0%	39.96%	19	14.93

5. Design Computer Program

5.1 ME Rigid Pavement Design

A computer program was developed using the model described herein to predict erosion and faulting performance. The program also considers other key distress types that occur in concrete pavement systems. The program allows for the design of Jointed Plain Concrete Pavements (JPCP) with and without dowels. For light duty pavements, JPCP is the appropriate pavement type and will be the focus of the below documentation. One of the main advantages of this program is that it can be calibrated with local data, if available.

5.2 Sensitivity Analysis (Light Duty)

A sensitivity analysis for both a light duty and heavy duty case has been performed on the model to validate the sensitivity of the inputs and demonstrate how precise the program accounts for various conditions in pavement design.

For the light duty case (e.g. passenger car parking lot), the base pavement structure for this analysis is a five inch concrete slab paved on compacted subgrade (sandy clay), jointed at 10 ft square intervals. The subgrade has a k-value of 100 psi/in. The Average Annual Daily Truck Traffic (ADTT) was set equal to 2 with annual growth rate of 2%. In this case, the ACI traffic category is considered A, which means the large majority of the traffic is passenger cars, with 2 trucks per day with axle weights corresponding to the corresponding axle load spectra (single axles ranging from 4 to 16 kips, and dual tandem axles ranging from 4 to 32 kips). The effective number of wet days is 50 days in a year (# of days in which the subgrade is wet). The erosion model was calibrated based on pavement sections located in Texas. Table 3 shows the main input parameters for the base analysis.

Table 3 Input Parameters for the Light Duty Base Analysis.

Pavement Type	JPCP
Analysis Period	20 Years
Slab Thickness	5"
Traffic Category (ACI 330)	A
ADTT	2
Joint Spacing	10'
Dowel Bar	No
Base Layer	No
Subgrade K-value	100 pci
Wet Days	50
Subgrade Erodibility	900
Calibration Data	Texas

When utilizing this model for evaluating a pavement design, a maximum allowable faulting threshold is established after a certain time period has passed. A typical value used by most agencies is 0.25 inches of faulting before maintenance is required. For the base case used in this sensitivity analysis, it resulted in 0.17 inches of faulting after 20 years which means the design is adequate.

Four cases were analyzed and compared to the base analysis. In each of these four cases only one variable has been changed and the rest of input values remained the same. Table 4 shows the sensitivity variables used for the study.

Table 4 Changed Parameters for Each of the Five Case Studies.

Case Number	Studied Input Parameter	Changed Value
Case 1	Traffic ADTT	0.1, 2, 4, 10
Case 2	Effective Wet Days	25, 50, 75, 100
Case 3	Stabilized Subgrade & Traffic ADTT	No & Yes Stabilization, 2 & 10 ADTT
Case 4	Slab Thickness	5, 5.5, 6 (ADTT 10)

Figure 5 compares the base analyzed structure with respect to ADTT traffic where the truck counts per day range from essentially zero (passenger cars only) up to 10. Figure 5 indicates that under these conditions, the maximum ADTT the pavement can withstand is 4 before the pavement thickness needs to increase, or an aggregate base or stabilized subgrade should be considered.

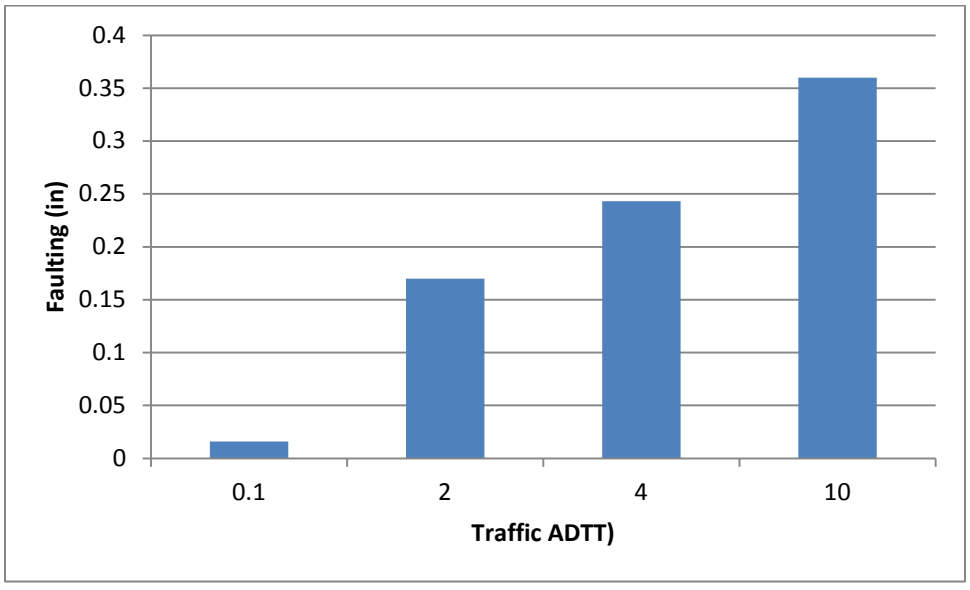

Figure 5 Light Duty Sensitivity Results on ADTT Traffic.

Figure 6 compares the base analyzed structure with respect to the number of effective wet days per year while the remaining conditions remain the same. The number of wet days is a function of the number of rain days per year (>0.1 in) as well as the joint sealant condition, and drainage. Figure 6 indicates that under these conditions, the pavement design is adequate since faulting remains under 0.25 inches.

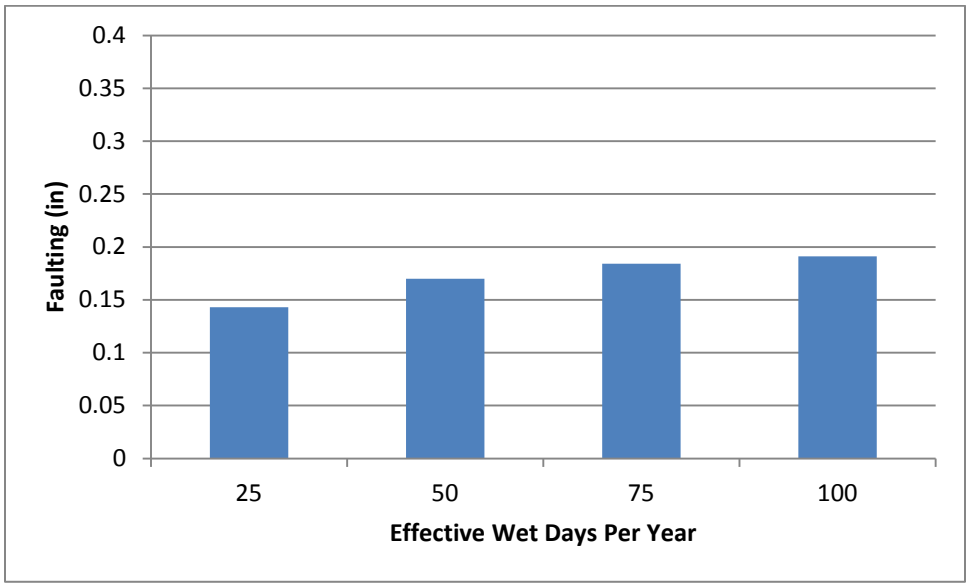

Figure 6 Light Duty Sensitivity Results on Number of Effective Wet Days Per Year.

Figure 7 compares the base analyzed structure with respect to using a stabilized subgrade (Lime, cement, or fly ash with an unconfined compressive strength of 150 psi) under two different ADTT levels. Figure 7 indicates that under these conditions, when stabilizing the subgrade, the faulting decreases to negligible levels even under increased traffic levels. While using this strategy was unnecessary with only 2 ADTT, stabilization would be necessary at 10 ADTT.

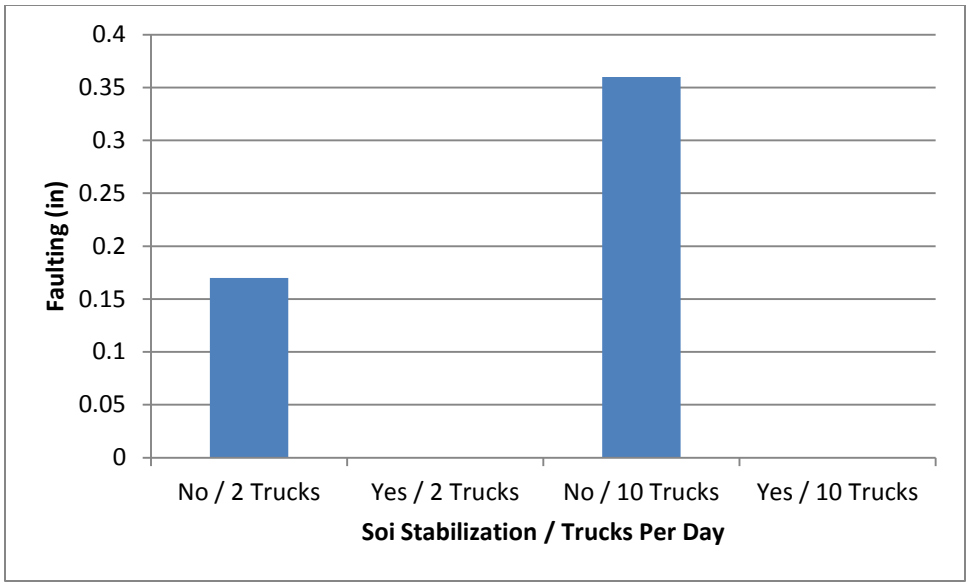

Figure 7 Light Duty Sensitivity Results on Soil Stabilization and ADTT.

Figure 8 compares the base analyzed structure with respect to concrete pavement thickness. This case was run using 10 ADTT rather than 2 (as was used as the base case previously). Figure 8 indicates that under these conditions, a 5.5 inch concrete pavement would be necessary to minimize faulting to an acceptable level.

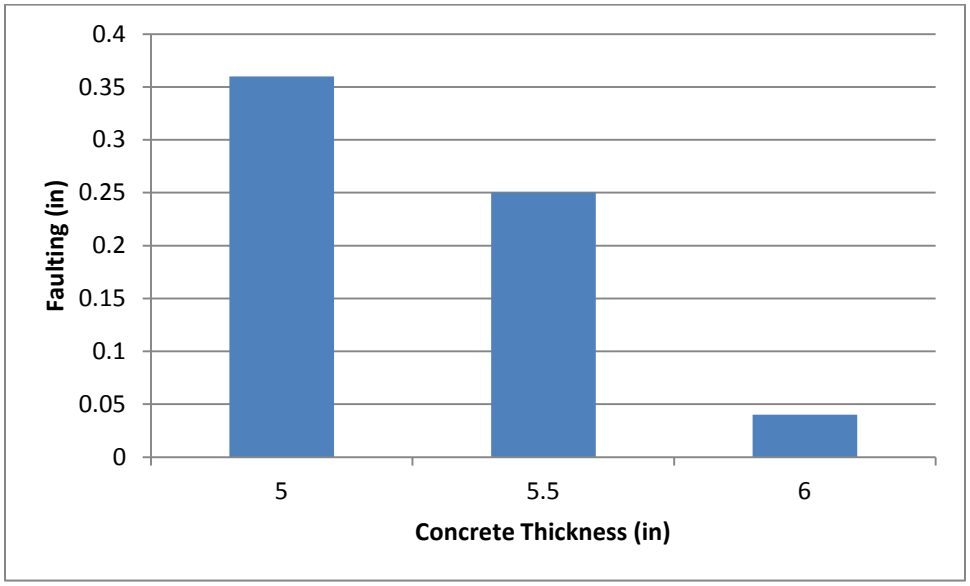

Figure 8 Light Duty Sensitivity Results on Concrete Pavement Thickness.

5.3 Sensitivity Analysis (Heavy Duty)

For the heavy duty case (e.g. distribution center), the base pavement structure for this analysis is a five inch concrete slab paved on compacted subgrade (sandy clay), jointed at 10 ft square intervals. The subgrade has a k-value of 100 psi/in. The Average Annual Daily Truck Traffic (ADTT) was set equal to 300 with annual growth rate of 2%. In this case, the ACI traffic category is considered C, which is large tractor trailers with axle weights corresponding to the corresponding axle load spectra (single axles ranging from 8 to 26 kips, and dual tandem axles ranging from 8 to 44 kips). The effective number of wet days is 50 days in a year (# of days in which the subgrade is wet). The erosion model was calibrated based on pavement sections located in Texas. Table 5 shows the main input parameters for the base analysis.

Table 5 Input Parameters for the Heavy Duty Base Analysis.

Pavement Type	JPCP
Analysis Period	20 Years
Slab Thickness	6.5"
Traffic Category (ACI 330)	C
ADTT	300
Joint Spacing	13'
Dowel Bar	No
Base Layer	No
Subgrade K value	100 pci
Wet Days	50
Subgrade Erodibility	900
Calibration Data	Texas

When utilizing this model for evaluating a pavement design, a maximum allowable faulting threshold is established after a certain time period has passed. A typical value used by most agencies is 0.25 inches of faulting before maintenance is required. For the base case used in this sensitivity analysis, it resulted in 0.20 inches of faulting after 20 years which means the design is adequate.

Four cases were analyzed and compared to the base analysis. In each of these four cases only one variable has been changed and the rest of input values remained the same. Table 6 shows the sensitivity variables used for the study.

Table 6 Changed Parameters for Each of the Five Case Studies.

Case Number	Studied Input Parameter	Changed Value
Case 1	Traffic ADTT	100, 300, 700
Case 2	Effective Wet Days	25, 50, 100
Case 3	Sub layer Type	Subgrade, Stabilized Subgrade, 4" Aggregate Base
Case 4	Slab Thickness	6, 6.5, 7 (ADTT 300)

Figure 9 compares the base analyzed structure with respect to ADTT traffic where the truck counts per day range from 100 to 700. Figure 9 indicates that under these conditions, the maximum ADTT the pavement can withstand is somewhere between 300 and 700 before the pavement thickness needs to increase, or an aggregate base or stabilized subgrade should be considered.

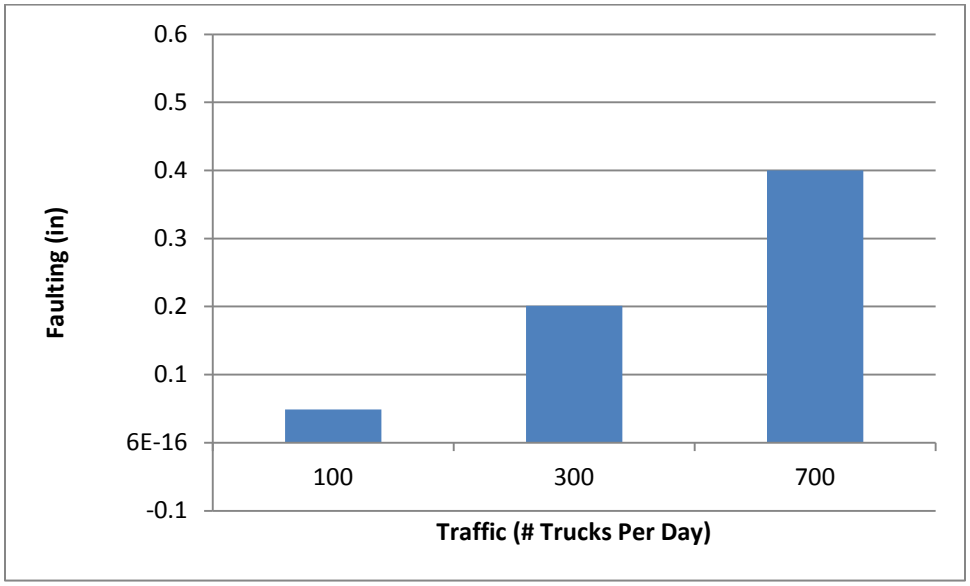

Figure 9 Heavy Duty Sensitivity Results on ADTT Traffic.

Figure 10 compares the base analyzed structure with respect to the number of effective wet days per year while the remaining conditions remain the same. The number of wet days is a function of the number of rain days per year (>0.1 in) as well as the joint sealant condition, and drainage. Figure 10 indicates that under these conditions, when the number of effective wet days reaches 100, the pavement design may need to be re-evaluated since the faulting threshold value has been reached.

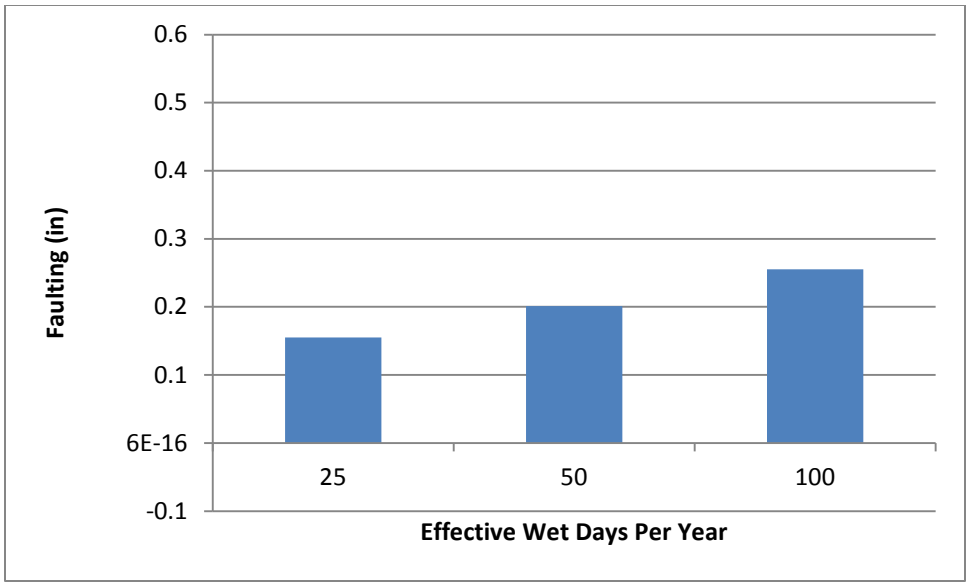

Figure 10 Heavy Duty Sensitivity Results on Number of Effective Wet Days Per Year.

Figure 11 compares the base analyzed structure with respect to using a natural subgrade, stabilized subgrade (lime, cement, or fly ash with an unconfined compressive strength of 150 psi), or a 4 inch thick aggregate base as the supporting layer underneath the 6.5 inch thick concrete pavement with 300 ADTT. Figure 10 indicates that under these conditions, when stabilizing the subgrade, or using a 4 inch thick aggregate base, the faulting decreases to negligible levels even though they may not be necessary since the faulting threshold value was not reached when using a natural subgrade.

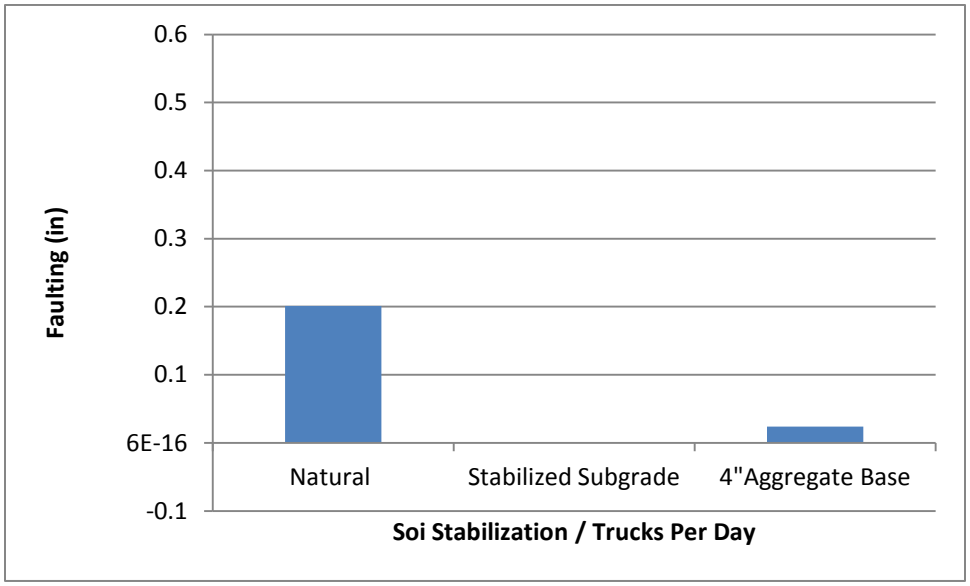

Figure 11 Heavy Duty Sensitivity Results on Soil Stabilization and ADTT.

Figure 12 compares the base analyzed structure with respect to concrete pavement thickness when the ADTT is 300 and the support layer is natural subgrade. Figure 12 indicates that under

these conditions, reducing the pavement thickness to 6 inches would drastically increase the faulting, while increasing the thickness to 7 inches would reduce faulting to negligible levels. The 6.5 inch thickness appears to be optimally designed.

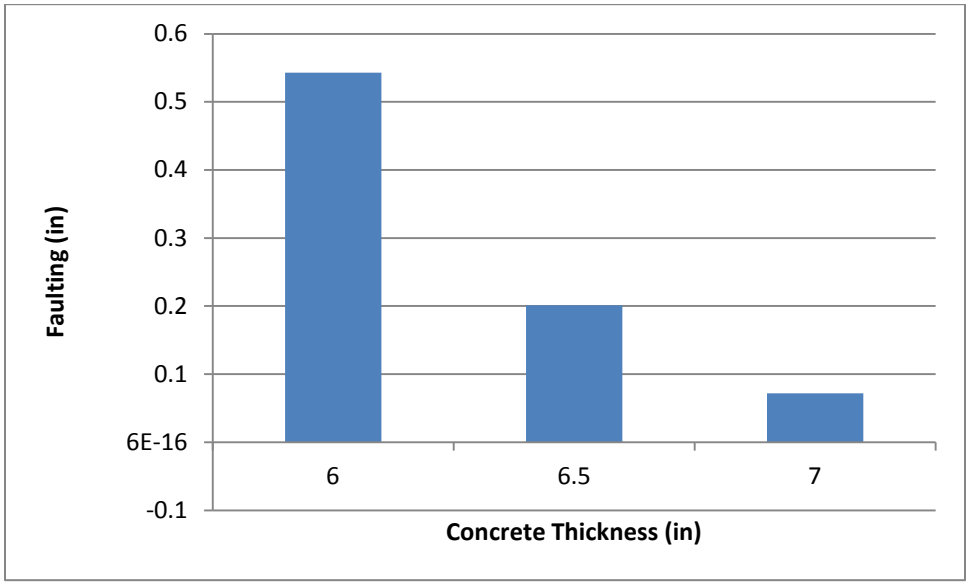

Figure 12 Heavy Duty Sensitivity Results on Concrete Pavement Thickness.

References

1. ACPA, *Subgrades and Subbases for Concrete Pavements*, 2007, American Concrete Pavement Association.
2. Neshvadian Bakhsh, K., D.G. Zollinger, and Y.-S. Jung. *Evaluation of Joint Sealant Effectiveness on Moisture Infiltration and Erosion Potential in Concrete Pavement*. in *Transportation Research Board 92nd Annual Meeting*. 2013.
3. Jung, Y.S. and D.G. Zollinger, *New Laboratory-Based Mechanistic-Empirical Model for Faulting in Jointed Concrete Pavement.* Transportation Research Record: Journal of the Transportation Research Board, 2011. **2226**(-1): p. 60-70.
4. K. T. Hall, J.A.C., T. E. Hoerner, K. D. Smith, A. M. Ioannides, and J. Armaghani, *Effectiveness of Sealing Transverse Contraction Joints in Concrete Pavements – Final Report*, 2008, U.S. Department of Transportation ,Federal Highway Administration.
5. ACI, *ACI 325, Guide for Design of Jointed Concrete Pavements for Streets and Local Roads*, 2002, American Concrete Institute.
6. Selezneva, O., J. Jiang, and S.D. Tayabji, *Preliminary Evaluation And Analysis Of LTPP Faulting Data-Final Report*, 2000.
7. ACI, *Guide for Design of Jointed Concrete Pavements for Streets and Local Roads*, in *ACI 325-12R-02*2002, American Concrete Institute: Farmington Hills, Michigan, USA.
8. *ASTM D6913 – 04* in *Standard Test Methods for Particle-Size Distribution (Gradation) of Soils Using Sieve Analysis*2009, American society for testing and materials.
9. *ASTM D4318 – 10*, in *Standard Test Methods for Liquid Limit, Plastic Limit, and Plasticity Index of Soils*2010, American Society for Testing and Materials.
10. *ASTM D2487 – 11*, in *Standard Practice for Classification of Soils for Engineering Purposes (Unified Soil Classification System)*2011, American Society for Testing and Materials.
11. Jung, Y.S., D.G. Zollinger, and A.J. Wimsatt, *Test Method and Model Development of Subbase Erosion for Concrete Pavement Design.* Transportation Research Record: Journal of the Transportation Research Board, 2010. **2154**(-1): p. 22-31.
12. Zollinger, D.G., et al., *Subbase and Subgrade Performance Investigation and Design Guidelines for Concrete Pavement*, 2012.
13. TxDoT, *Tex-242-F*, in *HAMBURG WHEEL-TRACKING TEST*2009, Texas Department of Transportation.
14. Zollinger, D.G., K.N. Baksh, *Test Methods & Results of Erosion Potential of Commonly Used Subgrade and Base Materials*, Texas Transportation Institute, August 2014
15. Bareither, C.A., et al., *Geological and physical factors affecting the friction angle of compacted sands.* Journal of geotechnical and geoenvironmental engineering, 2008. **134**(10): p. 1476-1489.
16. Lindeburg, M.R., *Civil engineering reference manual for the PE exam*. 2012: www. ppi2pass. com.
17. Ioannides, A., M.R. Thompson, and E.J. Barenberg, *Westergaard solutions reconsidered.* Transportation research record, 1985. **1043**: p. 13-23.
18. *ASTM D1883-05*, in *Standard Test Method for CBR (California Bearing Ratio) of Laboratory-Compacted Soils*, American Society for Testing and Materials.

19. *ASTM D4429-09a*, in *Standard Test Method for CBR (California Bearing Ratio) of Soils in Place*, American Society for Testing and Materials.
20. Sahin, H., *Characterization of expansive soil for retaining wall design*, in *Master Degree Thesis*2011, Texas A&MUniversity: College Station,Texas.
21. Fredlund, D.G. and A. Xing, *Equations for the soil-water characteristic curve.* Canadian Geotechnical Journal, 1994. **31**(4): p. 521-532.
22. Sahin, H., F. Gu, and R.L. Lytton, *Development of Soil Water Characteristic Curve for Flexible Base Materials Using the Methylene Blue Test.* Transportation Research Record: Journal of the Transportation Research Board 2013. **Under Press**.

Appendix A. The Modulus of Subgrade Reaction (k)

The modulus of subgrade reaction (k) is used as a primary input for rigid pavement design. It estimates the support of the layers below a rigid pavement surface course (the PCC slab). The k-value can be determined by field tests or by correlation with other tests. There is no direct laboratory procedure for determining k-value. The modulus of subgrade reaction was introduced because work done by Westergaard developed the k-value as a spring constant to model the support beneath the slab [17].

The most applicable test for rigid pavements is the plate bearing test as described in ASTM D 1196 or AASHTO T-222. The procedure consists of incrementally loading a stiff 760 mm (30 in.) diameter plate while measuring the deflection of the plate. The results of the test are expressed as Westergaard's modulus of subgrade reaction (k-value), which is the pressure on the plate divided by its deflection. It is recognized, however, that this test is seldom performed. Back-calculating k-values using falling weight deflectometer (FWD) data on existing pavements is typically a much more cost-effective approach to get an estimate of the k-value for various local soil types and conditions. Alternatively, the ACI 330R-08 Manual provides suggested values according to the soil classification.

Appendix B. The California Bearing Ratio (CBR)

The California Bearing Ratio (CBR) test is a simple strength test that compares the bearing capacity of a material with that of a well-graded crushed stone (thus, a high quality crushed stone material should have a CBR of 100%). It was developed by the California Division of Highways around 1930 and was subsequently adopted by numerous states, counties, U.S. federal agencies and internationally. As a result, most agency and commercial geotechnical laboratories in the U.S. are equipped to perform CBR tests. The CBR test is described in ASTM Standards D1883-05 (for laboratory-prepared samples) and ASTM D4429-09 (for soils in place in field) [8] [9]. The basic CBR test involves applying load to a small penetration piston at a rate of 1.3 mm (0.05") per minute and recording the total load at penetrations ranging from 0.64 mm (0.025 in.) up to 7.62 mm (0.300 in.). Figure 13 shows a CBR test device.

Figure 13 California Bearing Ratio Test Device.

Appendix C. Hamburg Wheel-Tracking Device (HWTD) [3] [13]

HWTD testing is mainly conducted under wet conditions in which erosion occurs due to mechanical and hydraulic shearing on the base layer generated by slab movement under an applied load. The configuration of the test device is shown in Figure 14. The test configuration consists of a subbase material 25.4 mm (1 in.) thick placed on a neoprene material below a jointed concrete block 25.4 mm (1 in.) thick. The device allows for testing a laboratory-compacted specimen or a core obtained from the field. A wheel load of 71.6 kg (158 lb) is applied at a 60-rpm load frequency. Measurements consist of the depth of erosion at 11 locations versus the number of wheel load passes [11] [12].

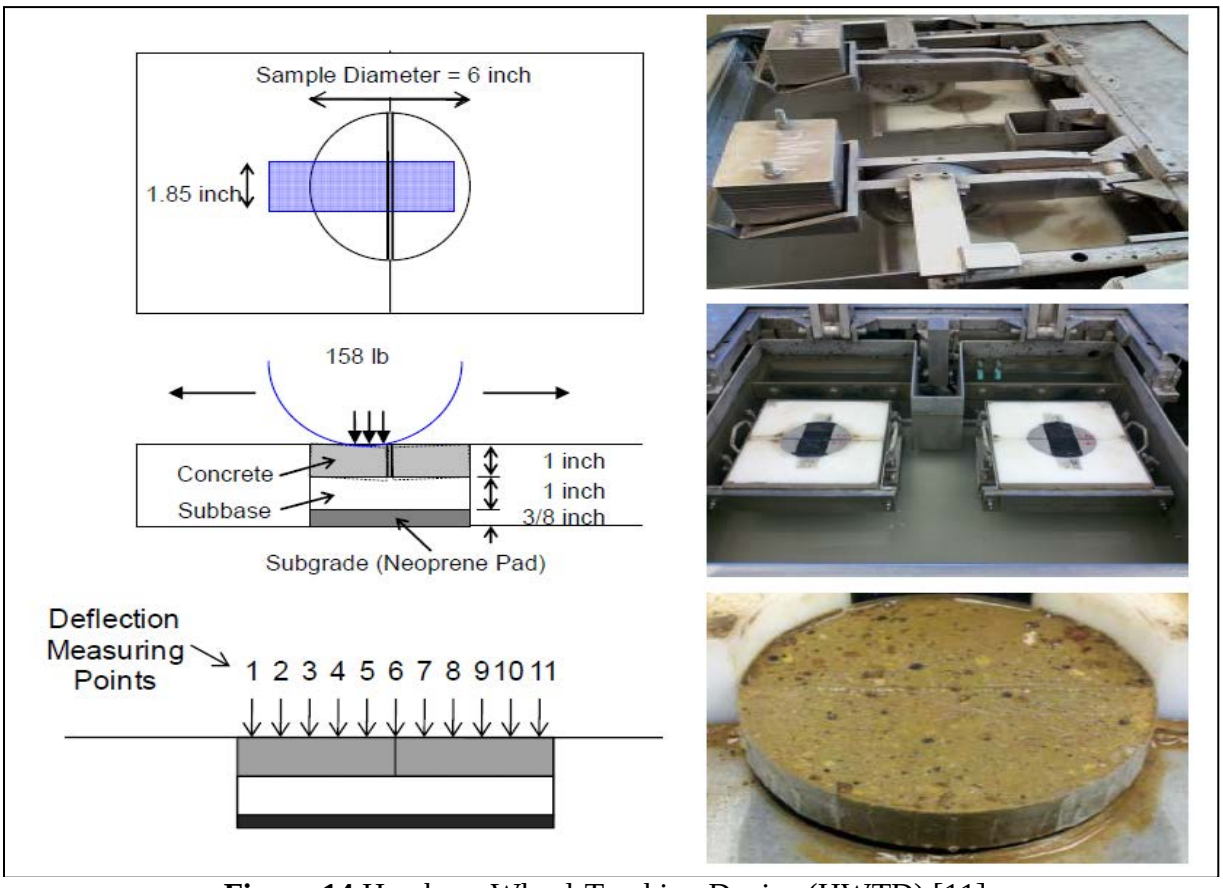

Figure 14 Hamburg Wheel-Tracking Device (HWTD) [11].

Samples are 6-inches in diameter and 1-inch thick. On top of the sample there is a concrete cap, the same size that has been split and sealed to simulate the joint. A wheel passes on the concrete cap causing deflection and erosion on the sample until the material fails.

Appendix D. Shear Strength Characteristics

Failure in soil materials can be defined by using Mohr-Coulomb shear failure theory;

$$\boldsymbol{\tau = \sigma * Tan(\varphi) + C} \qquad (7)$$

Where τ is the shear strength, σ is the normal stress. The quantity C is called the cohesion and the angle φ is called the angle of internal friction. These parameters can be achieved by performing shear tests such as "Direct shear test" or "Tri-axial shear test".

Direct shear test is relatively the easier to conduct but the major shortcoming is that the sample fails on a designated plane which may not be the weakest one (ASTM D 3080). Tri-axial Shear Test can overcome some of the serious disadvantages of the direct shear test. The tri-axial compression test is used to measure the shear strength of a soil under controlled drainage conditions. A cylindrical specimen of soil is encased and subjected to a confining fluid/air pressure and then loaded axially to failure. The test is called "tri-axial" because the three principal stresses are assumed to be known and are controlled. The major problem with this test is that it's very time-consuming and it takes a long time to achieve results especially for cohesive soils. Since many researchers have previously tested and documented the soil cohesion and friction parameters for the typical soil classifications, this testing does not need to be completed on a project-by-project basis. Table 6 shows the typical values for soil's cohesion and friction characteristics as indicated in the literature [6].

Table 6 Typical Strength Characteristic for Different Soil Categories[16].

Group Symbol	Cohesion (psi)	Friction Angle
GW	0	>38
GP	0	>37
GM	---	>34
GC	---	>31
SW	0	38
SP	0	37
SM	7.2	34
SM-SC	7.2	33
SC	13.6	31
ML	9.7	32
ML-CL	9.4	32
CL	12.5	28
OL	---	---
MH	10.4	25
CH	14.9	19
OH	---	---

Appendix E. Shear Strength Determination Using Soil Suction

As previously noted, shear strength is a key parameter in subgrade erosion performance. For cohesive soils, shear strength characteristics change with amount of moisture and the suction that exists in the soil. The relationship between shear strength and suction is discussed in this section.

E.1 Matric Suction-Confining Pressure-Shear Strength [20]

Matric suction is vacuum or negative pressure exerted by an unsaturated soil that induces water transport. The negative pressure results from the effect capillarity draw within the pore structure that makes up the 'matric' of a soil material. The relationship between matric suction, shear strength and confining pressure is shown in Figure 15. These relationships are derived from analysis of the failure envelope prescribed within a "Mohr's" circle.

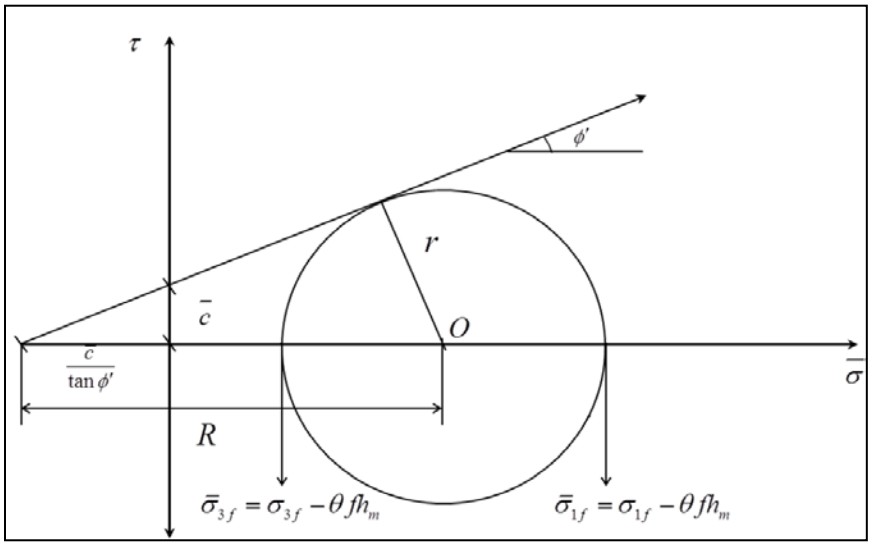

Figure 15 Mohr Failure Circle and Mohr Envelope [20].

Shear relationship with respect to suction is as follow:

$$\left(\frac{\sigma_{1f}-\sigma_{3f}}{2}\right) = \left(\frac{C*\cos\varphi}{1-\cos\varphi}\right) + \left(\frac{\sigma_{3f}-\theta*f*h_m}{1-\sin\varphi}\right) * \sin\varphi \qquad (8)$$

where :

σ_i = Normal Stresses
C = Cohesion
φ = Angle of internal friction
θ = Volumetric water content
h_m = Matric suction
f = Unsaturated shear factor

The under saturated shear factor can be calculated as:

$$f = 1 + \left(\frac{S_r - 85}{15}\right)\left(\frac{1}{\theta} - 1\right) \quad (9)$$

Therefore, in an unconfined compression test where $\sigma_3 = 0$ the equation for cohesion is:

$$C = \left(\frac{\sigma_{1f}}{2}\right)\left(\frac{1-\sin\varphi}{\cos\varphi}\right) + \theta * f * h_m * \tan\varphi \quad (10)$$

The effective friction angle, φ , can be estimated as a function of the plasticity index. The empirical expression for this purpose shown in Figure 16 is [20]:

$$\varphi = 0.0016PI^2 - 0.302PI + 36.208 \quad (11)$$

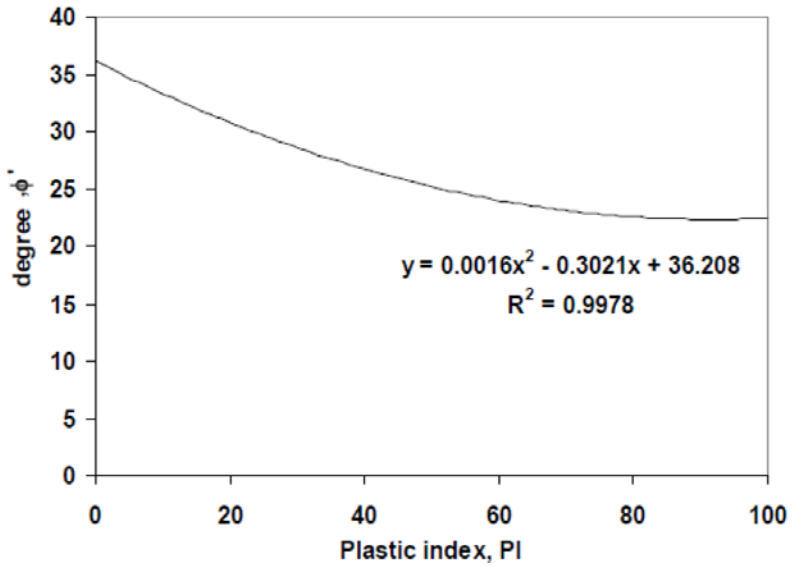

Figure 16 The Effective Friction Angle Versus Plasticity Index [20]

To illustrate the relation between matric suction, confining pressure and shear strength, a 3-D plot is generated that can be seen in Figure 17 [20].

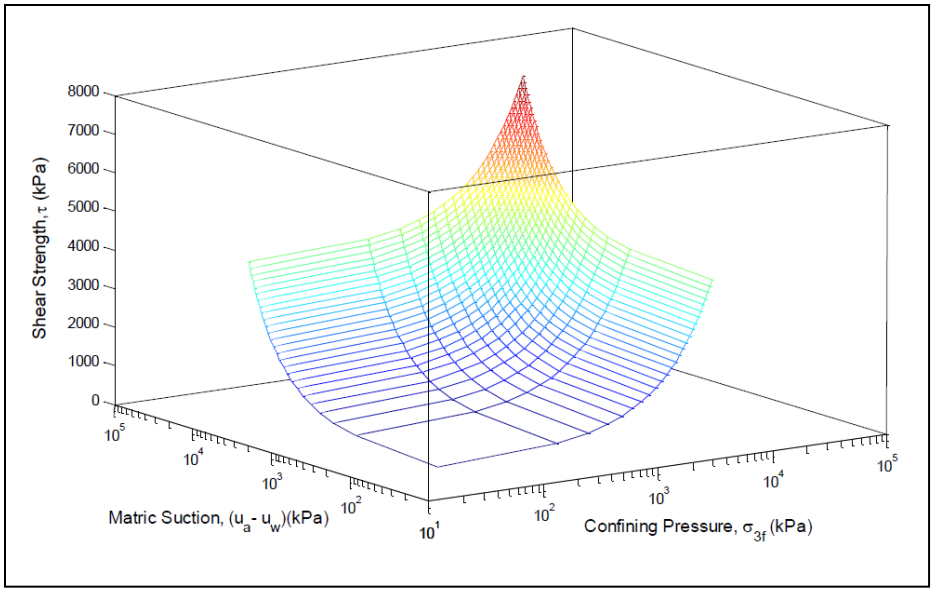

Figure 17 Three Dimensional Matric Suction, Shear Strength and Confining Pressure [20].

E.2 Soil Dielectric Characteristic Curve

Soil dielectric characteristic curve relation, denoted as SDCC, is the relation between soil dielectric value and soil suction proposed by Fredlund and Xing (1994) [21]. According to that model, the soil dielectric is a function of soil suction, maximum saturated dielectric of the soil and four parameters that are constant for each soil (Figure 18).

Since saturated dielectric of the soil can be measured easily, by having the four parameters in the Fredlund and Xing equation the SDCC curve can be plotted. Sahin found relationships between pfc value of the soil and these parameters [20]. Therefore, by knowing these parameters the SDCC curve can be plotted. That means for each known dielectric in the field, the suction value can be calculated. Figure 18 shows a sample of SDCC curve. In the model a,b, c and h_r are the four constant parameters.

$$\varepsilon_r = C(h) \times \left[\frac{d\varepsilon_{sat}}{\left[\ln\left[\exp(1) + \left(\frac{h}{a} \right)^b \right] \right]^c} \right]$$

$$C(h) = \left[1 - \frac{\ln\left(1 + \frac{h}{h_r}\right)}{\ln\left(1 + \frac{10^6}{h_r}\right)} \right]$$

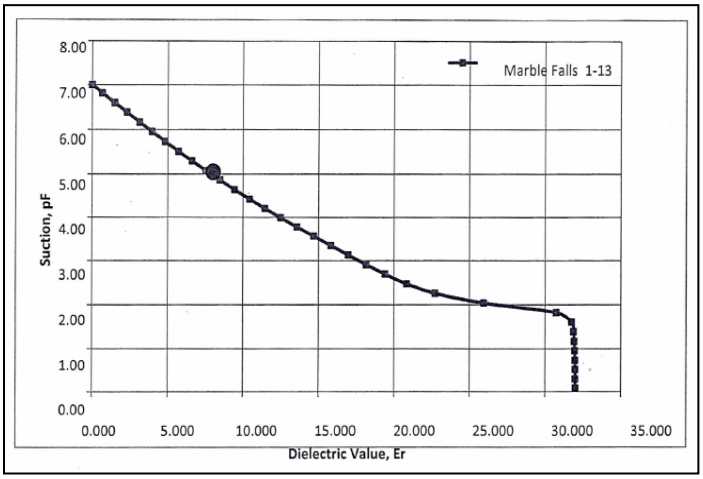

Figure 18 Soil Dielectric Characteristic Curve (SDCC) Relation [20].

E.3 Soil Water Characteristic Curve

Another relationship proposed by Fredlund and Xing (1994) relates soil moisture and soil suction that is useful to draw the Soil Water Characteristic Curve (SWCC) [1]. According to that model, the soil moisture is a function of soil suction, saturated volumetric content of the soil and four parameters that are constant for each soil (Figure 19).

$$\theta_w = C(h) \times \left[\frac{\theta_s}{\left[\ln\left[\exp(1) + \left(\frac{h}{a} \right)^b \right] \right]^c} \right]$$

$$C(h) = \left[1 - \frac{\ln\left(1 + \frac{h}{h_r} \right)}{\ln\left(1 + \frac{10^6}{h_r} \right)} \right]$$

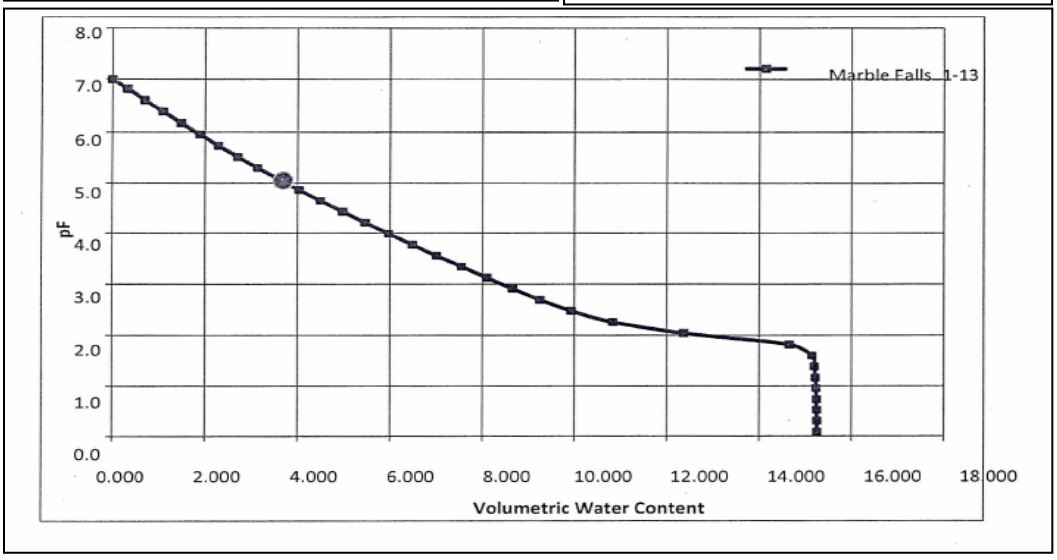

Figure 19 Soil Water Characteristic Curve (SWCC) Relation [20].

Sahin found relationships between pfc and these parameters [20]. Knowing these parameters and the saturated volumetric content of the soil the SWCC curve can be plotted. That means for each known suction value the water content can be calculated. Figure 19 shows a sample of SWCC curve. In the model a,b, c and h_r are the four constant parameters.

Therefore, dielectric value and pfc are correlated to generate soil dielectric characteristic curve. Additionally, this dielectric value is used to estimate material suction values. This suction which is an output from SDCC curve and percent fine content are employed to generate soil water characteristic curve. The output of SWCC gives instant moisture content of solid based on the suction value.

Appendix F. Determine the Soil PI Based on the Methylene Blue Test

In order to provide a means to obtain the soil PI in an expeditious manner, an alternative test procedure is explained in this section that is fast and easy to perform in the field. The direct outcome of this test is to find percent of clay in the soil, soil PI, and classification of the soil. These can help indirectly to estimate shear parameters and erodibility index.

Methylene Blue Test

The Methylene Blue Test yields a value (MBV) that provides an indication of the amount and activity of clay present in a soil sample. The Methylene Blue Test is a new, rapid method for measuring methylene blue value.

In contrast to time consuming titration tests (AASHTO T 330, EN 933), the Methylene Blue Test uses a single addition of methylene blue. In addition, the test measures the entire sand size fraction, rather than just the less than 75 micro millimeter fraction. The entire test can be complete in less than 10 minutes using a portable testing kit described below.

The test procedure involves the measurement of the amount of methylene blue dye adsorbed by a soil sample as an indication of the percent of clay fines in the sample by comparing the concentration of methylene blue in solution before and after mixing with the sample. The concentration of methylene blue solution is measured by colorimetery. A fixed dilution is used at the end of the test so that the methylene blue solution concentration is within the opening range of the colorimeter. Figure 20 illustrates the Methylene Blue Test procedure.

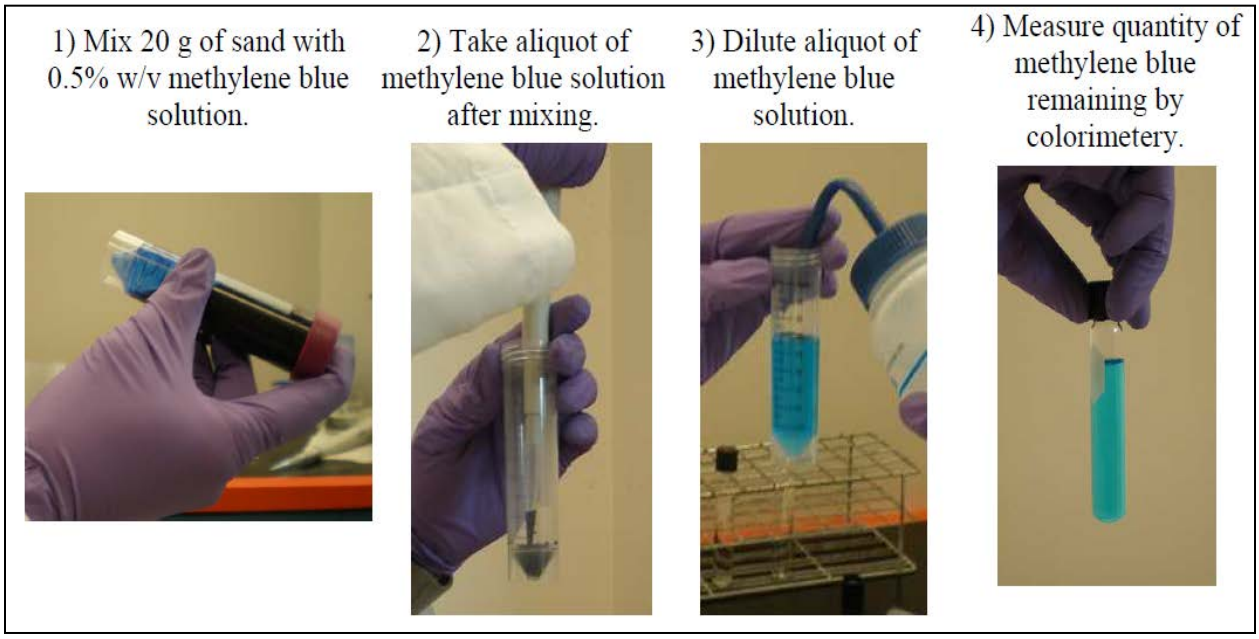

Figure 20 Methylene Blue Test Procedure [2].

Advantages of the test are listed as follows:

- Rapid (no sieving or tedious titration required);
- Portable (test equipment fits into a small toolbox as it shown in Figure 21);
- Comprehensive results (over a wide size range of aggregates);
- Simple procedure (no advanced training required); and
- Accurate and repeatable.

Test apparatus is shown in Figure 21 that includes:

1. Reader (colorimeter)
2. Micropipette
3. Portable balance
4. Test tubes
5. Syringe with filter
6. Methylene blue solution

Figure 21 Methylene Blue Test Apparatus.

Test Outcomes

The direct outcome of the MBV test is to define the percent of clay in the soil sample that can be used to get Plasticity Index (PI), Liquid Limit (LL), and cohesive strength with acceptable accuracy.

Plasticity Index

Sahin et al.[22] has performed several tests on different soils in order to define a relationship between MBV value and the plasticity index. This relation, for all of the material sample sources that were tested, is shown in Figure 22 where confidence level limits of 90 percent are given. A mathematical relation is formulated as follows [22]:

$$\boldsymbol{MBV = a.e^{0.1714(PI)}} \qquad (12)$$

The “a parameter” in the equation could differ for different soil types. The general form of the equation considers a = 1.7815 but the parameter can also be selected based on soil types that were tested in research done by Sahin to get more accurate results.

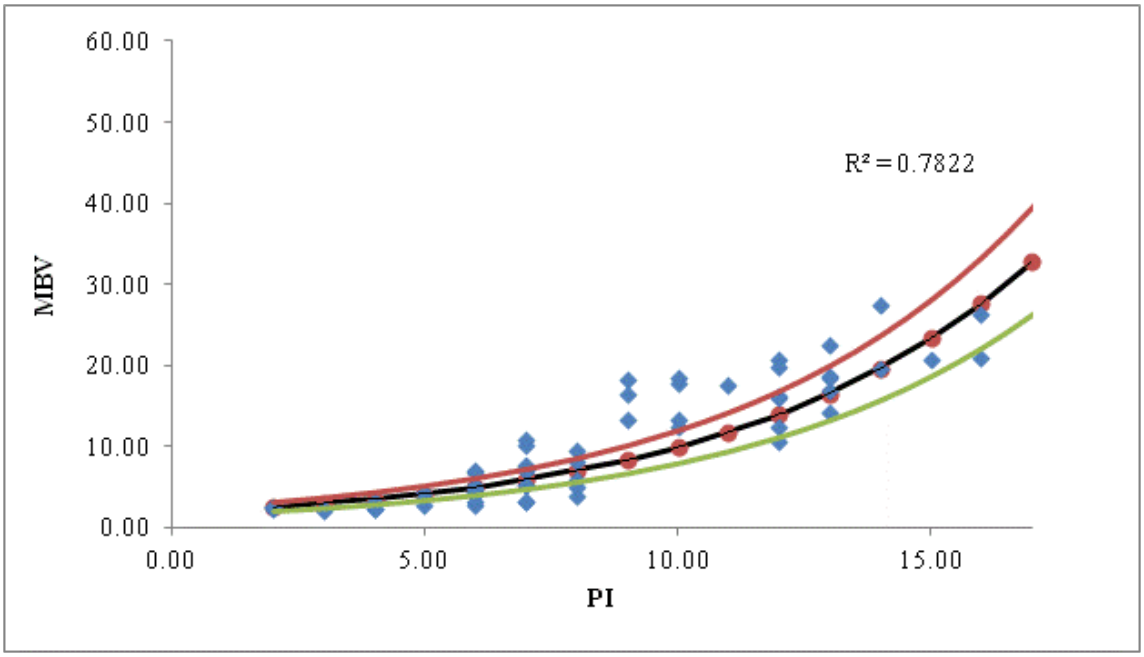

Figure 22 MBV and Plasticity Index relation with 90% Confidence Limits [2].

Percent of Clay

The extended laboratory test program by Sahin confirms a general relationship between the MBV and the percent of clay, pfc. As shown in Figure 23 this relationship presents a ‘C’ shaped curve that covers the entire methylene blue test range for soil materials.

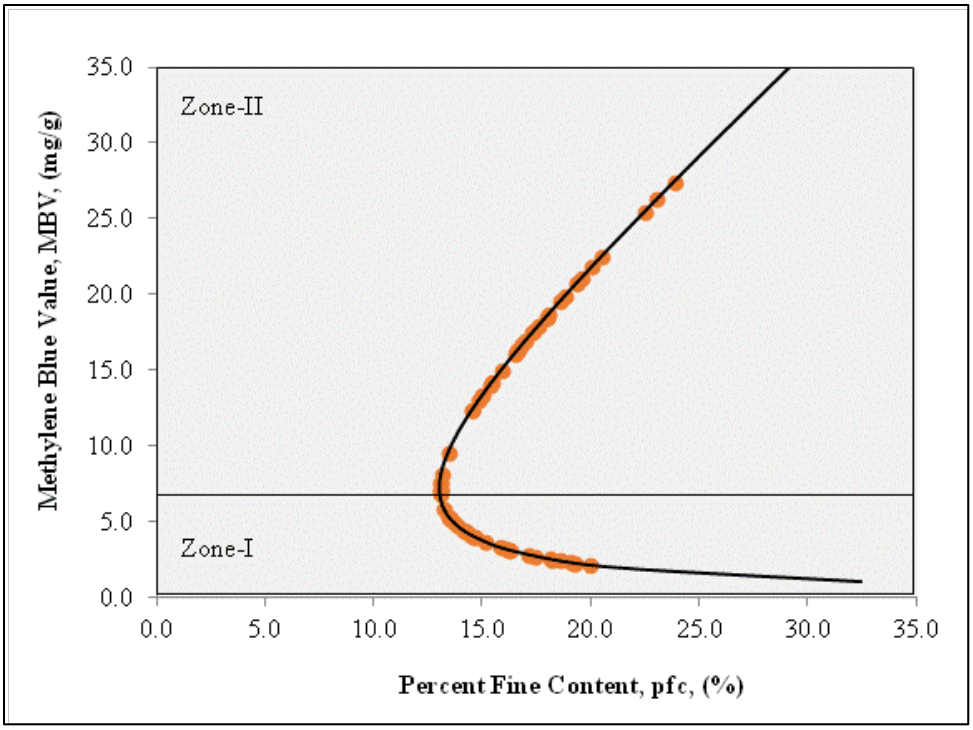

Figure 23 Relationship between MBV and Percent Fines Content (Only Clays) [22].

This curve is divided into two zones. The methylene blue value of 7.0 is considered to be the critical point. A material with MBV less than 7.0 is considered a relatively non-plastic soil suggesting from an erodibility standpoint to likely be of greater permeability respect to moisture movement perhaps yielding a lower number of wet days in the design process. If the MBV is larger than 7.0 the material has high plasticity and likely of lower permeability. For the same level of traffic, soils yielding MBV > 7 would perform at a lower level than those yielding MBV's greater than 7. A mathematical correlation model is determined between MBV and percent fines content. The model present quantitative amount of clay content as follows [22]:

$$\boldsymbol{pfc} = \frac{\mathbf{27.601}}{\boldsymbol{MBV}^{\mathbf{0.923}}} + \mathbf{1.552}\ (\boldsymbol{MBV}) \qquad (13)$$

Where MBV is the methylene blue value; pfc is the percent clay content. The coefficients are the general forms but there are tables based on soil types that help to get even more accurate values.

The percent of clay particles in the soil governs several characteristics of the soil such as cohesion, plasticity, saturation time, moisture volumetric change, etc. To be able to generate the soil dielectric characteristic curve relation, SDCC, or water characteristic curve, SWCC, the four parameters of Fredlund and Xing equation needs to be calculated (Figure 18 and Figure 19). These four parameters depend on pfc value. A relationship between the four parameters and pfc was proposed [20] and this study denoted that each parameter has a unique function based on the pfc. The pfc is employed to estimate four parameters and these four parameters are utilized to generate whole suction curves.

Suggested Test Procedure

This section suggests a fast yet promising test procedure that is helpful in order to gain needed inputs to carry out erosion design. To this end, Figure 24 shows a chart for how the required tests and equations described in this document are arranged.

The procedure consists mainly of three tests that can be performed quickly and easily especially under field conditions: the methylene blue test, the Percometer to measure the dielectric constant, and the dry gradation. Dry gradation can be performed only with two sieves that separate fines, sands and gravels (sieves number 4 and 200).

The methylene blue test result, MBV, helps to get the PI value (Equation 12) and percent of clay, pfc, according to Equation 13. These outputs along with simple dry gradation results make it possible to classify the soil according to ASTM 6913 [8]. This classification is useful to estimate the erodibility, ER according to Table 1.

The soil dielectric with percent fine that came from MB test helps to get suction and moisture content values [20] [1]. The Φ angle can be estimated having the plasticity index according to Equation 11 (with the PI previously determined from MB test). Finally, cohesion of the soil can be calculated according to Equation 10.

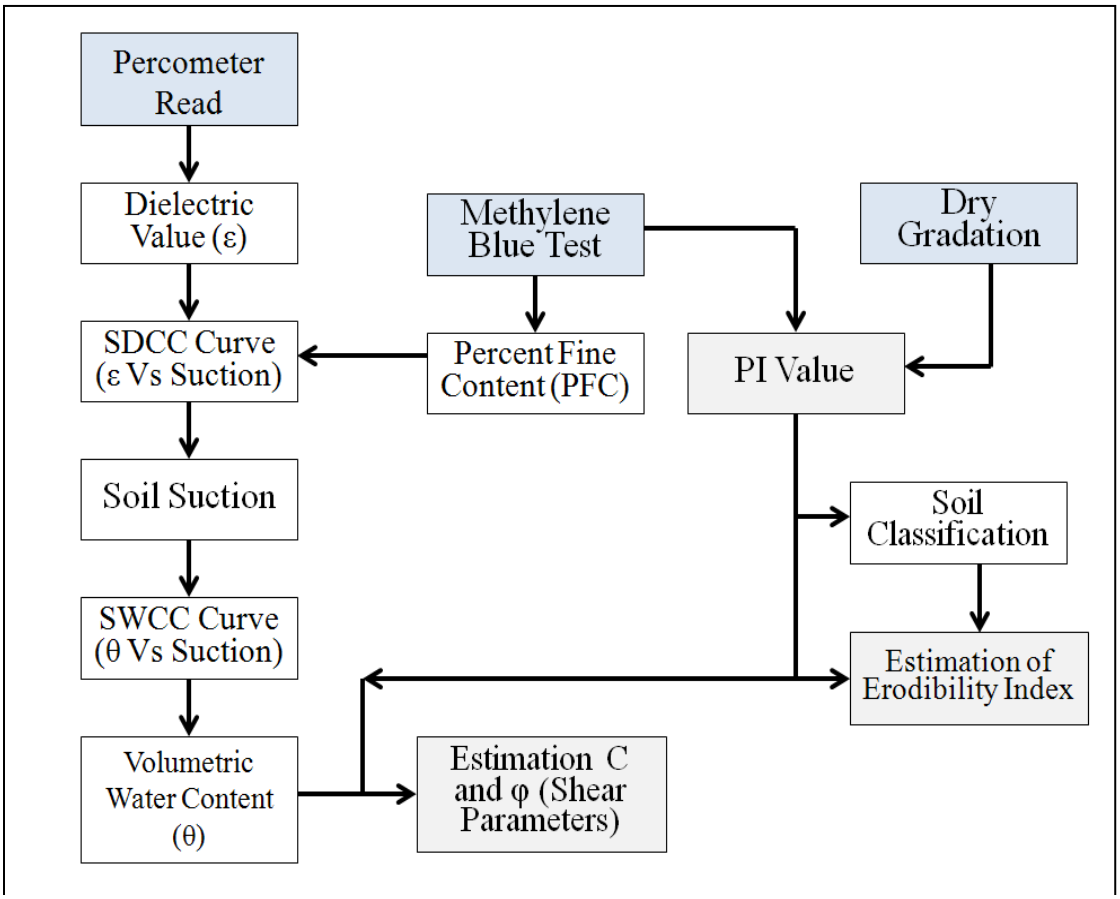

Figure 24 Suggested Test Procedure to Evaluate Subbase Parameters.

This page intentionally left blank.

TECHNICAL REPORT

SUBMITTED TO THE

READY MIXED CONCRETE (RMC) RESEARCH AND EDUCATION FOUNDATION

Test Methods & Results of Erosion Potential of Commonly Used Subgrade and Base Materials

Keivan Neshvadian Bakhsh
Graduate Research Assistant, Texas Transportation Institute

Dan Zollinger
Program Manager, Texas Transportation Institute

August 2014

TEXAS TRANSPORTATION INSTITUTE
The Texas A&M University System

Table of Contents

List of Figures

List of Tables

1. Background

One of the most important elements of concrete pavement design is the assessment of the supporting soil below the pavement and determining whether a subbase is required to meet the performance expectations specified by the project conditions. Evaluating the type and nature of the materials used as a subbase below the concrete slab is critical. An ideal subbase layer should provide sufficient strength, have moderate friction with the above concrete layer, and provide sufficient erosion resistance with uniform support. A subbase layer should also be adequately flexible to minimize curling and warping related stresses while reducing the potential for reflection cracking in the overlying concrete slab.

Many distresses in jointed concrete pavements occur when the sublayer loses its capability to provide adequate support below the slab. According to field observations and lab tests, when this occurs, faulting is typically the major performance issue for jointed concrete pavements [1, 2]; however, other distresses like cracking, and ultimately slab failure may occur. Faulting is costly to repair since it often requires extensive grinding or, in some cases, full depth repair which involves lane closures that impact the traveling public with delays, etc. [3] [4].

Subbase erosion directly contributes to the process of joint faulting. However, for erosion to occur a combination of factors must be present which include traffic loading, existence of water in the subbase/slab interface, and the erosion potential of the base material [2] (Figure 1). When the interface between the slab and the subbase is saturated with water, vertical slab movement due to loading propels the water back and forth under the slab creating a pumping action. This action hydraulically displaces loosened material that is no longer bound creating a void under the departure slab and leading to a building up of fines under the approach slab resulting in faulting and lack of the support beneath the slab [5].

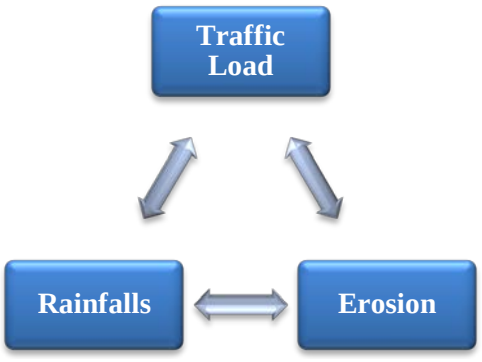

Figure 1 Three Main Elements Contributing in Subbase Erosion and PCC Faulting.

Despite the importance of erosion in jointed concrete pavements, little development has taken place to characterize key material properties that pertain to erosion or the resistance of slab-subbase interface. In many cases, the question is whether or not the subgrade material is sufficiently uniform and non-erodible to be used underneath a concrete slab. If the subgrade is adequate to meet the performance requirements, a subbase is not warranted which leads to more efficient designs and cost savings in raw materials, transportation, and placement. Another question that may need to be answered is whether or not simply improving the existing subgrade

through the addition of a stabilizing agent provides a non-erodible layer and uniform support thus eliminating the need for importing a subbase material.

Particularly with local roads and parking lots that bear lower volumes and weights of traffic, engineers need to appropriately design the underlying support layer in order to avoid extra expenses for construction of the pavement. Often a variety of local materials or stabilizing options may be available for construction; however, engineers need a method to evaluate their utility to meet specific performance needs. For highly trafficked highways, aggregate bases and/or stabilized materials are commonly used to provide the needed performance; however, for lighter duty pavements these materials may not be necessary. The research discussed herein was conducted in order to develop an evaluation process to assist the designer in making this determination specific to soil type, local climate, and traffic conditions.

A wide range of subgrade soil materials from seven locations in four states were tested and analyzed in order to evaluate the potential for erosion and the capability of the material to perform as a supporting layer. The selected samples cover different soil categories from non-plastic pure sand to high plasticity clay. The Hamburg Wheel-Tracking Device (HWTD) was used in order to test the subgrade samples. The following sections detail the material properties, HWTD, and the testing plan. Finally, the test results are presented in a database format.

2. Material Selection

This study focused on the assessment of key erosion parameters related to the use of various materials underneath a concrete slab. Accordingly, eight different soil samples were collected from project sites across the United States. These samples cover a range of different soil types including high plasticity clays to non-plastic beach sands. Figure 2 shows the U.S. soil texture classification map within which the colors represent different soil types encountered across the U.S. [6]. These are shown according to the USDA soil triangle which is shown next to the map. As can be seen, many areas consist of sand (non-cohesive soil), clay (cohesive soil) or combination of the two. Coastal areas, such as Florida, are an example of areas with sandy soils while concentrations of plastic clays can be seen in Texas, South Dakota or parts of California and Mississippi. Field samples collected in this study cover many of the common soil types encountered across the country.

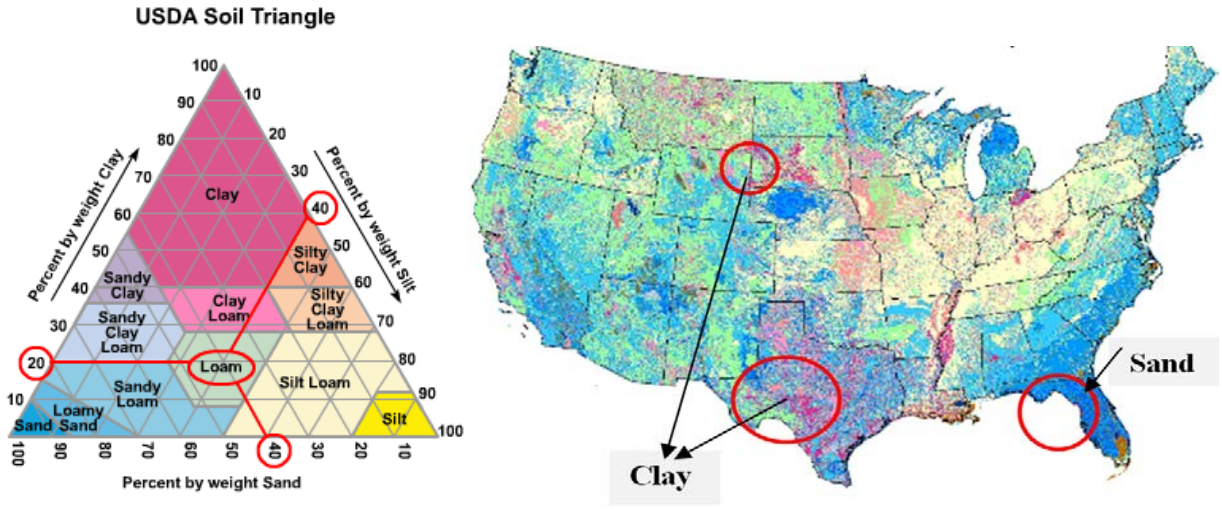

Figure 2 The Soil Classification Triangle and U.S. Soil Texture Classification Map [6].

2.1 Gradation and Classification

Dry and wet sieve analyses were performed on field soil samples to provide grading curves (ASTM D6913). Atterberg limits (liquid limit, plastic limit, and the plasticity index) on the fine portion of soils were determined (ASTM D4318). Soils were then classified according to the unified soil classification system (ASTM D2487) [7] [8] [9].

Results for the sieve analyses, grading curve, and Atterberg limits for each sample are shown in Appendix A and Appendix B. Table 1 summarizes the eight sample gradations and classifications. Sand is defined as particles of soil that pass a No. 4 (4.75 mm) sieve but are retained on the No. 200 (75 μm) sieve. Particles retrained on the No. 4 sieve (greater than 4.75 mm) are defined as gravel. Silt and clay are defined as particles that are smaller than 75 μm.[9]. Table 1 lists the samples in the order of increasing clay content and plasticity index.

The soil samples were divided into four subcategories. The first two samples were considered to be pure sands with them being more than 90% of sand and non-cohesive. The sand from Florida (sample number two) is finer compared to the sand from North Carolina (sample number one). The second set of samples were sandy but contained silt. While the two samples in this set have similar grading, the plasticity index was significantly different between the two, with the sandy silt from South Carolina having a higher plasticity index than the silty sand from Texas. The third set was a combination of clay and sandy soils. The one from Houston (sample number six) had a higher plasticity index compared to the one from San Angelo (sample number five). And finally the last two samples were clays with plasticity indexes of 20% and 40%, while containing almost 80% or more of minus 200 sieve-sized particles.

Figure 3 shows a comparison, distribution-wise, between a poorly graded sand and a fat clay demonstrating the significant differences in particle size. Figure 5 shows grading curves for the collected samples. Vertical dotted lines show the border between gravel-sand and sand-fine particles.

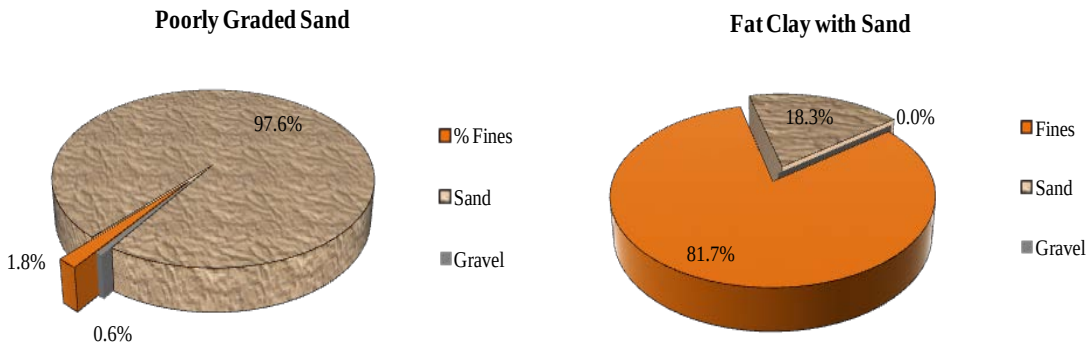

Figure 3 Comparison Between Two of the Sample's Gradation.

Figure 4 shows the plasticity indices, PI, and percent minus #200 sieve of the collected samples. As mentioned before, samples are listed in the order of increasing clay content, as well as the plasticity index. These figures demonstrate that these samples represent common soil and base types found in the United States and used as sublayers for construction of concrete pavements.

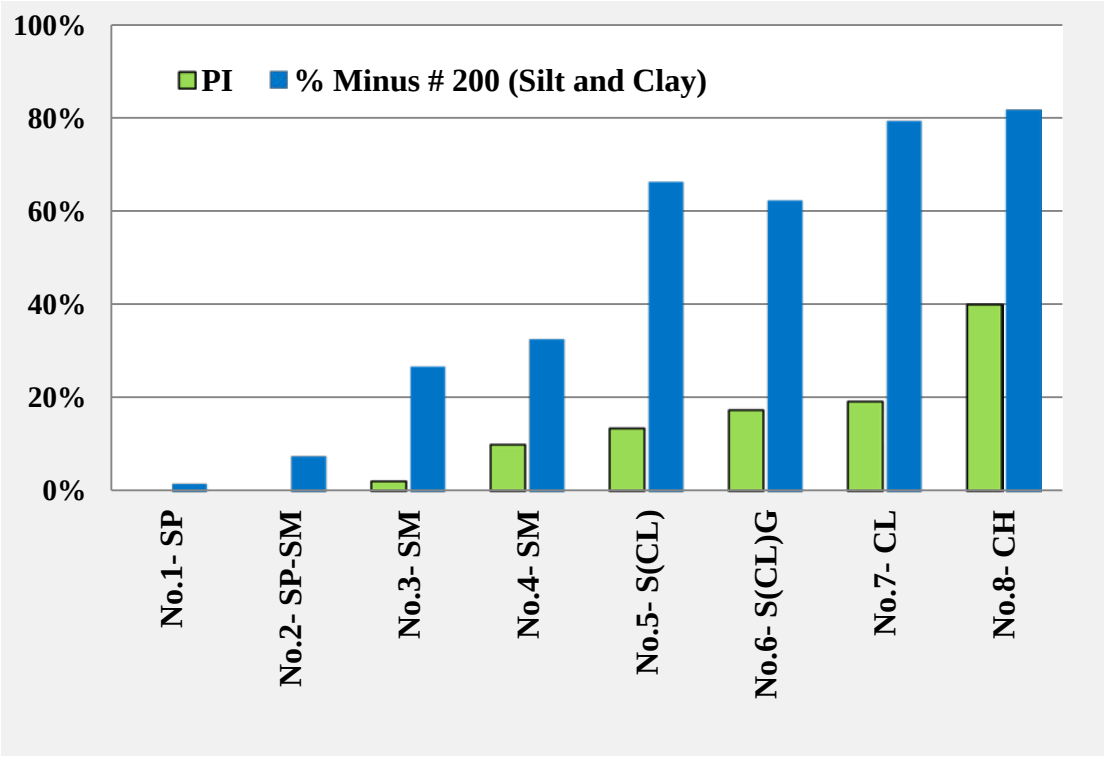

Figure 4 PI for Each Sample Along with the Percent of Minus 200 (Silt and Clay).

Table 1 Soil Samples Location and Classification.

No	Location	State	Group Symbol	Soil Category	Clay and Silt	Sand	Gravel	PI	Category for Fines
1	Greenville	NC	SP	Poorly Graded Sand	1.8%	97.6%	0.6%	NP*	NP
2	Delray Beach	FL	SP-SM	Poorly Graded Sand with Silt	7.7%	91.8%	0.5%	NP*	NP
3	College Station	TX	SM	Silty Sand	26.9%	69.3%	3.8%	2%	ML
4	Anderson	SC	SM	Sandy Silt	32.7%	63.7%	3.6%	10%	ML
5	San Angelo	TX	s(CL)	Sandy Lean Clay	66.3%	30.7%	3.0%	13%	CL
6	Houston	TX	s(CL)g	Sandy Lean Clay with Gravel	62.3%	22.6%	15.1%	17%	CL
7	Garland	TX	CL	Lean Clay with Sand	79.3%	20.7%	0.0%	19%	CL
8	Houston	TX	CH	Fat Clay with Sand	81.7%	18.3%	0.0%	40%	CH

*Non-Plastic

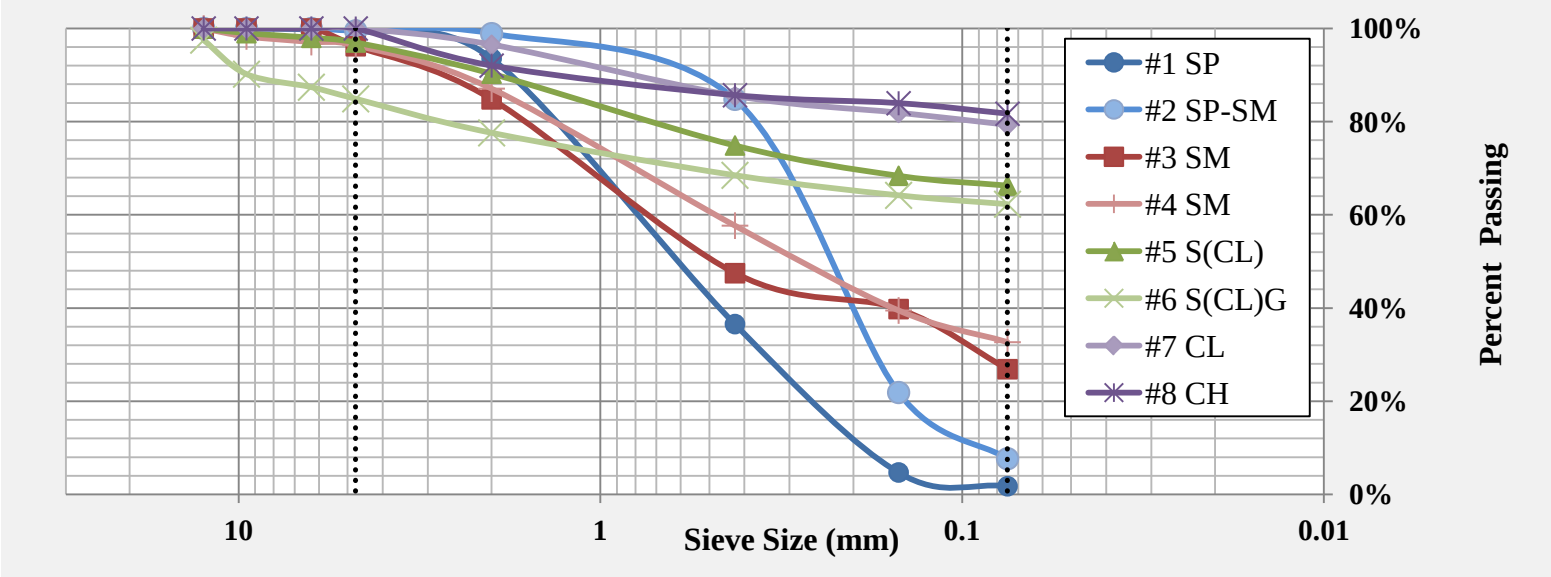

Figure 5 Grading Curves for Collected Samples.

2.2 Maximum Density and Optimum Moisture

Compaction tests were performed for all three samples in order to determine optimum water content and maximum dry density using ASTM D1557 and ASTM D698 [10] [11] [12]. Table 2 shows the compaction test results, optimum moisture and maximum dry density for the listed samples.

Table 2 Compaction Test Results for Samples.

No	Location	State	Group Symbol	Optimum Moisture	Max Dry Density (pcf)	Max Dry Density (Kg/m3)
1	Greenville	NC	SP	9.4%	114.3	1830.4
2	Delray Beach	FL	SP-SM	9.6%	109.9	1761.1
3	College Station	TX	SM	8.7%	127.6	2044.4
4	Anderson	SC	SM	21.6%	102.7	1644.9
5	San Angelo	TX	s(CL)	13.9%	110.5	1770.0
6	Houston	TX	s(CL)g	14.4%	117.9	1889.2
7	Garland	TX	CL	21.1%	101.4	1623.6
8	Houston	TX	CH	20.2%	111.2	1781.3

3. Method of Testing Erosion

3.1 Hamburg Wheel-Tracking Device

A variety of erosion tests were developed starting in the late 1970s using various testing devices, but none of those tests have been successfully used to develop a model or framework for pavement design. Most of the laboratory tests in this regard involve the application of loads on a material sample and defining erosion as related to weight loss, a parameter not particularly useful to mechanistic design analysis. The brush test method takes too long to run for practical purposes and the rotational shear device and jetting device can overestimate the amount of erosion due to the loss of aggregate-sized particles. The rolling wheel erosion test device tends to create an erosion mechanism not like the voiding that occurs under an actual concrete slab [13] [14]. The main problem with all these tests is the difficultly in determining the applied shear stress in the test. Jung and Zollinger developed a new test procedure to better lend itself to mechanistic interpretation to overcome these limitations. This test protocol involves measuring the erodibility of subgrade and base materials using the Hamburg Wheel-Tracking Device (Figure 6) (HWTD) [13] [15]. The test consists of two component layers, wherein the top is a concrete cap and the bottom consists of the base or subgrade material of interest.

HWTD testing is mainly conducted under a wet condition (sample is submerged during testing) and erosion occurs due to the mechanical and hydraulic shearing on the underlying layer generated by slab movement under an applied load. The configuration of the test device is

shown in Figure 6. The test configuration consists of a subgrade or base material, 154 mm (6 in.) in diameter and 25.4 mm (1 in.) thick, placed between a neoprene material (below) and a 25.4 mm (1 in.) thick jointed concrete block (above). The joint is sealed to simulate a joint in field conditions. A laboratory-compacted specimen or a core obtained from the field may be tested in the device. A wheel load of 71.6 kg (158 lb) is applied at a load frequency of 60-rpm. The depth of erosion at 11 locations is measured and then plotted versus the number of wheel load passes to graphically represent the erosion occurring in the base or soil sample [16] [5]. Erosion of the sublayer material is a result of the wheel load deflecting the concrete cap into the sublayer which induces shear stress and increased pore water pressure at the slab/sublayer interface. The HWTD is run until the point of failure in the sublayer.

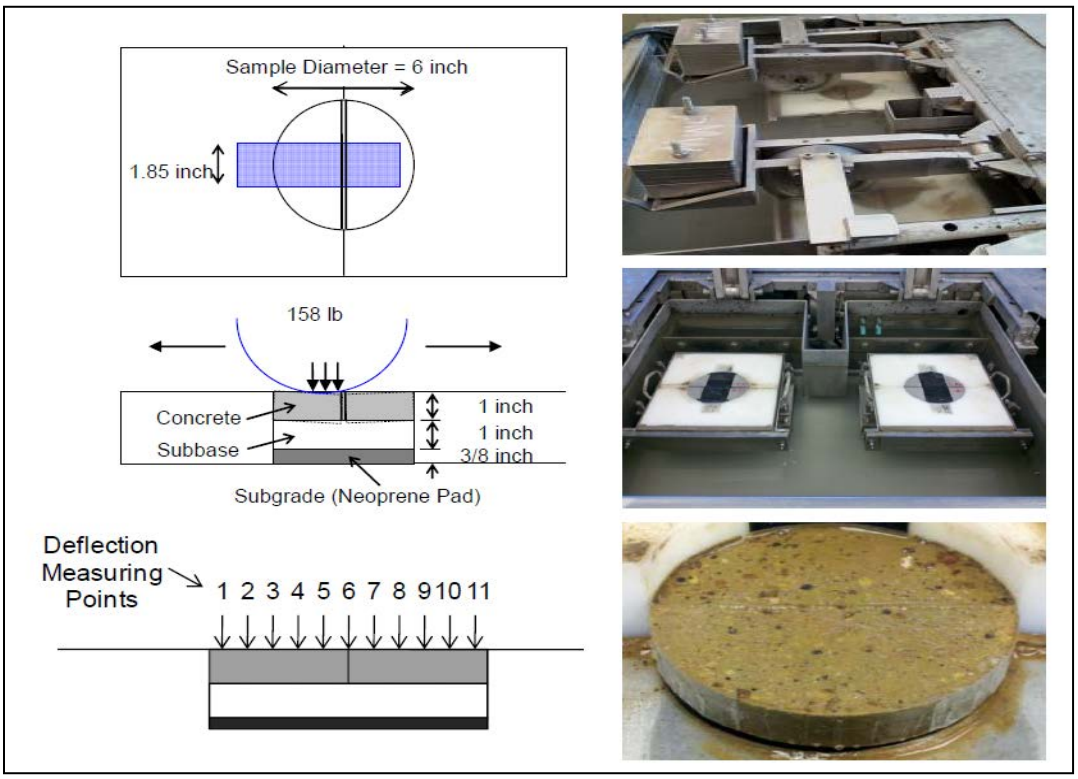

Figure 6 Hamburg Wheel – Tracking Device (HWTD) [16].

3.2 Test Plan

Since soil properties may change significantly due to changing moisture contents, some concern exists in regard to changes in a soil's resistance against erosion. Water plays a significant role in the erosion process, particularly when the subgrade or base materials are saturated. Cohesive soils, like clays, are more sensitive to moisture content but since they contain higher portions of fine particles, it may take longer for water to fully saturate them. The test plan for erosion testing was designed to address various moisture contents experienced by base and subgrade materials with boundary conditions ranging from completely dry to fully saturated conditions.

As previously explained, the HWTD contains a tank where the sample is placed and subjected to a passing wheel load. Under the wet condition, the tank is filled with water immediately prior to

starting the test, so when loading is applied, water is propelled along the sample interface. The water level is held at the interface between the concrete cap and soil. The wet Hamburg test represents the condition when the joint is holding water under traffic loading while the dry test represents the condition when joint is not holding water.

Erosion testing was completed according to the scenarios shown in Table 3. The test conditions represent different moisture conditions within the joint as well as the base or soil layer below the concrete cap. The test scenarios were developed to represent the range of field conditions in the vicinity of the joint and are assumed to be a function of the joint sealant effectiveness, prevailing weather conditions, as well as other factors such as base/soil permeability.

The first condition represents an extreme weather event with heavy rainfall wherein the subgrade becomes fully saturated. Under lab conditions, the wet HWTD testing was performed using a pre-saturated, fully submerged sample. The second test condition simulates a pavement joint shortly after a storm event has begun but the base/soil has yet to become fully saturated. The third test pertains to a dry but moist condition and represents the joint condition after a rain event where excess water has dissipated from the slab/base or slab/soil interface but the base/soil is still wet. The fourth test considers the case where the sample and tank are both dry representing the in-situ conditions without significant rainfall over a long period of time.

Table 3 Erosion Tests using Hamburg Wheel-Tracking Device (HWTD).

No	Test Type	Sample's Moisture Content	Material for the Test
1	Wet	Saturated	Clay Only
2	Wet	Optimal Moisture	All Soils
3	Dry	Optimal Moisture	All Soils
4	Dry	Dry	Clay Only

Non-cohesive sandy soils, which have fewer fine particles and generally higher permeability values compared to cohesive clay soils, drain water much faster. Figure 7 demonstrates the behavior of sand versus clay when exposed to the same amount of moisture. Since sands typically have more interconnected and larger pores, water can directly pass through the soil. In clays, the pores are less interconnected and much smaller, leading to reduced permeability. Clays tend to absorb water and permeation happens very slowly. Due to this phenomenon, the clay materials in this research project were tested using a wider range of moisture contents to simulate potential field conditions. Therefore, four moisture contents were prepared for two of the clay samples (Samples 7 and 8). For the remaining samples, one wet and one dry test was carried out at the optimum moisture conditions (Table 3).

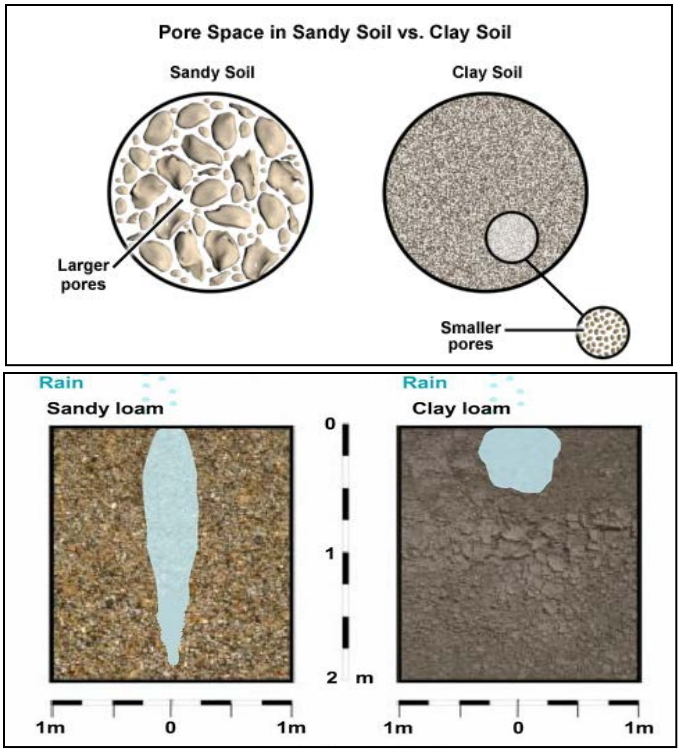

Figure 7 Schematic View Comparing the Infiltration and Permeability of Sand vs. Clay.

3.3 Stabilized Samples

Clay soils are found in many areas across the U.S. and designers are forced to use it as a foundation material because of limited construction budgets or lack of quality fill materials. However, water can dramatically change clay's performance behavior and strength. Although not the focus of this research, clay soils may absorb a significant amount of water causing them to swell and damage structures like building foundations and pavements.

Clay soils may be stabilized with lime, cement, or other products to improve performance as a supporting layer under a concrete slab through long-term strength gain from pozzolanic reaction. Cement and lime have consistently been found to be among the most effective stabilizers for road and airfield applications [17].

In order to evaluate the effectiveness of stabilization protecting against erosion under concrete pavements, the two clay samples (lean clay and fat clay) were stabilized and tested using the HWTD. Four stabilized tests were performed for each of the two clay samples; three cement stabilized (3%, 5% and 7% cement) and one lime stabilized sample. The effective percent of lime was measured based on pH measurements (TXDOT-121E) and used to make lime treated samples [18]. The pH test determines the minimum percent lime needed for a soil-lime mixture to attain a pH of 12.4. Cation exchange occurs at this pH, resulting in modification of the soil particle structure to achieve improved workability and decreased swell and plasticity. Appendix C shows the pH test results for clays. The effective percent of lime was found to be 2% for the lean clay (based on field observations, this sample may have been treated with lime in the field prior to sampling) and 4% for the fat clay.

Also, in order to test how sand's behavior changes after stabilization, one of the sand samples was stabilized and tested under wet conditions using the HWTD.

4. Test Results

4.1 Dry and Wet Erosion Tests (At Optimum Moisture)

For each of the samples, a dry test and wet test (HWTD tank dry or full) was performed. For these tests, the sample was compacted to its maximum dry density and optimum moisture condition using ASTM D 698 or D 1557 (Table 3, Test numbers 2 and 3). HWTD results were plotted as number of passes versus measured deflection in millimeters to determine erosion potential. Erodibility of the sample is defined as the load displacement in mm at 1 million load repetitions. The higher the erodibility the less resistance the material has against erosion.

For dry conditions, the water tank is totally dry: however, the moisture inside the sample is assumed to remain constant during the test (which for this section of the report the samples are at the optimum moisture content). Under wet conditions, testing was also conducted with the moisture level in the sample initially at optimum (and the water level brought to the slab-subbase interface). It is assumed that the samples take on moisture during the wet condition tests, but this cannot be verified due to the damage done to the sample during the test. Table 4 and Figure 8 show results of the erosion tests for both dry and wet conditions. The wet erosion rate was found to be, on average, 20 times greater than the dry erosion rate for unstabilized subgrade samples. Figure 9 shows the dry erosion test results and Figure 10 shows the wet erosion test results.

Table 4 Results of Dry and Wet Erosion Tests (At Optimum Moisture) for all Unstabilized Samples.

Sample	**Soil Category**	**Dry Hamburg on $W_{Optimum}$ (mm/million)**	**Wet Hamburg on $W_{Optimum}$ (mm/million)**
#1_SP	Poorly Graded Sand	90	4'500
#2_SP-SM	Poorly Graded Sand with Silt	20	2'400
#3_SM	Silty Sand	95	1'600
#4_SM	Sandy Silt	130	1'600
#5_s(CL)	Sandy Lean Clay	110	3'000
#6_s(CL)g	Sandy Lean Clay with Gravel	130	3'100
#7_CL	Lean Clay with Sand	60	900
#8_CH	Fat Clay with Sand	60	840

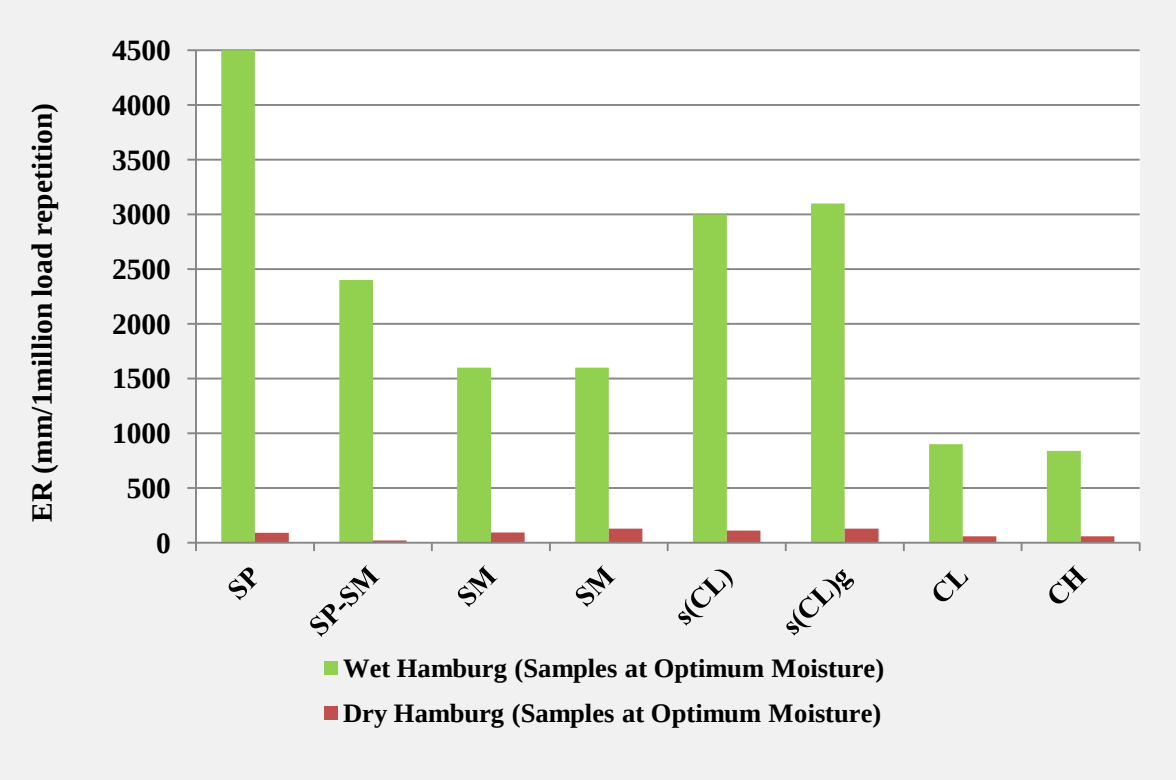

Figure 8 Erosion Tests Results for all Unstabilized Samples (Wet and Dry Tests).

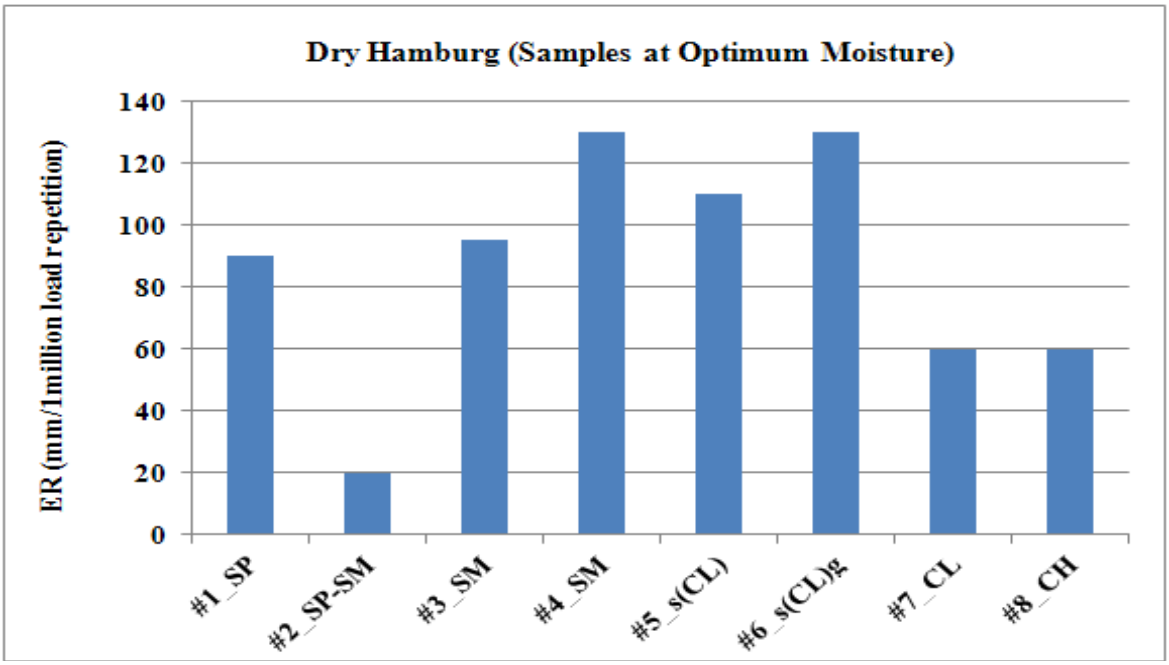

Figure 9 Dry Erosion Tests Results for all Unstabilized Samples.

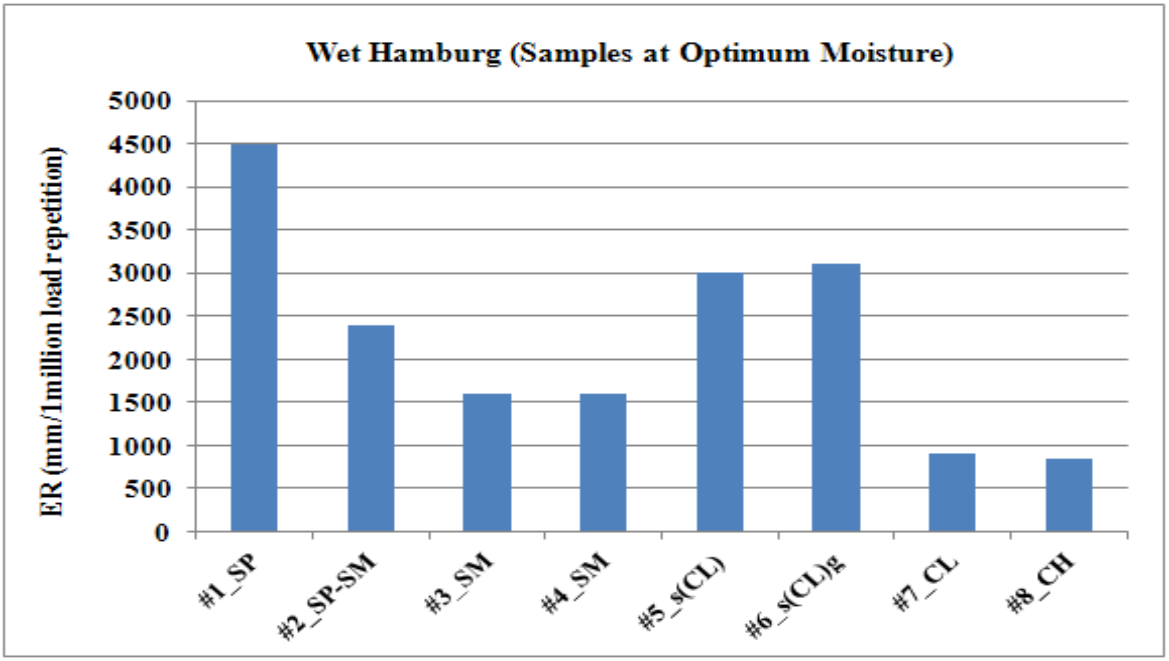

Figure 10 Wet Erosion Tests Results for all Unstabilized Samples.

As previously discussed, samples were prepared from four subcategories of soils: sand, combination of silt and sand, combination of sand and clay, and clayey soils. Except for the sand, each of the materials from the other subcategories performed nearly the same under the wet and dry test conditions. As expected, the subgrade materials show relatively low erodibility in the dry condition and a high rate of erosion in the wet condition. Figure 11 shows the results of Hamburg tests for both the wet and dry samples from each subcategory. Individual results from each soil category under dry and wet conditions are shown on Figures 12 and 13, respectively. Appendix D includes graphs of all erosion test results collected for each sample.

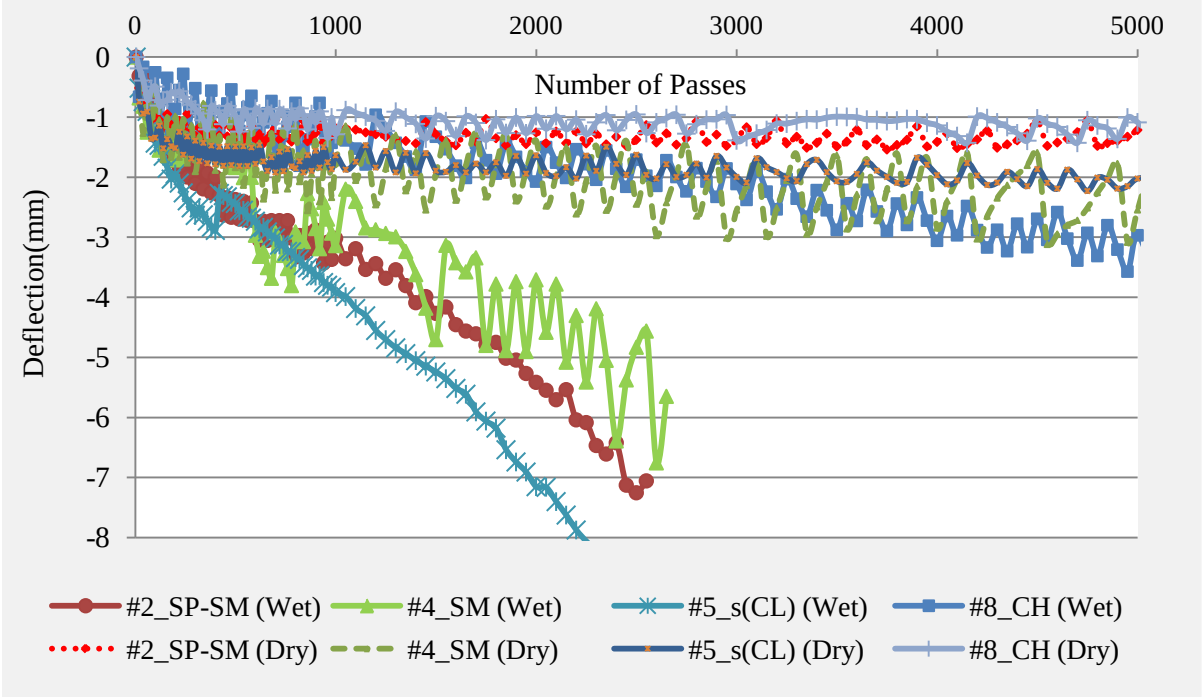

Figure 11 Hamburg Test Results for each Subcategory Sample in both the Wet and Dry Condition.

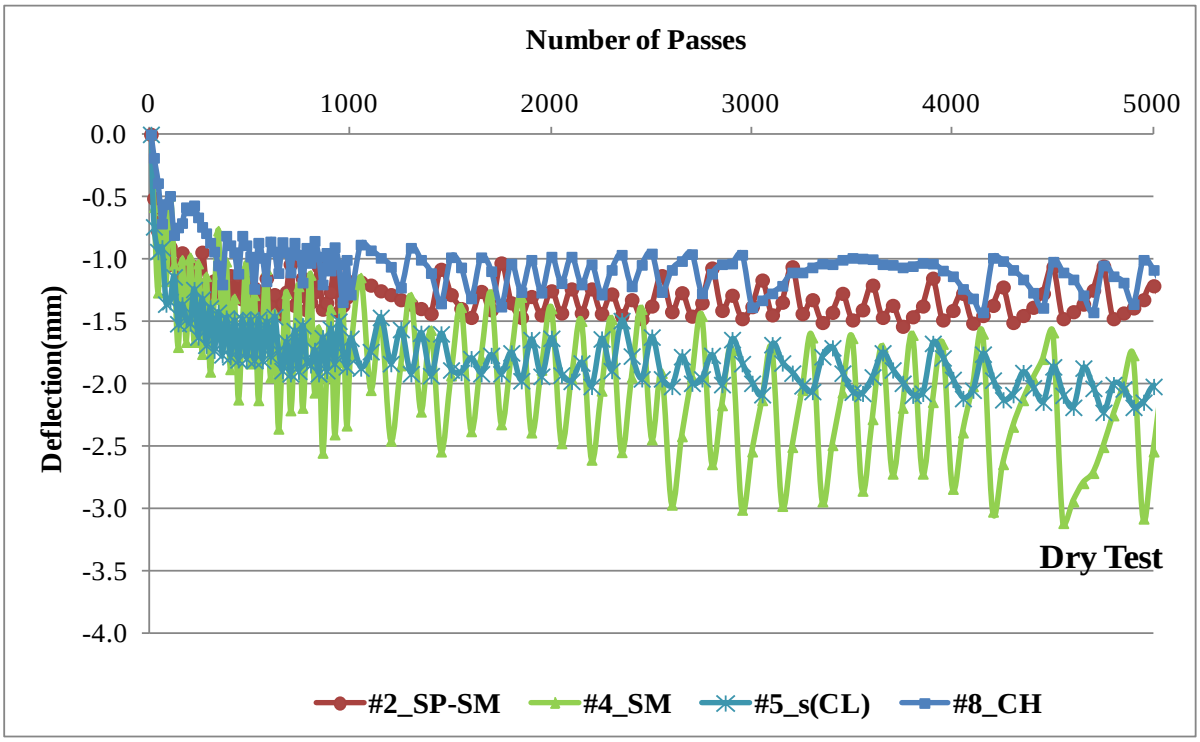

Figure 12 Hamburg Test Results for Each Soil Subcategory in the Dry Condition.

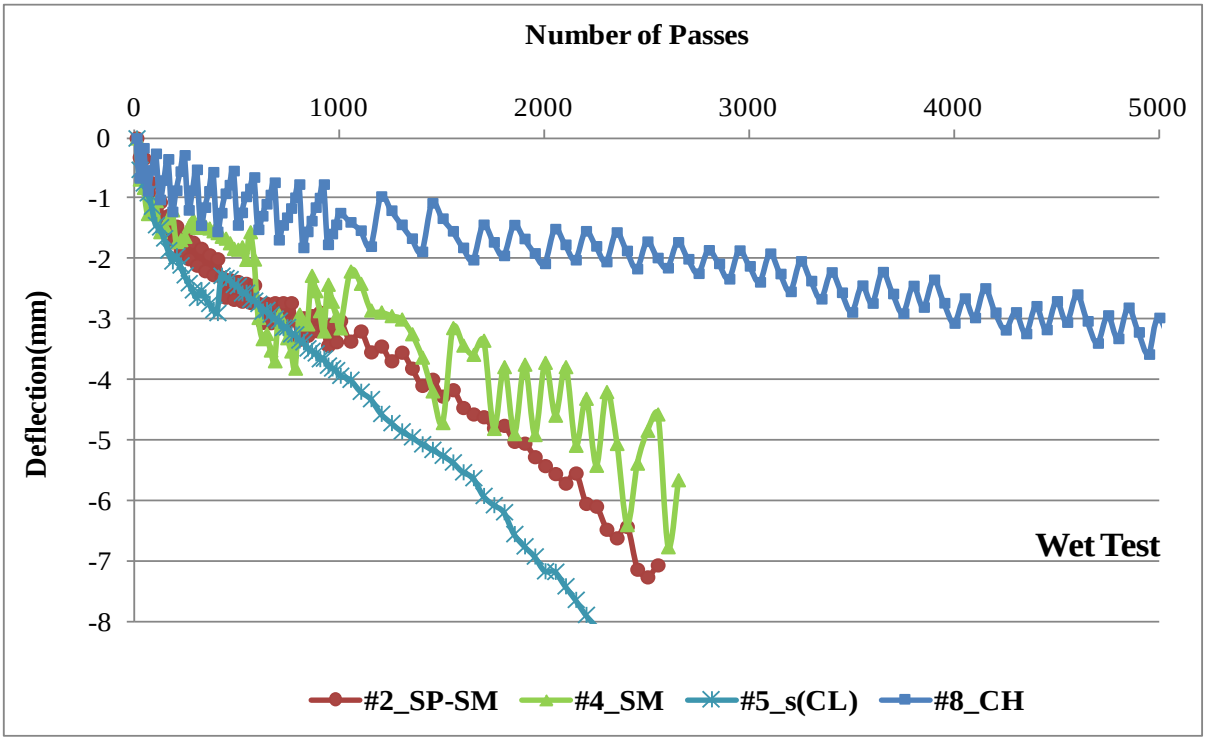

Figure 13 Hamburg Test Results for each Soil Subcategory in the Wet Condition.

Prior to testing, it was anticipated that the HWTD would clearly replicate the assumption that the combination of traffic load and water would wash away abraded material below the concrete cap. Based on the results presented in Figures 8 through 13, it is evident that the subbase/subgrade materials tested are weaker in the wet condition which was expected since water significantly decreases the shear strength of the material. Among all samples, the clays (specifically samples 7 and 8) were more resistant against erosion both in the dry and wet condition (see results in Figures 8, 9, and 10).

4.2 Erosion Tests on Clays

Clays are expected to show very good shear strength when dry but the strength characteristics change as a function of water content. To investigate the effect of moisture on the shear strength, four moisture conditions were explored on each clay soil (Table 3). The dry and wet conditions were discussed previously. Two additional tests were performed by exposing the clay samples to extreme conditions: The first was created by oven drying the sample and testing under dry condition (with the tank empty). The second condition was developed by completely pre-saturating the sample and testing under the wet condition (tank was full). Testing the additional clay samples allowed testing to occur under four different moisture conditions resulting an evaluation of erodibility effects with respect to the moisture content of the sample. Table 5 and Figure 14 show results of HWTD testing on lean and fat clay material at these four moisture and tank combinations.

Table 5 Results for Hamburg Test on Lean Clay and Fat Clay at Various Moisture and Tank Combinations.

Test Method	Dry Test	Dry Test	Wet Test	Wet Test
Sample's Moisture Content	Oven Dried	Optimum	Optimum	Saturated
ER for #7_CL (PI~20)	30	60	900	13600
ER for #8_CH (PI~40)	30	60	840	32400

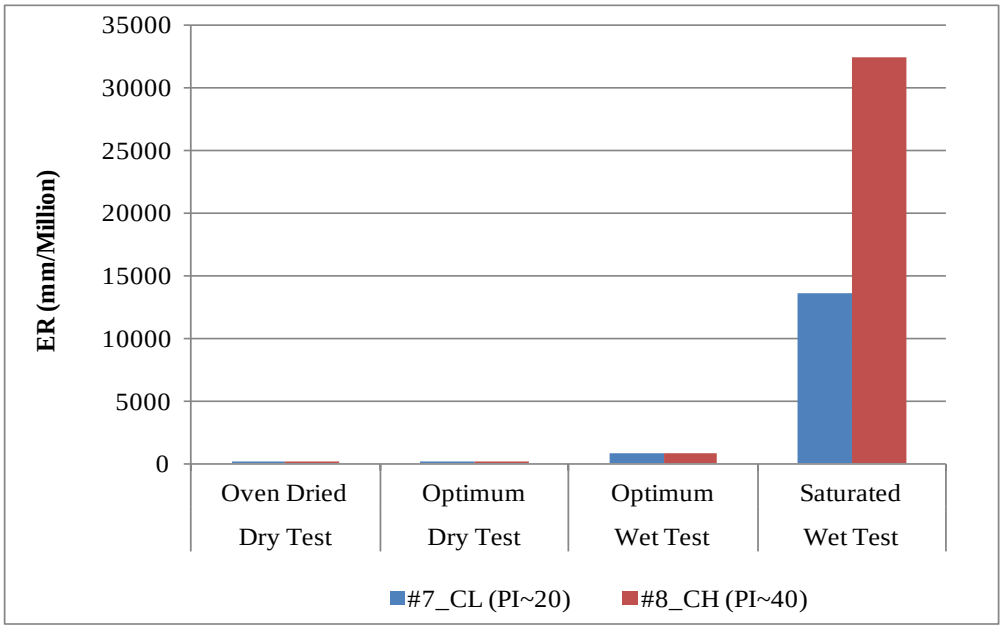

Figure 14 Results for Hamburg Test on Lean Clay and Fat Clay at Various Moisture and Tank Combinations.

Results show that both clays are resistant to erosion and behave similarly when they are dry or at the optimum moisture content, regardless of the tank condition (wet or dry). However, when the clay becomes fully saturated and exposed to additional moisture (i.e. the wet tank condition) the clays become extremely weak and the erodibility index is greater.

It should be noted that saturation of the whole clay layer may occur when the pavement is subjected to multiple wet days and the joint seals are performing poorly. In order to saturate the one-inch thick clay samples, they were kept in a moisture room for one week prior to testing. The saturation moisture content for the lean clay soil was determined to be 49.2% and 61.4% for the fat clay. Figures 15 and 16 show the plot of Hamburg tests for lean and fat clay at the four moisture and tank combinations.

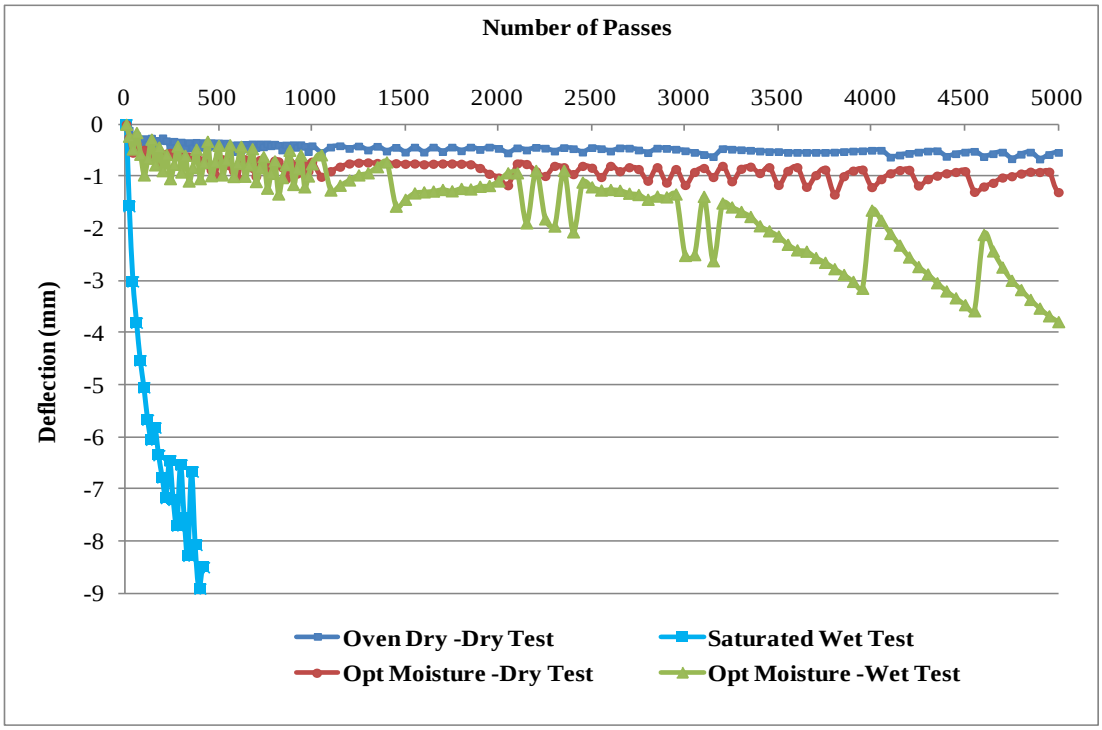

Figure 15 Hamburg Tests for Lean Clay, Sample Number 7.

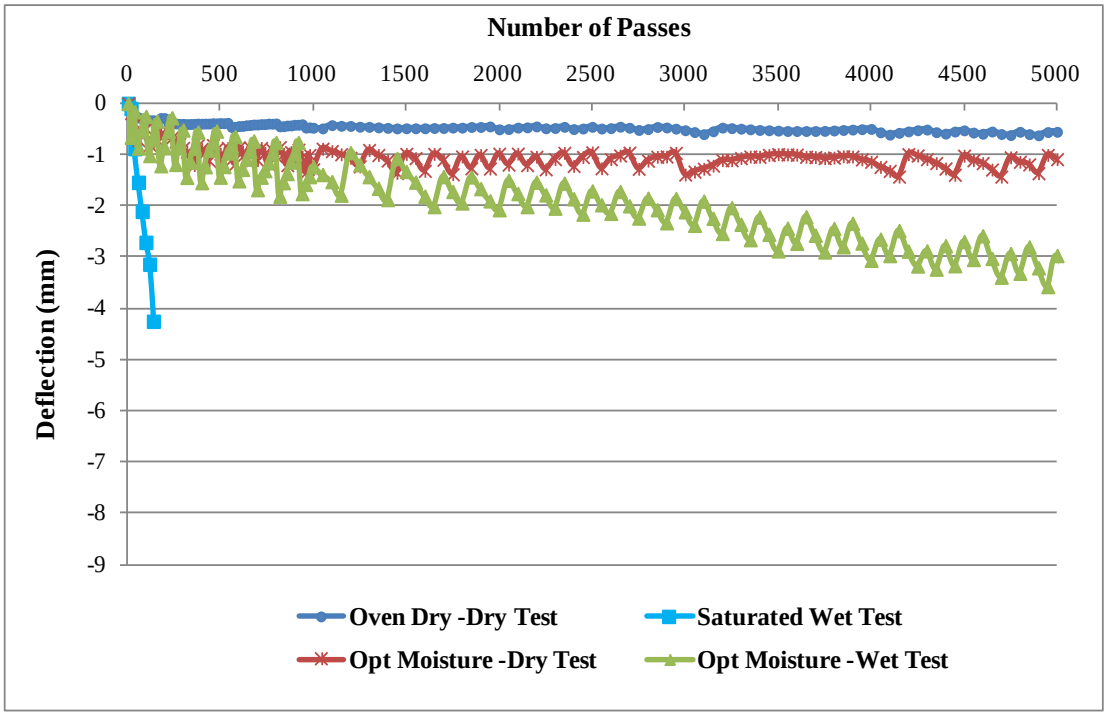

Figure 16 Hamburg Tests for Fat Clay, Sample Number 8.

4.3 Stabilized Clay Samples

In order to evaluate the effectiveness of soil stabilization on erosion potential, four stabilized conditions were tested for the two clay samples described above. Three stabilization conditions were developed using cement at contents of 3%, 5% and 7%. One additional sample for each clay sample was prepared with lime. Samples were cured for 28 days and tested immediately after removal from the moisture room. The samples were also tested in the saturated condition because it was assumed that the erosion rate would have been minimal if tested dry or at optimum moisture. Effective percent of added lime was measured based on pH measurements following the Tex-121E test method [18]. The effective percent of lime was found to be 2% for the lean clay (based on field observations, this sample may have been treated with lime in the field prior to sampling) and 4% for the fat clay (see Appendix C for results from Tex-121-E). Table 6 and Figure 17 show results from HWTD testing on the stabilized clay samples. Figures 18 and 19 show the plot of HWTD testing for stabilized lean clay and fat clay samples.

Table 6 Results for Hamburg Test on Stabilized Clays.

Test Method	Wet Test in Saturation	Wet Test in Saturation	Wet Test in Saturation	Wet Test in Saturation	Wet Test in Saturation
% Stabilized	0% Cement	3% Cement	5% Cement	7% Cement	Effective % of Lime
ER for #7_CL (PI~20)	13600	6400	3500	1100	3400
ER for #8_CH (PI~40)	32400	8200	5300	2200	4200

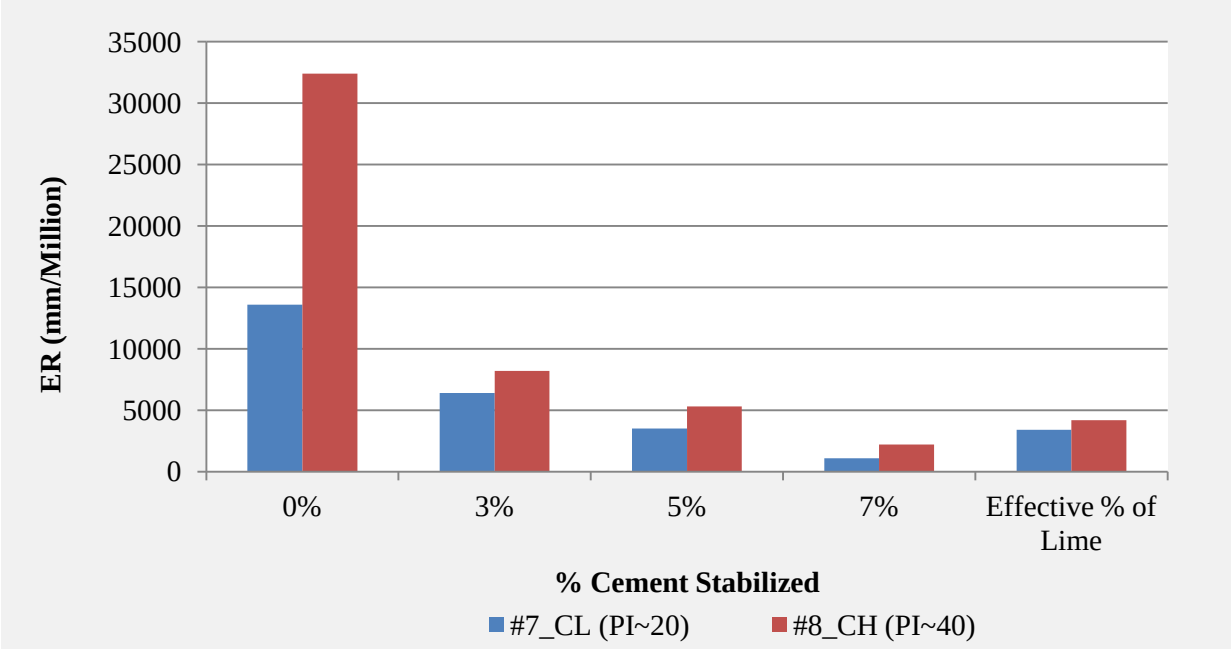

Figure 17 Results for Hamburg Test on Stabilized Clays.

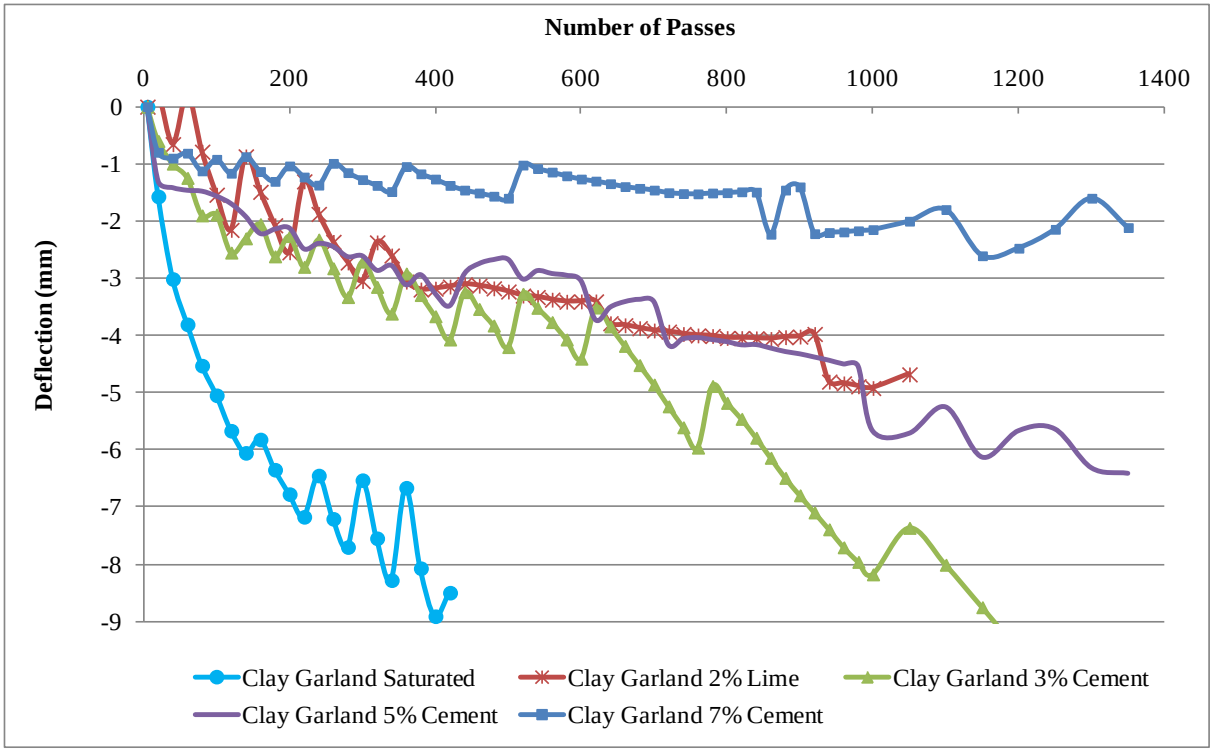

Figure 18 Hamburg Tests for Stabilized Lean Clay, Sample Number 7.

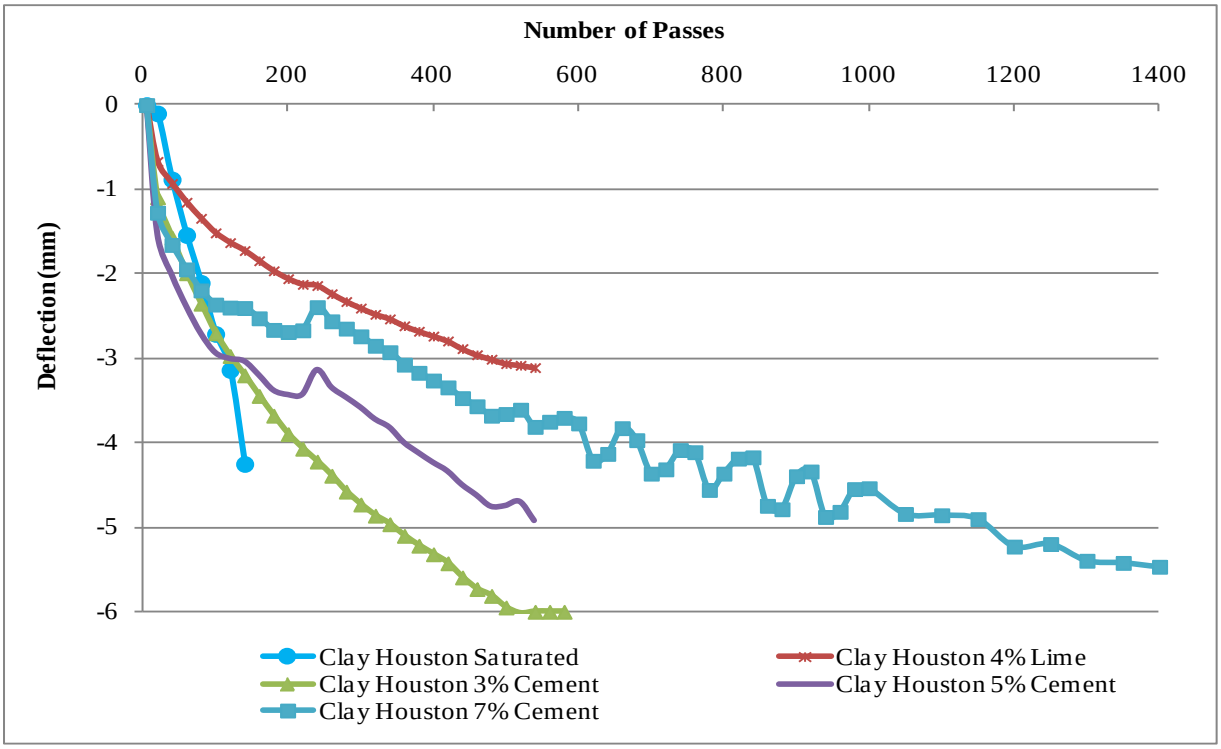

Figure 19 Hamburg Tests for Stabilized Fat Clay, Sample Number 8.

As expected, stabilization significantly improved the resistance of the samples against erosion. Clays with less plasticity are shown to be stronger against erosion in the saturated condition when tested in the HWTD. Even though high plasticity clays have higher cohesiveness compared to low plastic clays, they absorbed more water when saturated; hence the reverse effect occurs because moisture weakens the high plasticity clay.

4.4 Stabilized Sand Samples

Three sand samples were stabilized and tested in the HWTD. The beach sand from North Carolina tested in four different conditions which included unstabilized, stabilized with 6 percent lime, 6 percent cement, and a combination of 3 percent cement and 3 percent lime. Samples were cured for 14 days and tested immediately after removal from the moisture room. As with the clay samples, the sand samples were tested at saturated moisture conditions. Table 7 and Figure 20 show the final results from the HWTD testing. Figure 21 shows the plot of deflection versus the number of passes and demonstrates the rate of erosion for each sample.

Table 7 Results of HWTD Testing on Stabilized Sand.

Test Method	Wet Test in Saturation	Wet Test in Saturation	Wet Test in Saturation	Wet Test in Saturation
% Stabilized	Non-Stabilized	6% Lime	3% Lime +3%Cement	6% Cement
ER for #1_Sand (SP)	4500	3100	2500	1070

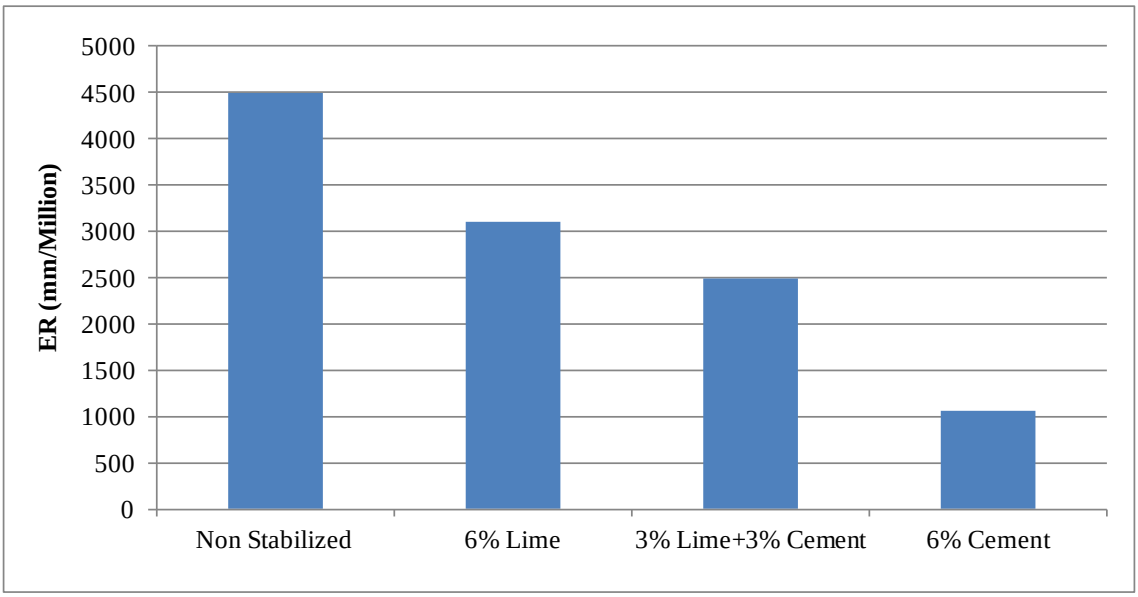

Figure 20 Results of HWTD Testing on Stabilized Sand.

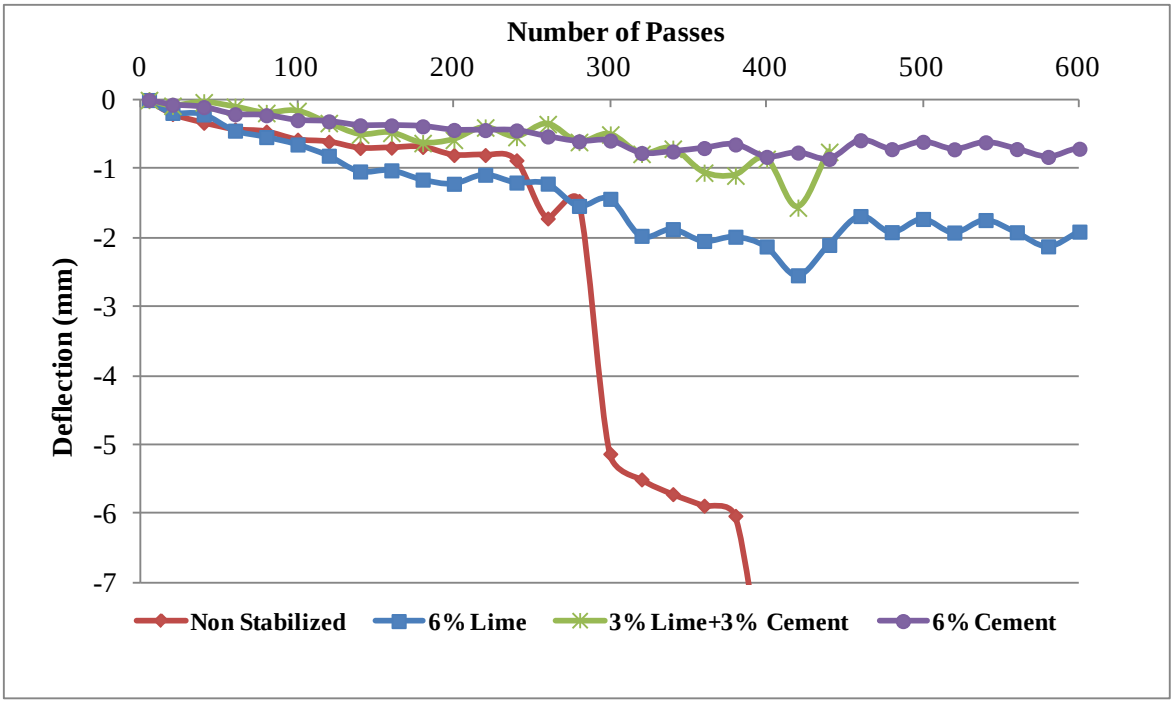

Figure 21 Hamburg Tests for Stabilized Sand, Sample Number 1.

As expected, stabilization improved the resistance of sand against erosion when tested using the HWTD. Additionally, cement stabilization showed better erodibility resistance as compared to lime stabilization.

5. Conclusions and Discussions

Several important conclusions can be drawn from the analysis of this test program and are summarized as follows:

- Water is a critical factor in the sublayer erosion process underneath a slab.
- Subgrade materials, when exposed to water, show considerably less resistance against erosion compared to dry conditions. Existence of water significantly decreases the shear strength at the slab/sublayer interface; therefore, greatly increasing the potential of erosion in the sublayer material. The wet erosion rate was found to be, on average, 20 times greater than the dry erosion rate for unstabilized sublayer samples.
- All the samples showed acceptable performance in the absence of water. Even though erosion occurred in dry tests, the rate of dry erosion was low for all samples.
- Cohesiveness increases the soil shear strength; therefore, increasing the resistance against erosion. Sands were found to be highly erodible, particularly when the slit and/or clay content are/is lower. Sandy soils have little cohesive strength thus making them

susceptible to erosion. Clays, which typically have higher cohesiveness, on the other hand were found to be more resistant against erosion.

- While dried clays are very resistant against erosion, clays become extremely weak when completely saturated. It should be noted that complete saturation of the whole clay layer rarely occurs unless a pavement system is in an extremely rainy climate with unsealed joints and poor drainage system.

- The results suggest that clays could be used as a suitable subgrade in a dry climate for minor roads or parking lots but using clays should be avoided in places with heavy rain and when unsealed joints may be used. Another potential problem with clays in changing moisture conditions is volume change that may cause damage to a concrete slab.

- Stabilization significantly improved the resistance of all samples against erosion. Seven percent cement caused a decrease in erodibility index by 14 times in fat clays. Stabilization also improved the resistance of sand against erosion.

- Cement stabilization showed better erodibility resistance as compared to lime stabilization. Also, stabilization has greater impact on clay as compared to sands mainly because of faster and stronger chemical reactions of clay particles.

References

1. Selezneva, O., J. Jiang, and S.D. Tayabji, *Preliminary Evaluation And Analysis Of LTPP Faulting Data-Final Report*, 2000.
2. Neshvadian Bakhsh, K., D.G. Zollinger, and Y.-S. Jung. *Evaluation of Joint Sealant Effectiveness on Moisture Infiltration and Erosion Potential in Concrete Pavement*. in *Transportation Research Board 92nd Annual Meeting*. 2013.
3. Jung, Y.S., D.G. Zollinger, and T.J. Freeman, *Evaluation and Decision Strategies for the Routine Maintenance of Concrete Pavement.* 2009.
4. Freeman, T.J. and D.G. Zollinger, *Guidelines for Routine Maintenance of Concrete Pavement*, 2008.
5. Zollinger, D.G., et al., *Subbase and Subgrade Performance Investigation and Design Guidelines for Concrete Pavement*, 2012.
6. *"USDA/The COMET Program"*. [Web] 2012 [cited 2012 10 September]; Basic Hydrologic Science Course, Runoff Processes,Section Four: Soil Properties].
7. *ASTM D6913 – 04* in *Standard Test Methods for Particle-Size Distribution (Gradation) of Soils Using Sieve Analysis*2009, American society for testing and materials.
8. *ASTM D4318 – 10*, in *Standard Test Methods for Liquid Limit, Plastic Limit, and Plasticity Index of Soils*2010, American Society for Testing and Materials.
9. *ASTM D2487 – 11*, in *Standard Practice for Classification of Soils for Engineering Purposes (Unified Soil Classification System)*2011, American Society for Testing and Materials.
10. *ASTM D698 – 07*, in *Standard Test Methods for Laboratory Compaction Characteristics of Soil Using Standard Effort (12 400 ft-lbf/ft3 (600 kN-m/m3))*2007, American Society for Testing and Materials.
11. *ASTM D1557 – 09*, in *Standard Test Methods for Laboratory Compaction Characteristics of Soil Using Modified Effort (56,000 ft-lbf/ft3(2,700 kN-m/m3))*2009, American Society for Testing and Materials.
12. *ASTM D2216 – 10*, in *Standard Test Methods for Laboratory Determination of Water (Moisture) Content of Soil and Rock by Mass1*2010, American Society for Testing and Materials.
13. Jung, Y.S. and D.G. Zollinger, *New Laboratory-Based Mechanistic-Empirical Model for Faulting in Jointed Concrete Pavement.* Transportation Research Record: Journal of the Transportation Research Board, 2011. **2226**(-1): p. 60-70.
14. De Beer, M., *Aspects of Erodibility Lightly Cementitious Materials*. South African Council for Scientific Industrial Research. . 1989: Flexible Pavement Programme.
15. TxDoT, *Tex-242-F*, in *HAMBURG WHEEL-TRACKING TEST*2009, Texas Department of Transportation.

16. Jung, Y.S., D.G. Zollinger, and A.J. Wimsatt, *Test Method and Model Development of Subbase Erosion for Concrete Pavement Design.* Transportation Research Record: Journal of the Transportation Research Board, 2010. **2154**(-1): p. 22-31.

17. Kawamura, M. and S. Diamond, *Stabilization of clay soils against erosion loss*, 1975.

18. *Tex-121-E*, in *SOIL-LIME TESTING*2002, Texas Department of Transportation.

19. Sahin, H., F. Gu, and R.L. Lytton, *Development of Soil Water Characteristic Curve for Flexible Base Materials Using the Methylene Blue Test.* Transportation Research Record: Journal of the Transportation Research Board 2013. **Under Press**.

20. Lindeburg, M.R., *Civil engineering reference manual for the PE exam*. 2012: www. ppi2pass. com.

Appendix A. Soil Samples Classifications

Sample Number 1.
Location: Greenville, North Carolina
Color: White-Gray

Non-Plastic (LL= 14.2%, PL: Not Applicable)
Coefficient of Uniformity (Cu) = 4.44
Coefficient of Curvature (Cc) = 0.85

Category: **Poorly Graded Sand**
Group Symbol: SP

Table 8 Gradation Table for Sample No. 1, Poorly Graded Sand.

Sieve mesh size (mm)	Sieve Number	Percent Retained	Percent Passing	Particles	
9.52	3/8"	0.00%	100.0%	Gravel	0.6%
4.750	4	0.57%	99.4%		
2.000	10	5.85%	93.6%	Sand	97.6%
0.425	40	57.00%	36.6%		
0.150	100	31.83%	4.7%		
0.075	200	2.95%	1.8%		
Pan	Pan	1.79%	0.0%	Fines	1.8%

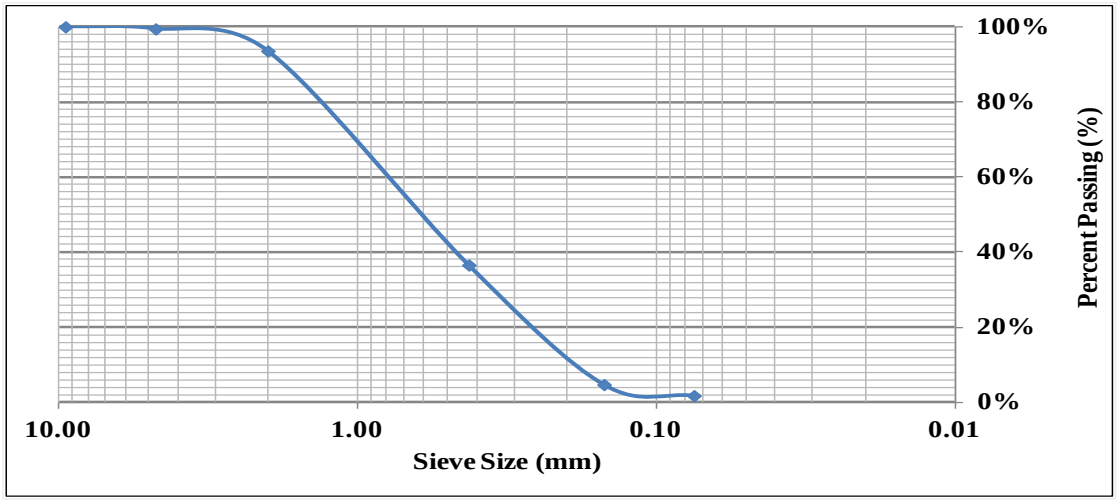

Figure 22 Gradation Curve for Sample No. 1, Poorly Graded Sand.

Sample Number 2.
Location: Delray Beach, Florida
Color: Very Dark Brown

Non-Plastic (LL= 16.1%, PL: Not Applicable)
Coefficient of Uniformity (Cu) = 2.78
Coefficient of Curvature (Cc) = 1.36

Category: **Poorly Graded Sand with Silt**
Group Symbol: SP-SM

Table 9 Gradation Table for Sample No. 2, Poorly Graded Sand with Silt.

Sieve mesh size (mm)	Sieve Number	Percent Retained	Percent Passing	Particles	
6.300	1/4"	0.0%	100.0%	Gravel	0.5%
4.750	4	0.5%	99.5%		
2.000	10	0.6%	98.9%	Sand	91.8%
0.425	40	14.1%	84.8%		
0.150	100	62.9%	21.9%		
0.075	200	14.2%	7.7%		
Pan	Pan	7.7%	0.0%	Fines	7.7%

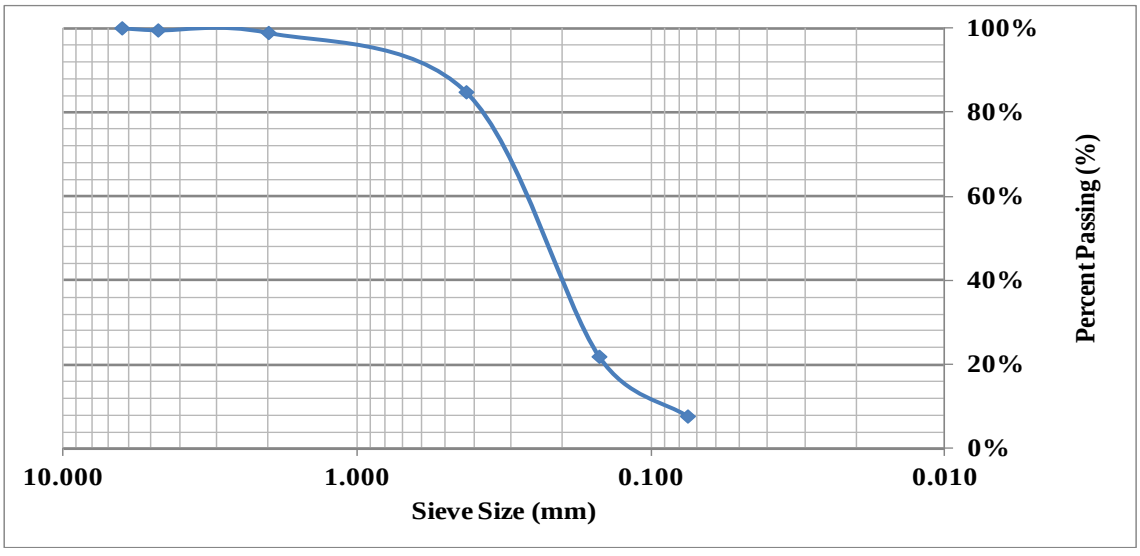

Figure 23 Gradation Curve for Sample No. 2, Poorly Graded Sand with Silt.

Sample Number 3.
Location: College Station, Texas
Color: Light Brown

PI= 2.09%
(LL= 20.01%, PL: 17.92%)
Classification of Fine Portion: Low Plasticity Silt (ML)

Category: **Silty Sand**
Group Symbol: SM

Table 10 Gradation Table for Sample No. 3, Silty Sand.

Sieve mesh size (mm)	Sieve Number	Percent Retained	Percent Passing	Particles	
12.50	1/2"	0.00%	100.00%	Gravel	3.8%
4.750	4	3.80%	96.20%		
2.000	10	11.40%	84.80%	Sand	69.3%
0.425	40	37.30%	47.50%		
0.150	100	7.70%	39.80%		
0.075	200	12.90%	26.90%		
Pan	Pan	26.90%	0.00%	Fines	26.9%

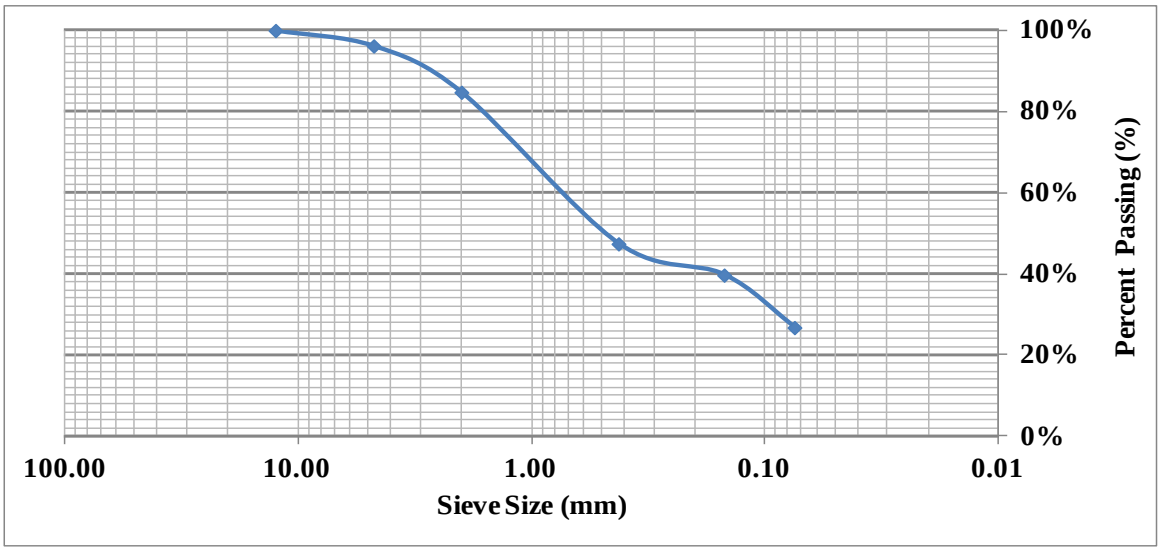

Figure 24 Gradation Curve for Sample No. 3, Silty Sand.

Sample Number 4.
Location: Anderson, South Carolina
Color: Brick Red

PI= 9.91%
(LL= 41.99%, PL: 32.08%)
Classification of Fine Portion: Low Plasticity Silt (ML)

Category: **Sandy Silt**
Group Symbol: SM

Table 11 Gradation Table for Sample No. 4, Sandy Silt.

Sieve mesh size (mm)	Sieve Number	Percent Retained	Percent Passing	Particles	
9.52	3/8"	0.80%	99.2%	Gravel	3.6%
4.750	4	2.80%	96.4%		
2.000	10	9.30%	87.1%	Sand	63.7%
0.425	40	29.40%	57.7%		
0.150	100	18.20%	39.5%		
0.075	200	6.80%	32.7%		
Pan	Pan	32.70%	0.0%	Fines	32.7%

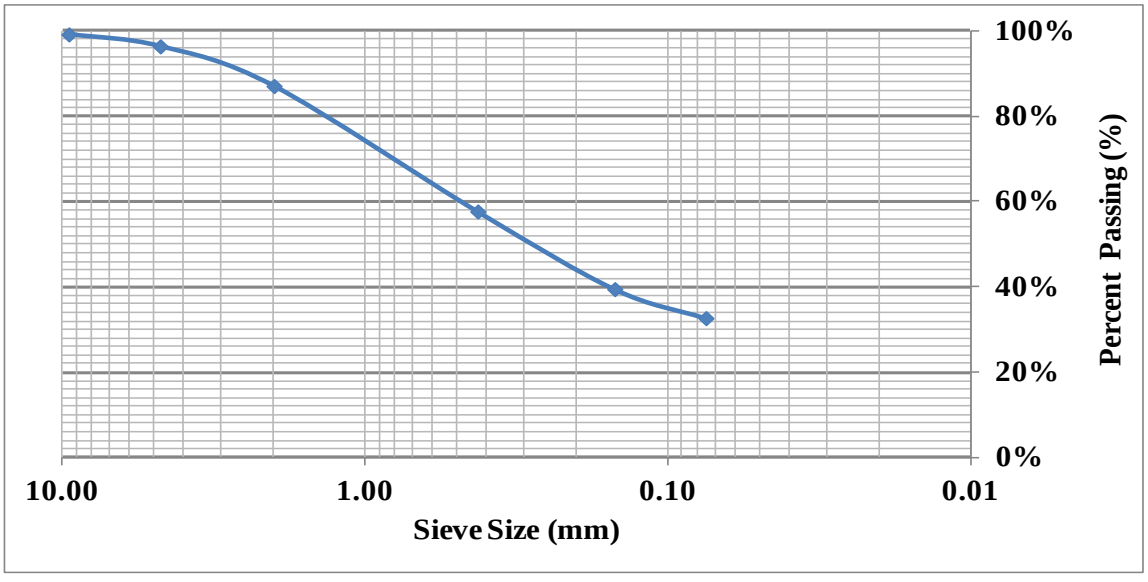

Figure 25 Gradation Curve for Sample No. 4, Sandy Silt.

Sample Number 5.
Location: San Angelo, Texas
Color: Dark Brown

PI= 13.36%
(LL= 32.36%, PL: 19.00%)
Classification of Fine Portion: Low Plasticity Clay (CL)

Category: **Sandy Lean Clay**
Group Symbol: s(CL)

Table 12 Gradation Table for Sample No. 5, Sandy Lean Clay.

Sieve mesh size (mm)	Sieve Number	Percent Retained	Percent Passing	Particles	
12.50	1/2"	0.0%	100.0%	Gravel	3.0%
4.750	4	3.0%	97.0%		
2.000	10	6.7%	90.3%	Sand	30.7%
0.425	40	15.4%	74.9%		
0.150	100	6.5%	68.4%		
0.075	200	2.1%	66.3%		
Pan	Pan	66.3%	0.0%	Fines	66.3%

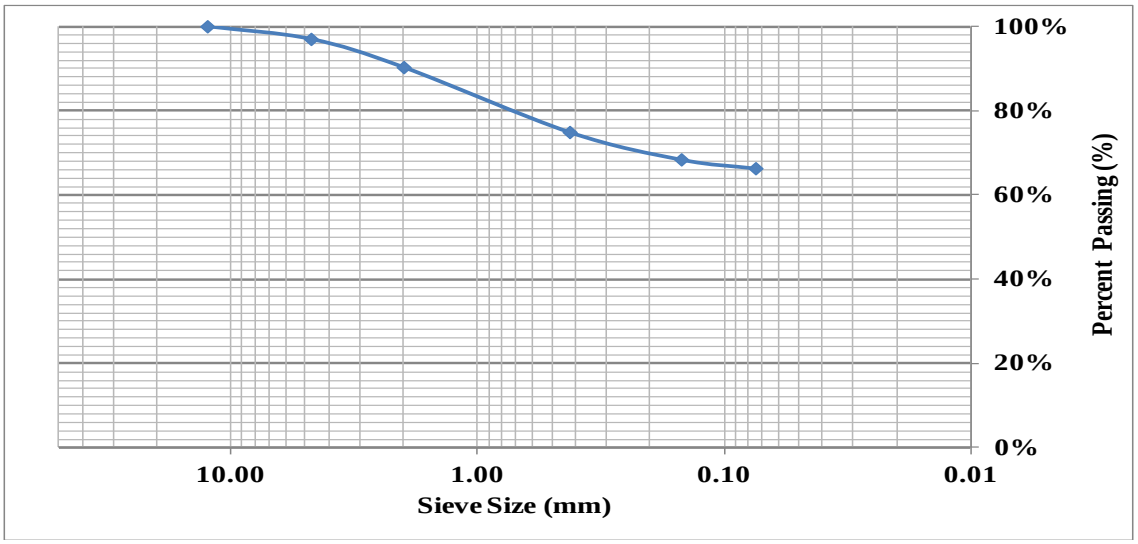

Figure 26 Gradation Curve for Sample No. 5, Sandy Lean Clay.

Sample Number 6.
Location: Houston, Texas
Color: Brown

PI= 17.34%
(LL= 33.59%, PL: 16.25%)
Classification of Fine Portion: Low Plasticity Clay (CL)

Category: **Sandy Lean Clay with Gravel**
Group Symbol: s(CL)g

Table 13 Gradation Table for Sample No. 6, Sandy Lean Clay with Gravel.

Sieve mesh size (mm)	Sieve Number	Percent Retained	Percent Passing	Particles	
12.50	1/2"	2.5%	97.5%	Gravel	15.1%
4.750	4	12.6%	84.9%		
2.000	10	7.3%	77.6%	Sand	22.6%
0.425	40	9.1%	68.5%		
0.150	100	4.3%	64.2%		
0.075	200	1.9%	62.3%		
Pan	Pan	62.3%	0.0%	Fines	62.3%

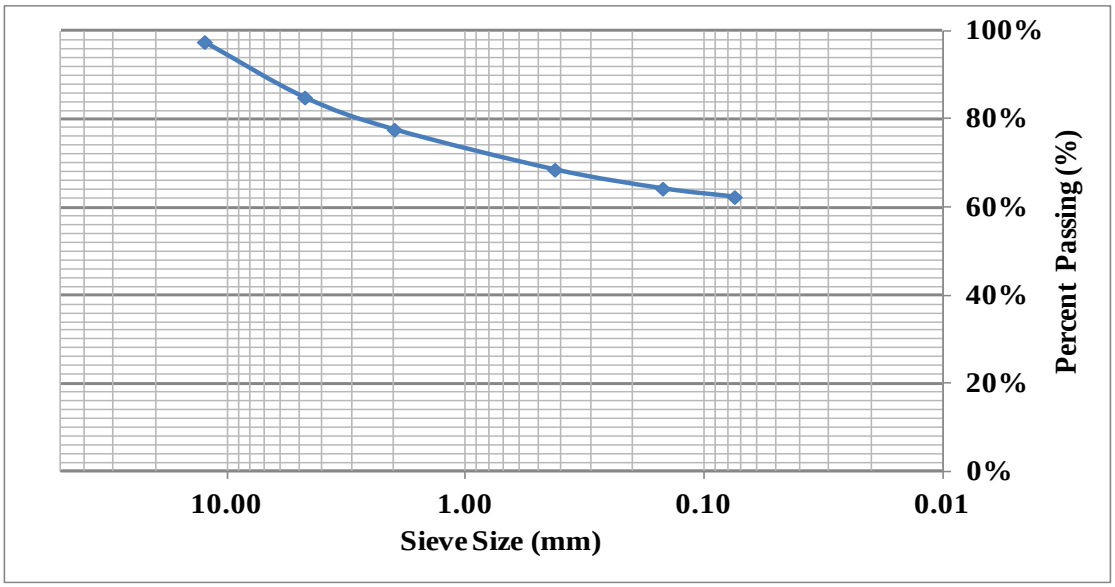

Figure 27 Gradation Curve for Sample No. 6, Sandy Lean Clay with Gravel.

Sample Number 7.
Location: Garland, Texas
Color: Grayish Brown

PI= 19.17%
(LL= 41.78%, PL: 22.61%)
Classification of Fine Portion: Low Plasticity Clay (CL)

Category: **Lean Clay with Sand**
Group Symbol: CL

Table 14 Gradation Table for Sample No. 7, Lean Clay with Sand.

Sieve mesh size (mm)	Sieve Number	Percent Retained	Percent Passing	Particles	
12.50	1/2"	0.00%	100.0%	Gravel	0.0%
4.750	4	0.00%	100.0%		
2.000	10	3.50%	96.5%	Sand	20.7%
0.425	40	11.00%	85.5%		
0.150	100	3.60%	81.9%		
0.075	200	2.60%	79.3%		
Pan	Pan	79.30%	0.0%	Fines	79.3%

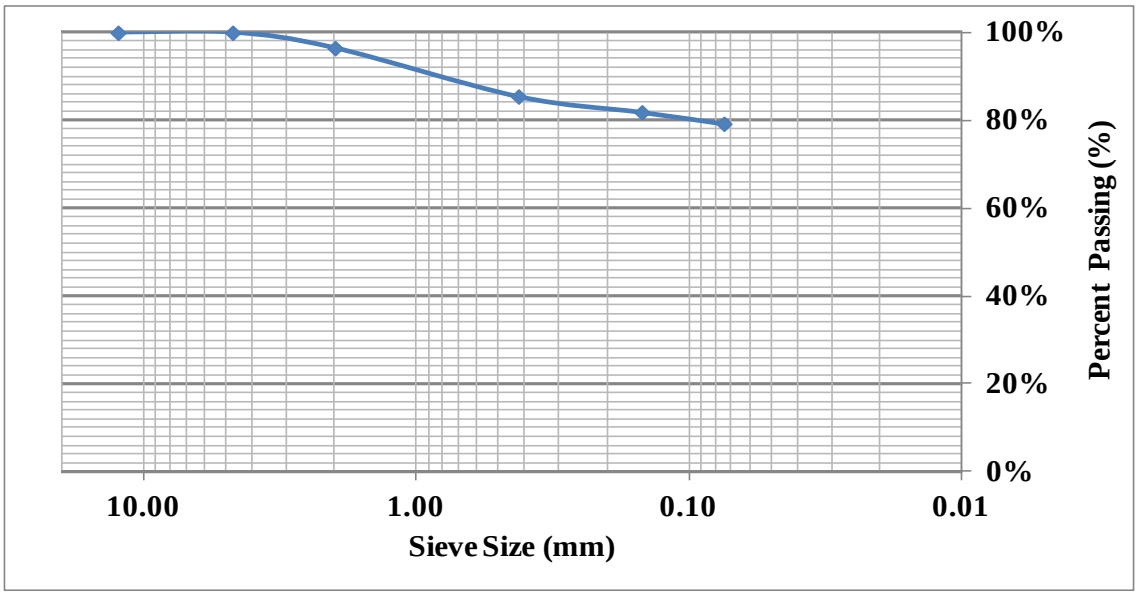

Figure 28 Gradation Curve for Sample No. 7, Lean Clay with Sand.

Sample Number 8.
Location: Houston, Texas
Color: Dark Grayish Brown

PI= 39.96%
(LL= 61.48%, PL: 21.52%)
Classification of Fine Portion: High Plasticity Clay (CH)

Category: **Fat Clay with Sand**
Group Symbol: CH

Table 15 Gradation Table for Sample No. 8, Fat Clay with Sand.

Sieve mesh size (mm)	Sieve Number	Percent Retained	Percent Passing	Particles	
12.50	1/2"	0.00%	100.0%	Gravel	0.0%
4.750	4	0.00%	100.0%		
2.000	10	7.96%	92.0%	Sand	18.29%
0.425	40	6.36%	85.7%		
0.150	100	1.72%	84.0%		
0.075	200	2.25%	81.7%		
Pan	Pan	81.71%	0.0%	Fines	81.71%

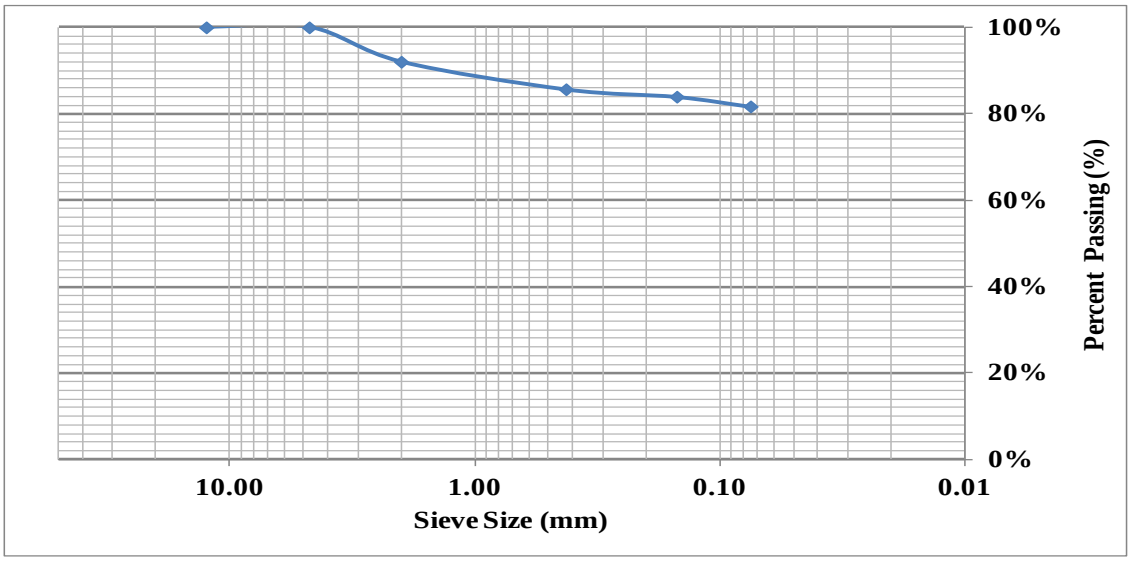

Figure 29 Gradation Curve for Sample No. 8, Fat Clay with Sand.

Appendix B. Soil Samples Atterberg Limits

Table 16 Atterberg Limits for Samples.

No	Location	State	Category	LL(%)	PL(%)	PI(%)	Category for Fines
1	Greenville	NC	Poorly Graded Sand	14.20	NP	NP	NP
2	Delray Beach	FL	Poorly Graded Sand with Silt	16.10	NP	NP	NP
3	College Station	TX	Silty Sand	20.01	17.92	2.09	ML
4	Anderson	SC	Sandy Silt	41.99	32.08	9.91	ML
5	San Angelo	TX	Sandy Lean Clay	32.36	19.00	13.36	CL
6	Houston	TX	Sandy Lean Clay with Gravel	33.59	16.25	17.34	CL
7	Garland	TX	Lean Clay with Sand	41.78	22.61	19.17	CL
8	Houston	TX	Fat Clay with Sand	61.48	21.52	39.96	CH

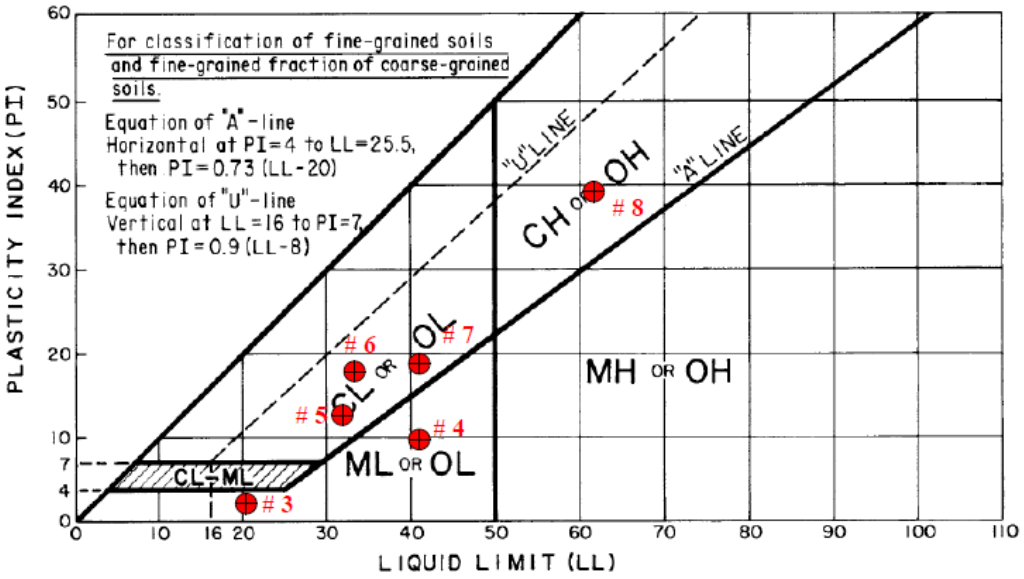

Figure 30 Fine Particles Classifcation for Samples (ASTM D2487).

Appendix C. Lime Stabilization on Clay Samples

The pH test determines the minimum percent lime needed for a soil-lime mixture to attain a pH of 12.4. Cation exchange occurs at this pH, resulting in modification of the soil particle structure to achieve improved workability and decrease swell and plasticity. Series of 30 g samples of soil were placed in separate containers. Series of lime equivalent to 0, 2, 4, 6, 8, and 10% of the 30 g soil samples were added to the soil and mixed with 150 ml (5 fl. oz.) of distilled water to each combination, and stirred vigorously. The pH was measured for each sample and recordings were plotted to find the effective percent of added lime for the soil. Figure 31 shows the pH measurement device. Figure 32 and 33 show the plotted graph for lean and fat clay in this study (sample number 7 and 8). The effective percent of lime is 2% for the lean clay and 4% for the fat clay.

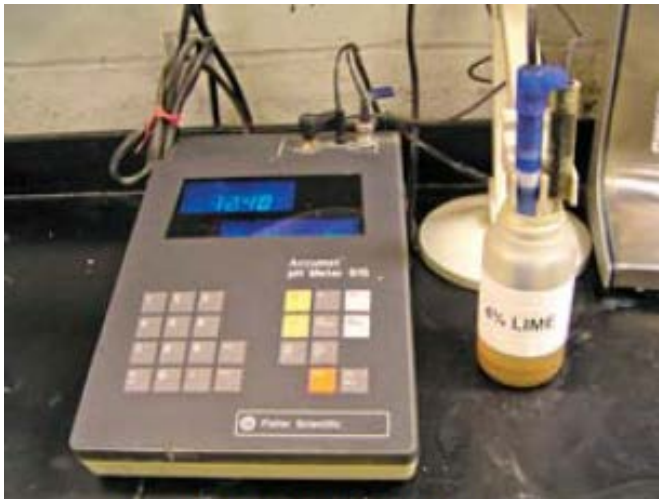

Figure 31 pH Measurement Device.

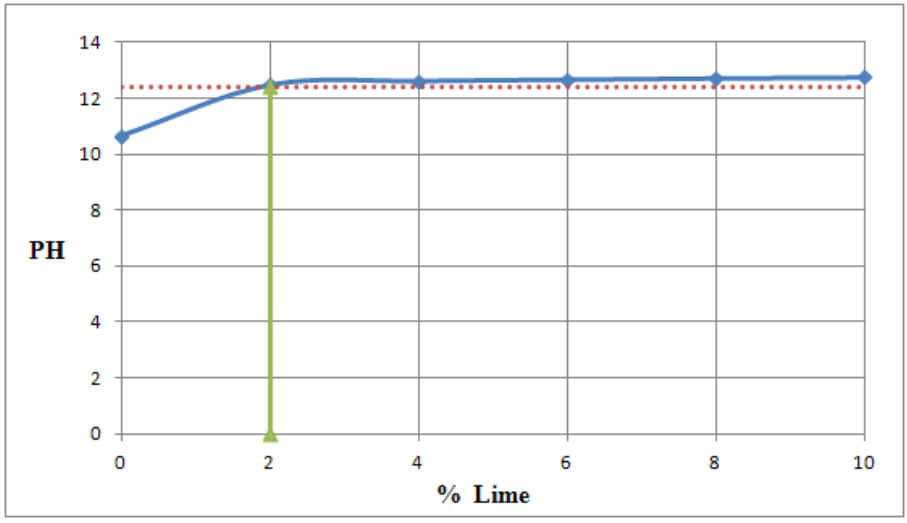

Figure 32 pH Test Plot for Lean Clay, Sample No. 7.

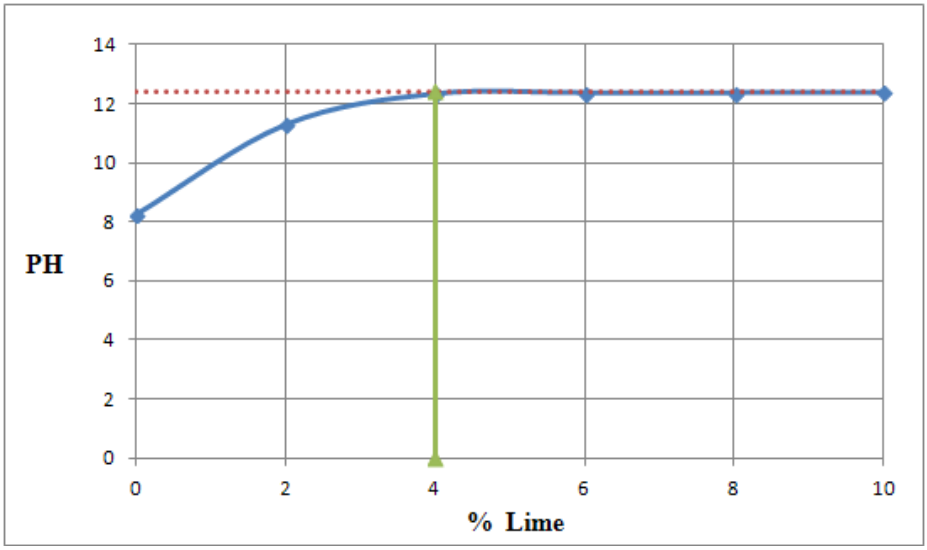

Figure 33 pH Test Plot for Fat Clay, Sample No. 8.

Appendix D. Hamburg Test Results

Erosion test results for each of the collected sample are shown in this Appendix.

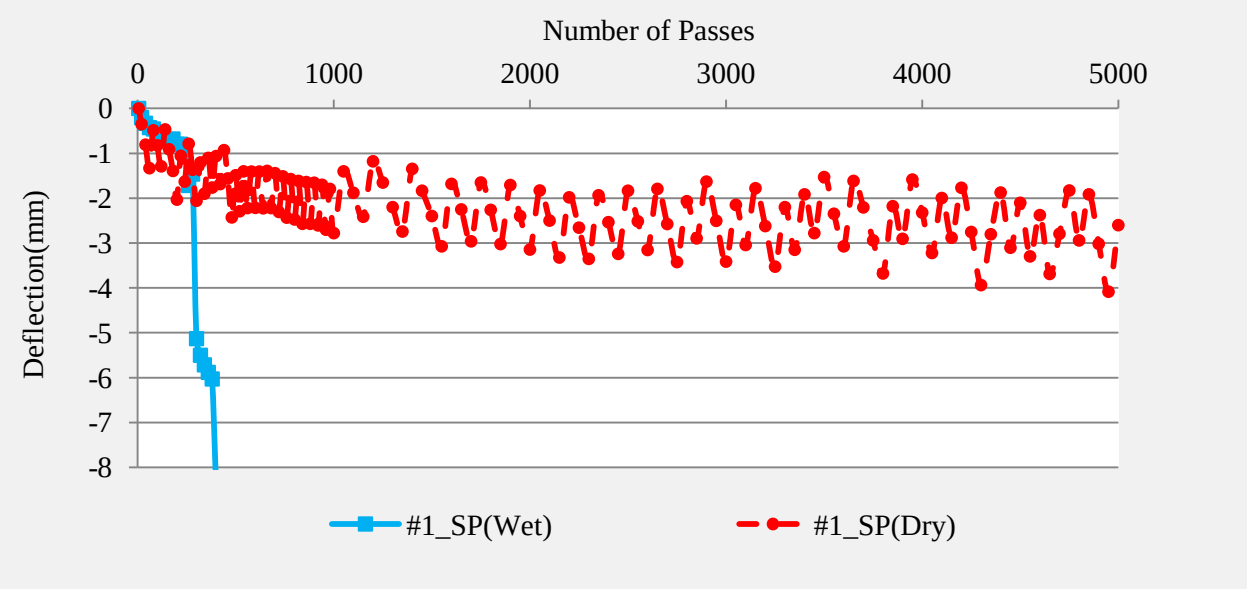

Figure 34 Erosion Test Results for Poorly Graded Sand.

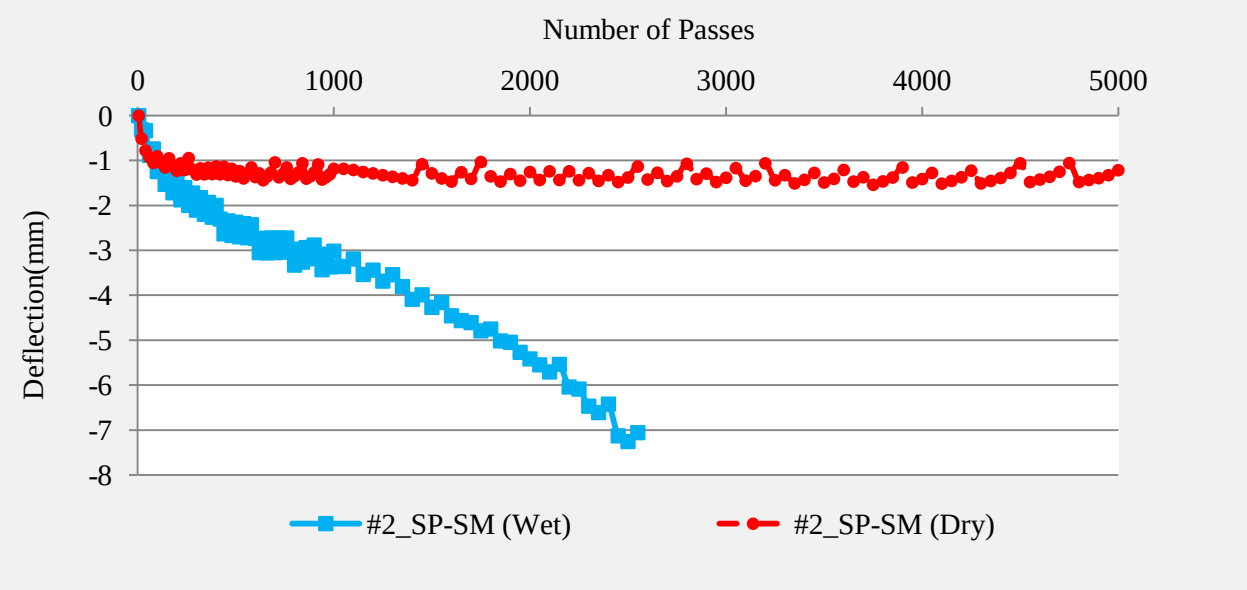

Figure 35 Erosion Test Results for Poorly Graded Sand with Silt.

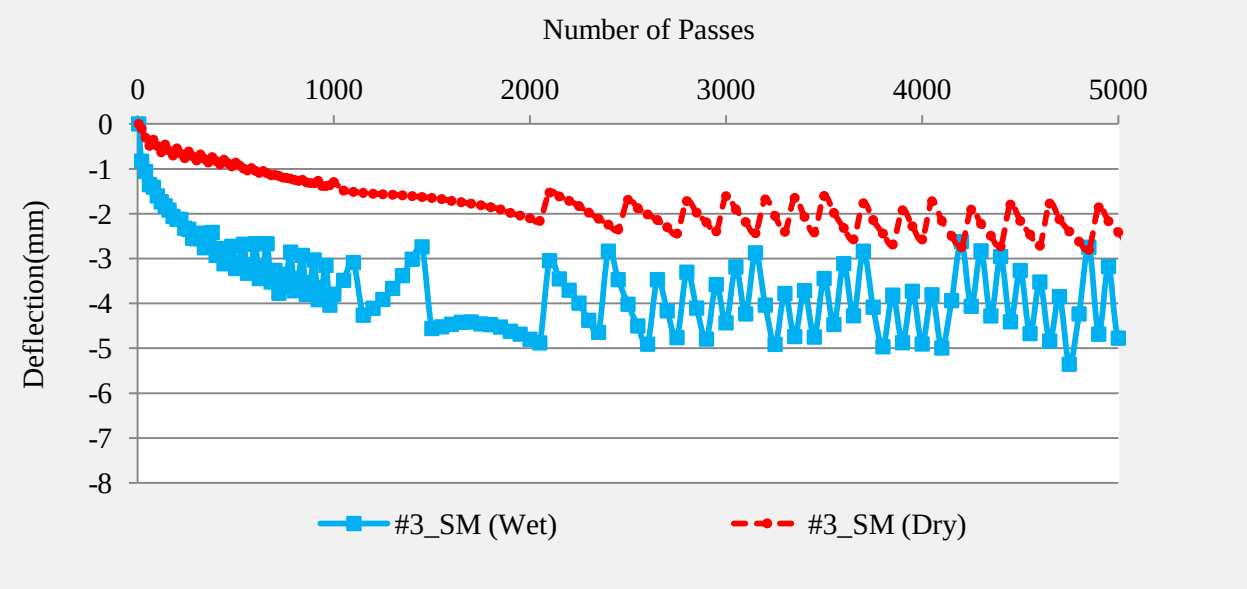

Figure 36 Erosion Test Results for Silty Sand.

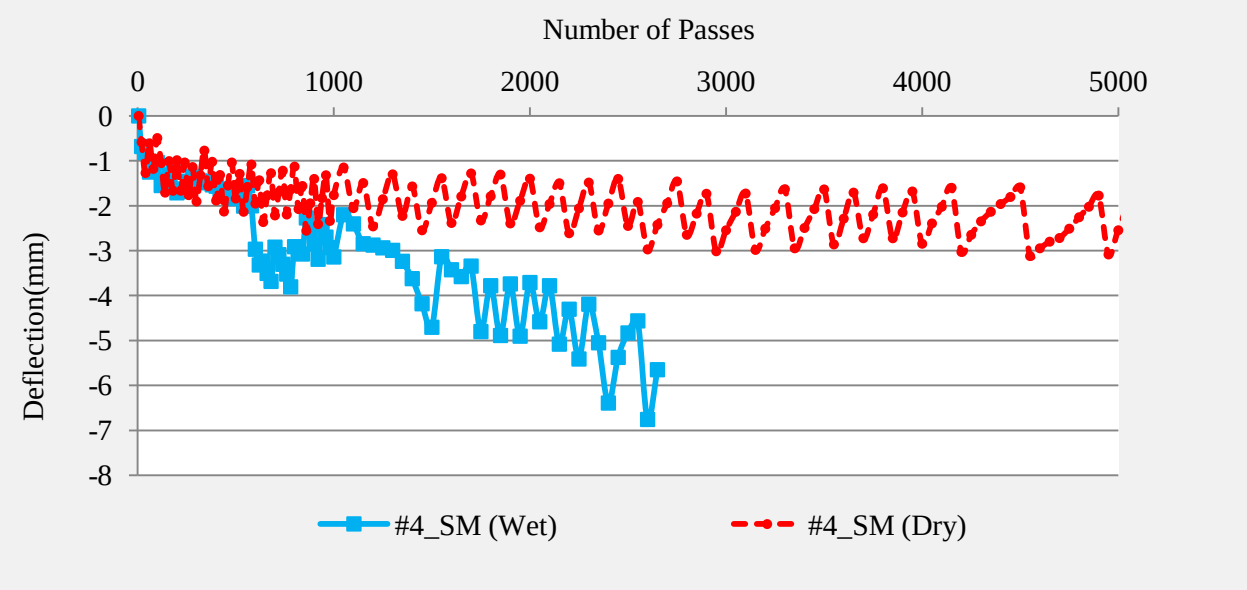

Figure 37 Erosion Test Results for Sandy Silt.

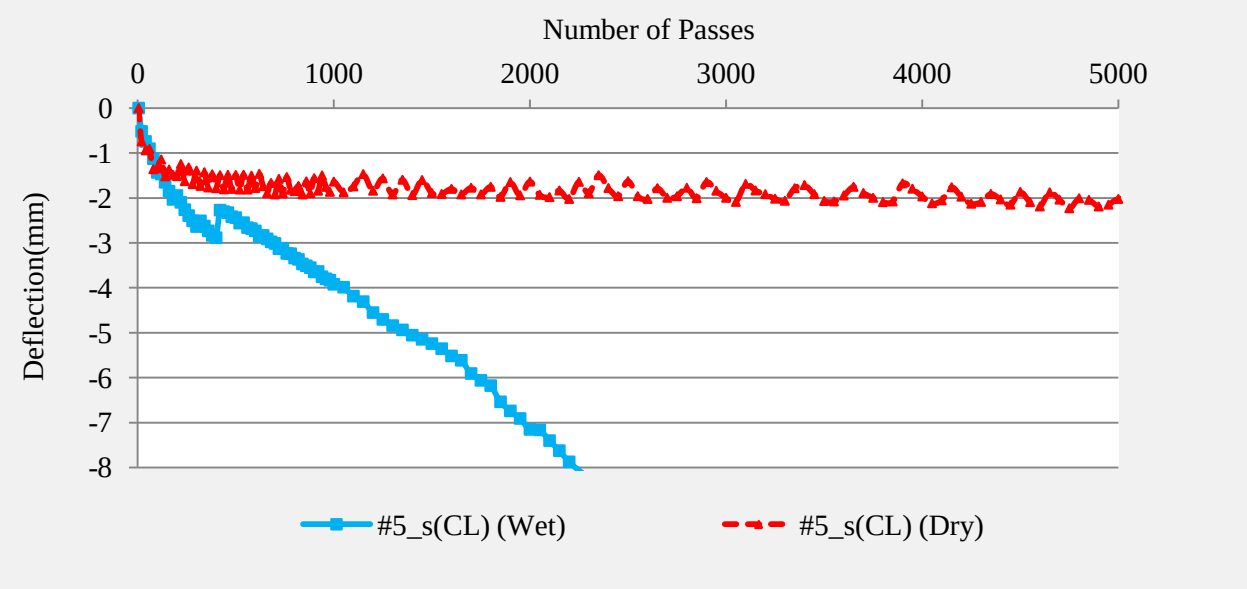

Figure 38 Erosion Test Results for Sandy Lean Clay.

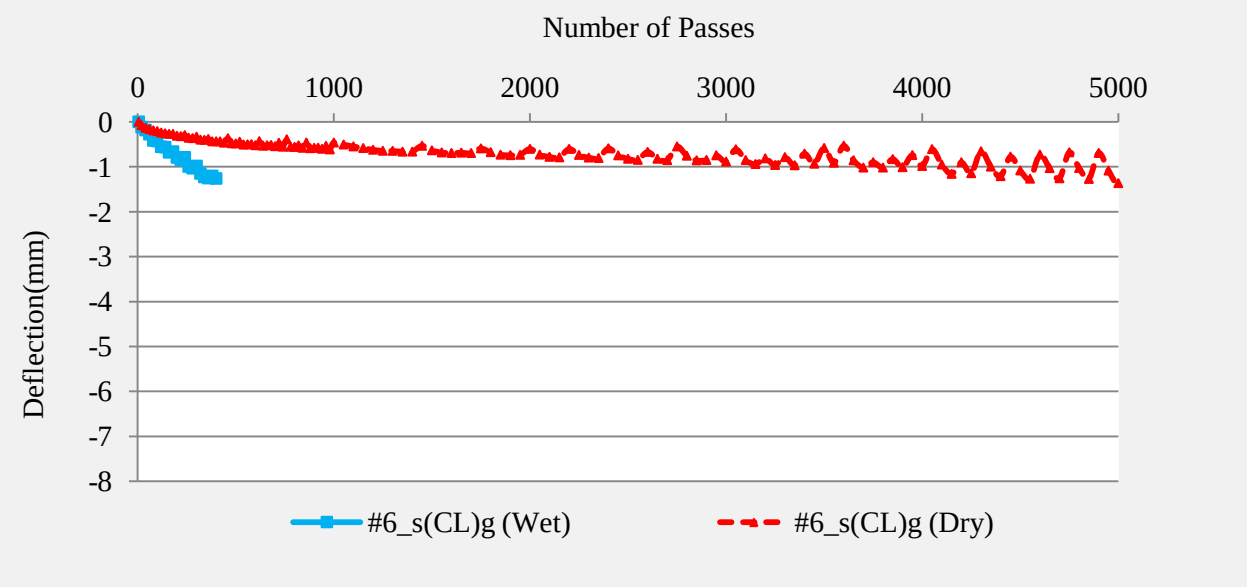

Figure 39 Erosion Test Results for Sandy Lean Clay with Gravel.

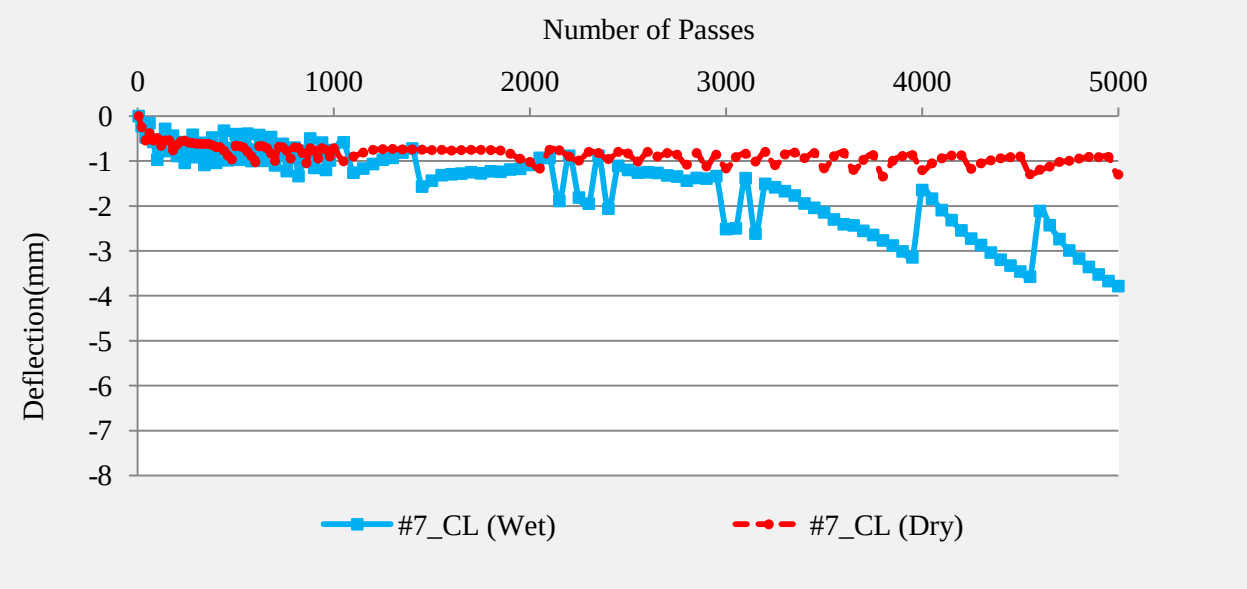

Figure 40 Erosion Test Results for Lean Clay with Sand.

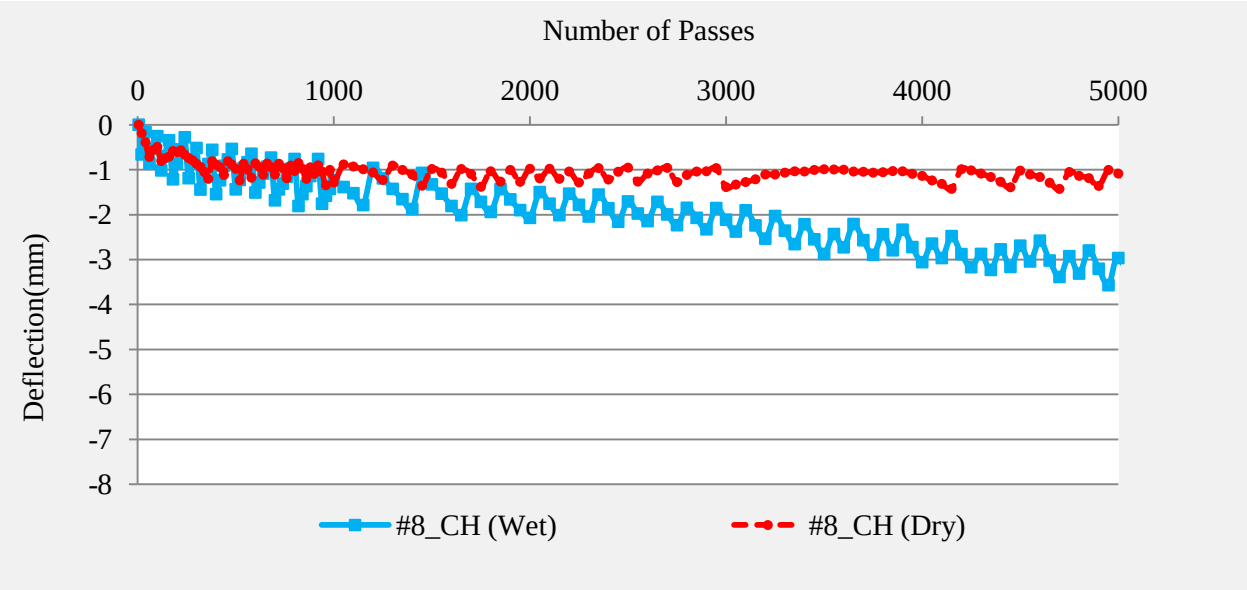

Figure 41 Erosion Test Results for Fat Clay with Sand.

Appendix E. Suggested Test Procedure; Methylene Blue Test

In order to define the soil classification, another test method is suggested. The Methylene Blue Value (MBV) provides an indication of amount and activity of clay present in soil sample. The MBV is a new, rapid method for measuring Methylene Blue Value. In contrast to time consuming traditional tests, the Methylene Blue Test is quick and is completed in nearly 10 minutes. The apparatus is portable and the procedure is simple. The direct outcome of the MBV test is to define the percent of clay in the soil sample. That can be used to get Plasticity Index (PI), Liquid Limit (LL), and Cohesion value with an acceptable accuracy. Appendix E contains an explanation of MBV test. It also includes comparison of values gained by common test methods for one of the soil samples (sample number four) to the values gained by MBV method which shows the accuracy of the MBV test results.

E.1 Principle and Procedure

The test measures the amount of methylene blue dye adsorbed onto clay by comparing the concentration of methylene blue in solution before and after mixing with sand. The concentration of methylene blue solution is measured by colorimetery. A fixed dilution is used at the end of the test so that the methylene blue solution concentration is within the opening range of the colorimeter. Figure 42 shows Methylene Blue Test procedure.

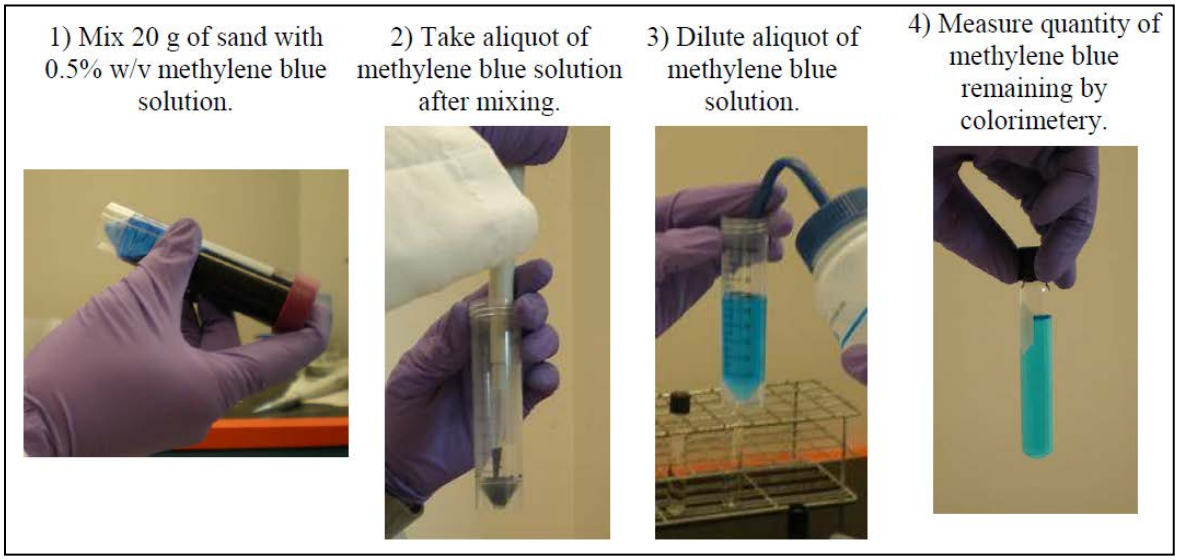

Figure 42 Methylene Blue Test Procedure.

Advantages of the test are listed as follows:

- Rapid (No sieving or tedious titration required);
- Portable (Devices fit into a small toolbox as is shown in Figure 43);
- Comprehensive results (It measures full size fraction of aggregates);
- Simple procedure (No advanced training required); and
- Accurate and repeatable.

E.2 Test Kit Contents

Test apparatus is shown in Figure 43 that includes

1. Reader (Colorimeter)
2. Micropipette
3. Portable balance
4. Test tubes
5. Syringe with filter
6. Methylene blue solution

Figure 43 Methylene Blue Test Apparatus.

E.3 Test Outcome

The direct outcome of the MBV test is to define the percent of clay in the soil sample. That can be used to get Plasticity Index (PI), Liquid Limit (LL), and Cohesion value with an acceptable accuracy.

E.3.1 Plasticity Index

Sahin et al, [19] has performed several tests on different soils in order to define a relationship between MBV value and the plasticity index. This relation, for some of the aggregate sources that were tested, is shown in Figure 44. The confidence level limits of 90 percent are given. A mathematical relation is formulated as follows [19]:

$$MBV = a.e^{0.1714(PI)}$$

The “a parameter” in the equation could differ for different soil types. The general form of the equation considers the “a parameter” equal to 1.7815 but the parameter can be selected based on soil types that were tested in research done by Sahin to get more accurate results.

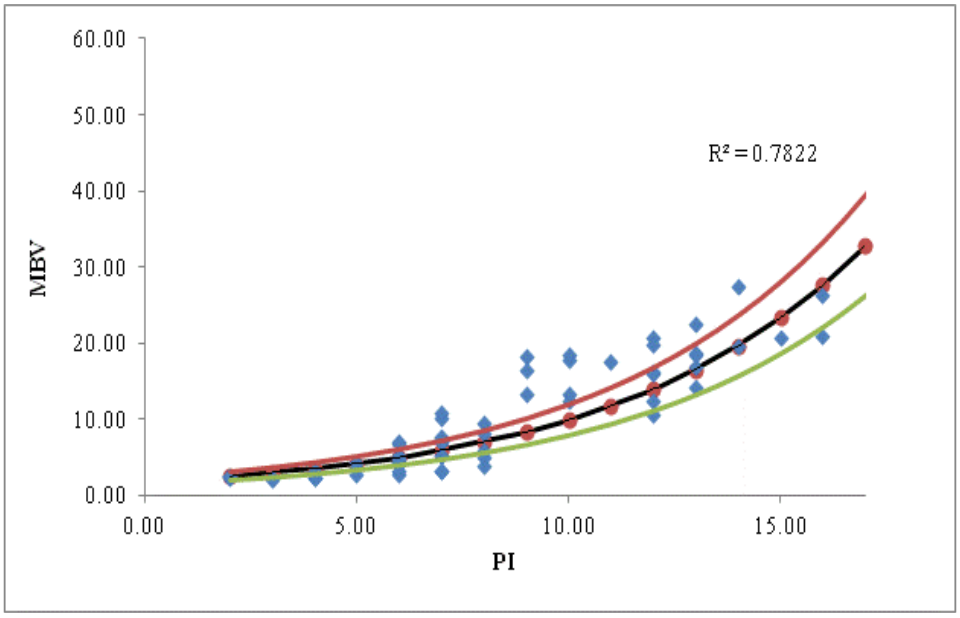

Figure 44 MBV and Plasticity Index Relation with 90% Confidence Limits [19].

E.3.2 Percent of Clay

The extended laboratory test program by Sahin confirms a general relationship between the MBV and the percent of clay, pcf. As shown in Figure 45 this relationship presents a 'C' shaped curve that covers the entire methylene blue test range for soil materials [19].

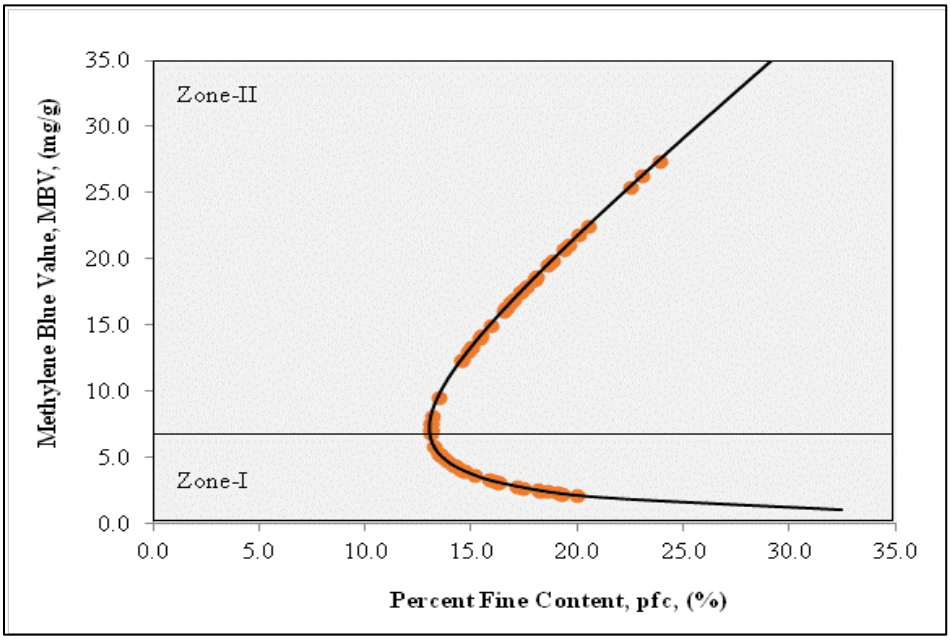

Figure 45 Relationship Between MBV and Percent Fines Content (Only Clays) [19].

This curve is divided into two zones. The MBV of 7.0 is considered to be the critical point. A material with MBV less than 7.0 is considered a relatively non-plastic soil. If the MBV is larger

than 7.0 the material has high plasticity. A mathematical correlation model is determined between MBV and percent fines content. The model present quantitative amount of clay content as follows [19]:

$$pcf = \frac{27.601}{MBV^{0.923}} + 1.552\ (MBV)$$

Where MBV is the methylene blue value; pcf is the percent clay content. The coefficients are the general forms but there are tables based on soil types that help to get even more accurate values.

E.3.3 Cohesion and Friction Angle

Failure in soil materials can be defined by using Mohr-Coulomb shear failure theory;

$$\tau = \sigma * tg\varphi + C$$

Where τ is the shear strength, σ is the normal stress. The quantity C is referred to as the cohesion and the angle φ is called the angle of internal friction. These parameters can be obtained from tri-axial shear or similar testing. To circumvent the amount of time involved in conducing such testing, cohesion and φ angle data has been summarized in Table 17. The data is provided with respect to the Uniform Soil Classification (ASTM D2487) type has an alternative given the soil group category is known. MBV and sieve analysis soil data can also be useful to determine the ASTM D2487 soil type. Table 17 shows the typical values for soil's cohesion and friction characteristics [20].

Table 17 Typical Strength Characteristic for Different Soil Categories [20].

Group Symbol	Cohesion (psi)	Friction Angle
GW	0	>38
GP	0	>37
GM	---	>34
GC	---	>31
SW	0	38
SP	0	37
SM	7.2	34
SM-SC	7.2	33
SC	13.6	31
ML	9.7	32
ML-CL	9.4	32
CL	12.5	28
OL	---	---
MH	10.4	25
CH	14.9	19
OH	---	---

E. 4 Test Validation with Lab Data

In order to validate the MBV test and corresponding values, one of the soil samples was tested. The sandy silt from Anderson, South Carolina (Sample No.4) was tested and the MBV value for the sample is 6.44. Also, the hydrometric analysis was performed in order to find the percent of clay. The total percent of fines (clay and silt) was known from sieve analysis (32.07%). Horiba la-910 was used for hydrometric analysis. Horiba LA-910 is a laser scattering particle size analyzer. Hydrometric results are shown in Figure 46. Accordingly, 12.2% of the sample is clay (particle size smaller than 2 micro millimeters).

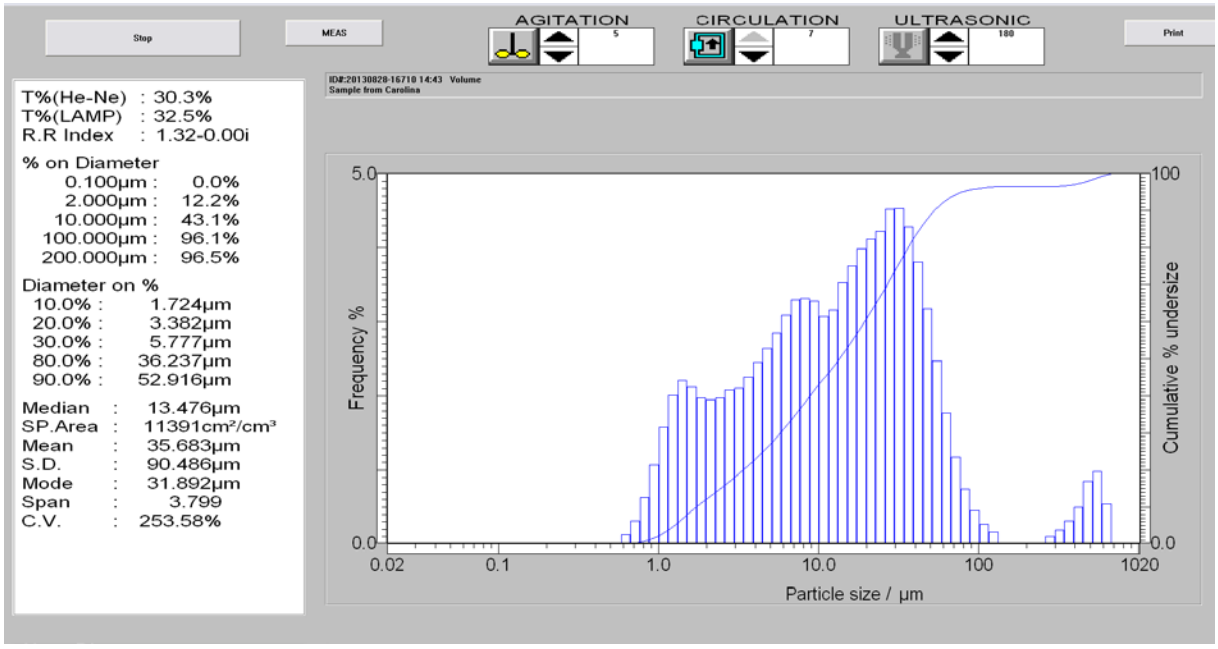

Figure 46 Hydrometric Results for South Carolina Sandy Silt.

Table 18 shows the test results on South Carolina sample using traditional test methods. Table 19 compares values calculated by traditional test methods versus the values using MBV value. It can be seen that errors are negligible and the MBV results are close to the common test results.

Table 18 Test Results on South Carolina Sample Using Traditional Test Methods.

Sample Location	Group Symbol	Category	Percent of Fines	Percent of Sand	Percent of Gravel	PI	Percent of Clay
Anderson, Sc	SM	Sandy Silt	32.7%	63.7%	3.6%	9.92%	12.20%

Table 19 Comparison of Values Gained By Common Methods Vs. Values Using MBV.

MBV	PI	% of Error	pcf	% of Error
6.44	9.52%	4.05%	11.72%	3.94%